9 SPECIAL TOPICS AND MODELING TECHNIQUES

The Eiffel Tower, Paris
(Filip Fuxa/Shutterstock)

In this chapter, we consider some modifications and extensions of the matrix stiffness method developed in the preceding chapters. Also considered herein are techniques for modeling certain special features (or details) of structures, so that more realistic analytical models can be created and more accurate structural responses predicted from the analysis.

We begin by discussing an alternative formulation of the stiffness method in Section 9.1. As this alternative formulation involves the structure stiffness matrix for all the coordinates (including the restrained coordinates) of the structure, it is less efficient for computer implementation than the formulation used in the preceding chapters. Nonetheless, an understanding of this alternative formulation provides some important insights into the stiffness method of analysis. In Sections 9.2 and 9.3, we consider some techniques for reducing a structure's degrees of freedom, and/or the number of structure stiffness equations to be processed simultaneously. These techniques are useful in handling the analysis of large structures. Section 9.4 is devoted to the modeling of inclined roller supports; in the following two sections, we develop techniques for modeling the effects of offset connections (Section 9.5), and semirigid connections (Section 9.6), in the analysis. The inclusion of shear deformation effects in the analysis of beams, grids and frames is considered in Section 9.7; and in Section 9.8, we cover the analysis of structures composed of nonprismatic members. Finally, we conclude the chapter by discussing a procedure for efficiently storing and solving the systems of linear equations that arise in the analysis of large structures.

9.1 THE STRUCTURE STIFFNESS MATRIX INCLUDING RESTRAINED COORDINATES—AN ALTERNATIVE FORMULATION OF THE STIFFNESS METHOD

In the formulation of the matrix stiffness method, as developed in the preceding chapters, the conditions of zero (or known) joint displacements corresponding to restrained coordinates are applied to the member force-displacement relationships before the stiffness relations for the entire structure are assembled. This approach yields structure stiffness relations that contain only the degrees of freedom as unknowns. Alternatively, the stiffness method can be formulated by first establishing the stiffness relations for all the coordinates (free and restrained) of the structure, and then applying the restraint conditions to the structure stiffness relations, which now contain both the degrees of freedom, and the support reactions, as unknowns.

In the alternative formulation, the structure's restrained coordinates are initially treated as free coordinates, and the stiffness relations for all the coordinates of the structure are expressed as

$$\underset{NC \times 1}{\mathbf{P}^*} \quad - \quad \underset{NC \times 1}{\mathbf{P}_f^*} \quad = \quad \underset{NC \times NC}{\mathbf{S}^*} \quad \underset{NC \times 1}{\mathbf{d}^*} \tag{9.1}$$

with

$$NC = NCJT(NJ) = NDOF + NR \tag{9.2}$$

In Eqs. (9.1) and (9.2), *NC* denotes the number of structure coordinates; $\mathbf{P}^*$ represents the joint forces (i.e., the known external loads and the unknown support reactions); $\mathbf{P}_f^*$ denotes the fixed-joint forces, due to member loads, temperature changes, and fabrication errors, at the locations, and in the directions, of the structure coordinates; $\mathbf{S}^*$ represents the stiffness matrix for the structure coordinates (free and restrained); and $\mathbf{d}^*$ denotes the joint displacements (i.e., the unknown degrees of freedom and the known displacements corresponding to the restrained coordinates). The structure stiffness matrix $\mathbf{S}^*$ and fixed-joint force vector $\mathbf{P}_f^*$ can be determined by assembling the member global stiffness matrices $\mathbf{K}$ and fixed-end force vectors $\mathbf{F}_f$, respectively, using the member code number technique described in the preceding chapters. The application of this technique remains essentially the same, except that now those elements of $\mathbf{K}$ and $\mathbf{F}_f$ that correspond to the restrained coordinates are no longer discarded, but are added (stored) in their proper positions in $\mathbf{S}^*$ and $\mathbf{P}_f^*$.

As indicated in the preceding paragraph, the structure stiffness relations (Eq. (9.1)) contain two types of unknown quantities; namely, the unknown joint displacements and the unknown support reactions. To separate the two types of unknowns, we rewrite Eq. (9.1) in partitioned-matrix form:

$$\begin{bmatrix} \mathbf{P} \\ \hline NDOF \times 1 \\ \hline \mathbf{R} \\ NR \times 1 \end{bmatrix} - \begin{bmatrix} \mathbf{P}_f \\ \hline NDOF \times 1 \\ \hline \mathbf{R}_f \\ NR \times 1 \end{bmatrix} = \left[\begin{array}{c|c} \mathbf{S} & \mathbf{S}_{FR} \\ \hline NDOF \times NDOF & NDOF \times NR \\ \hline \mathbf{S}_{RF} & \mathbf{S}_{RR} \\ NR \times NDOF & NR \times NR \end{array}\right] \begin{bmatrix} \mathbf{d} \\ \hline NDOF \times 1 \\ \hline \mathbf{d}_R \\ NR \times 1 \end{bmatrix} \tag{9.3}$$

in which, $\mathbf{P}$, $\mathbf{R}$, $\mathbf{P}_f$, $\mathbf{S}$, and $\mathbf{d}$ denote the same quantities as in the preceding chapters; $\mathbf{R}_f$ denotes the structure fixed-joint forces corresponding to the restrained coordinates; and $\mathbf{d}_R$ denotes the *support displacement vector*. Note that the $\mathbf{P}_f$ and $\mathbf{R}_f$ vectors contain structure fixed-joint forces due to member loads, temperature changes, and fabrication errors. The effects of support displacements are not included in $\mathbf{P}_f$ and $\mathbf{R}_f$, but are directly incorporated into the analysis through the support displacement vector $\mathbf{d}_R$. Each element of the submatrix $\mathbf{S}_{FR}$ in Eq. (9.3) represents the force at a free coordinate caused by a unit displacement of a restrained coordinate. The other two submatrices, $\mathbf{S}_{RF}$ and $\mathbf{S}_{RR}$, can be interpreted in an analogous manner. By multiplying the two partitioned matrices on the right-hand side of Eq. (9.3), we obtain two matrix equations,

$$\mathbf{P} - \mathbf{P}_f = \mathbf{S}\mathbf{d} + \mathbf{S}_{FR}\mathbf{d}_R \tag{9.4a}$$

$$\mathbf{R} - \mathbf{R}_f = \mathbf{S}_{RF}\mathbf{d} + \mathbf{S}_{RR}\mathbf{d}_R \tag{9.4b}$$

which can be rearranged as

$$\boxed{\mathbf{P} - \mathbf{P}_f - \mathbf{S}_{FR}\mathbf{d}_R = \mathbf{S}\mathbf{d}} \tag{9.5a}$$

$$\boxed{\mathbf{R} = \mathbf{R}_f + \mathbf{S}_{RF}\mathbf{d} + \mathbf{S}_{RR}\mathbf{d}_R} \tag{9.5b}$$

The procedure for analysis essentially consists of first solving Eq. (9.5a) for the unknown joint displacements **d**, and then substituting **d** into Eq. (9.5b) to evaluate the support reactions **R**. With **d** known, the member end displacements and end forces can be obtained using the procedures described in the preceding chapters. In the case of structures with no support displacements, $\mathbf{d}_R = \mathbf{0}$, and Eqs. (9.5) reduce to

$$\mathbf{P} - \mathbf{P}_f = \mathbf{S}\mathbf{d} \tag{9.6a}$$

$$\mathbf{R} = \mathbf{R}_f + \mathbf{S}_{RF}\mathbf{d} \tag{9.6b}$$

The main advantages of the alternative formulation are that support displacements can be incorporated into the analysis in a direct and straightforward manner, and the reactions can be more conveniently calculated by using the structure stiffness relations. However, since the alternative formulation uses the stiffness matrix for all of the structure's coordinates, it requires significantly more computer memory space than the standard formulation developed in the preceding chapters, which uses the stiffness matrix for only the free coordinates of the structure. For this reason, the alternative formulation is not considered to be as efficient for computer implementation as the formulation developed in the preceding chapters [14].

The application of the alternative formulation is illustrated by the following example.

EXAMPLE 9.1 Determine the joint displacements, member local end forces, and support reactions for the plane frame of Fig. 9.1(a), due to the combined effect of the loading shown and a

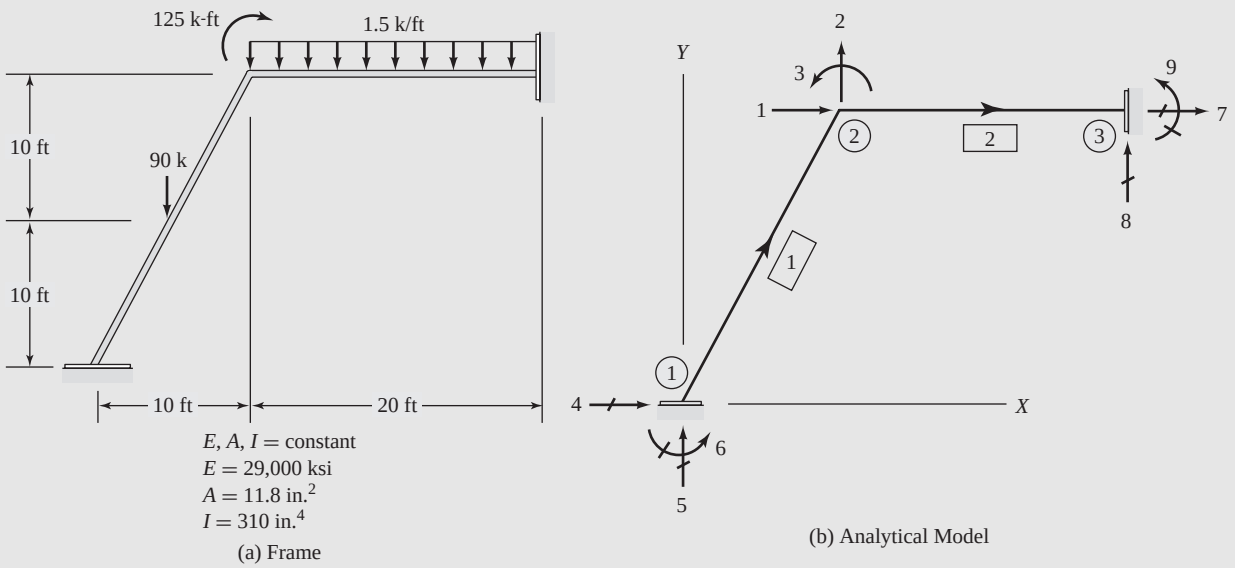

Fig. 9.1

settlement of 1 in. of the left support. Use the alternative formulation of the matrix stiffness method.

SOLUTION This frame was analyzed in Example 6.6 for external loading, and in Example 7.4 for the combined effect of the loading and the support settlement, using the standard formulation.

Analytical Model: See Fig. 9.1(b). In this example, we use the same analytical model of the frame as used previously, so that the various member matrices calculated in Example 6.6 can be reused. The frame has three degrees of freedom and six restrained coordinates. Thus, the total number of structure coordinates is nine.

Structure Stiffness Matrix: By storing the element of the member global stiffness matrices $\mathbf{K}_1$ and $\mathbf{K}_2$, calculated in Example 6.6, in their proper positions in the 9×9 structure stiffness matrix $\mathbf{S}^*$, we obtain, in units of kips and inches, the following stiffness matrix for all the structure coordinates.

$$\mathbf{S}^* = \begin{bmatrix} \mathbf{S} & \mathbf{S}_{FR} \\ \mathbf{S}_{RF} & \mathbf{S}_{RR} \end{bmatrix} = \begin{array}{c} \begin{matrix} 1 & 2 & 3 & 4 & 5 & 6 & 7 & 8 & 9 \end{matrix} \\ \left[\begin{array}{ccc:ccc:ccc} 1{,}685.3 & 507.89 & 670.08 & -259.53 & -507.89 & 670.08 & -1{,}425.8 & 0 & 0 \\ 507.89 & 1{,}029.2 & 601.42 & -507.89 & -1{,}021.4 & -335.04 & 0 & -7.8038 & 936.46 \\ 670.08 & 601.42 & 283{,}848 & -670.08 & 335.04 & 67{,}008 & 0 & -936.46 & 74{,}917 \\ \hdashline -259.53 & -507.89 & -670.08 & 259.53 & 507.89 & -670.08 & 0 & 0 & 0 \\ -507.89 & -1{,}021.4 & 335.04 & 507.89 & 1{,}021.4 & 335.04 & 0 & 0 & 0 \\ 670.08 & -335.04 & 67{,}008 & -670.08 & 335.04 & 13{,}401.5 & 0 & 0 & 0 \\ -1{,}425.8 & 0 & 0 & 0 & 0 & 0 & 1{,}425.8 & 0 & 0 \\ 0 & -7.8038 & -936.46 & 0 & 0 & 0 & 0 & 7.8038 & -936.46 \\ 0 & 936.46 & 74{,}917 & 0 & 0 & 0 & 0 & -936.46 & 149{,}833 \end{array}\right] \end{array} \begin{matrix} 1 \\ 2 \\ 3 \\ 4 \\ 5 \\ 6 \\ 7 \\ 8 \\ 9 \end{matrix} \quad \textbf{(1)}$$

Structure Fixed-Joint Force Vector Due to Member Loads: Similarly, by storing the elements of the member global fixed-end force vectors $\mathbf{F}_{f1}$ and $\mathbf{F}_{f2}$, calculated in Example 6.6, in the 9×1 structure fixed-joint force vector $\mathbf{P}_f^*$, we obtain

$$\mathbf{P}_f^* = \begin{bmatrix} \mathbf{P}_f \\ \mathbf{R}_f \end{bmatrix} = \begin{array}{c} \left[\begin{array}{c} 0 \\ 60 \\ -750 \\ \hdashline 0 \\ 45 \\ 1{,}350 \\ 0 \\ 15 \\ -600 \end{array}\right] \end{array} \begin{matrix} 1 \\ 2 \\ 3 \\ 4 \\ 5 \\ 6 \\ 7 \\ 8 \\ 9 \end{matrix} \quad \textbf{(2)}$$

Joint Load Vector: From Example 6.6,

$$\mathbf{P} = \begin{bmatrix} 0 \\ 0 \\ -1{,}500 \end{bmatrix} \begin{matrix} 1 \\ 2 \\ 3 \end{matrix} \quad \textbf{(3)}$$

Support Displacement Vector: From the analytical model of the structure in Fig. 9.1(b), we observe that the given 1 in. settlement of the left support occurs at the location and

in the direction of restraint coordinate 5. Thus, the support displacement vector can be expressed as

$$\mathbf{d}_R = \begin{bmatrix} 0 \\ -1 \\ 0 \\ 0 \\ 0 \\ 0 \end{bmatrix} \begin{matrix} 4 \\ 5 \\ 6 \\ 7 \\ 8 \\ 9 \end{matrix} \tag{4}$$

Joint Displacements: By substituting $\mathbf{S}$ and $\mathbf{S}_{FR}$ from Eq. (1), $\mathbf{P}_f$ from Eq. (2), $\mathbf{P}$ from Eq. (3), and $\mathbf{d}_R$ from Eq. (4) into Eq. (9.5a), we write the stiffness relations for the free coordinates of the frame as

$$\mathbf{P} - \mathbf{P}_f - \mathbf{S}_{FR}\mathbf{d}_R = \mathbf{S}\mathbf{d}$$

$$\begin{bmatrix} 0 \\ 0 \\ -1{,}500 \end{bmatrix} - \begin{bmatrix} 0 \\ 60 \\ -750 \end{bmatrix} - \begin{bmatrix} -259.53 & -507.89 & 670.08 & -1{,}425.8 & 0 & 0 \\ -507.89 & -1{,}021.4 & -335.04 & 0 & -7.8038 & 936.46 \\ -670.08 & 335.04 & 67{,}008 & 0 & -936.46 & 74{,}917 \end{bmatrix} \begin{bmatrix} 0 \\ -1 \\ 0 \\ 0 \\ 0 \\ 0 \end{bmatrix}$$

$$= \begin{bmatrix} 1{,}685.3 & 507.89 & 670.08 \\ 507.89 & 1{,}029.2 & 601.42 \\ 670.08 & 601.42 & 283{,}848 \end{bmatrix} \begin{bmatrix} d_1 \\ d_2 \\ d_3 \end{bmatrix}$$

or

$$\begin{bmatrix} -507.89 \\ -1{,}081.4 \\ -414.96 \end{bmatrix} = \begin{bmatrix} 1{,}685.3 & 507.89 & 670.08 \\ 507.89 & 1{,}029.2 & 601.42 \\ 670.08 & 601.42 & 283{,}848 \end{bmatrix} \begin{bmatrix} d_1 \\ d_2 \\ d_3 \end{bmatrix}$$

By solving these equations, we determine the joint displacements to be

$$\mathbf{d} = \begin{bmatrix} 0.017762 \text{ in.} \\ -1.0599 \text{ in.} \\ 0.00074192 \text{ rad} \end{bmatrix} \begin{matrix} 1 \\ 2 \\ 3 \end{matrix} \tag{5}$$ **Ans**

Note that these joint displacements are identical to those calculated in Example 7.4. The joint displacement vector for all the coordinates (free and restrained) of the structure can be expressed as

$$\mathbf{d}^* = \begin{bmatrix} \mathbf{d} \\ \hdashline \mathbf{d}_R \end{bmatrix} = \begin{bmatrix} 0.017762 \text{ in.} \\ -1.0599 \text{ in.} \\ 0.00074192 \text{ rad} \\ \hdashline 0 \\ -1 \text{ in.} \\ 0 \\ 0 \\ 0 \\ 0 \end{bmatrix} \begin{matrix} 1 \\ 2 \\ 3 \\ 4 \\ 5 \\ 6 \\ 7 \\ 8 \\ 9 \end{matrix} \tag{6}$$

Support Reactions: To evaluate the support reaction vector $\mathbf{R}$, we substitute $\mathbf{S}_{RF}$ and $\mathbf{S}_{RR}$ from Eq. (1), $\mathbf{R}_f$ from Eq. (2), $\mathbf{d}_R$ from Eq. (4), and $\mathbf{d}$ from Eq. (5) into Eq. 9.5(b): $\mathbf{R} = \mathbf{R}_f + \mathbf{S}_{RF}\mathbf{d} + \mathbf{S}_{RR}\mathbf{d}_R$. This yields

$$\mathbf{R} = \begin{bmatrix} 25.316 \text{ k} \\ 97.409 \text{ k} \\ 1{,}431.7 \text{ k-in.} \\ -25.325 \text{ k} \\ 22.576 \text{ k} \\ -1{,}537 \text{ k-in.} \end{bmatrix} \begin{matrix} 4 \\ 5 \\ 6 \\ 7 \\ 8 \\ 9 \end{matrix} \qquad \textbf{Ans}$$

Note that these support reactions are the same as those calculated in Example 7.4.

Member End Displacements and End Forces:

Member 1 Using member code numbers and Eq. (6), we obtain

$$\mathbf{v}_1 = \begin{bmatrix} v_1 \\ v_2 \\ v_3 \\ v_4 \\ v_5 \\ v_6 \end{bmatrix} \begin{matrix} 4 \\ 5 \\ 6 \\ 1 \\ 2 \\ 3 \end{matrix} = \begin{bmatrix} d_4^* \\ d_5^* \\ d_6^* \\ d_1^* \\ d_2^* \\ d_3^* \end{bmatrix} = \begin{bmatrix} 0 \\ -1 \\ 0 \\ 0.017762 \\ -1.0599 \\ 0.00074192 \end{bmatrix}$$

Next, we use the member transformation matrix $\mathbf{T}_1$ from Example 6.6, to calculate

$$\mathbf{u}_1 = \mathbf{T}_1\mathbf{v}_1 = \begin{bmatrix} -0.89443 \\ -0.44721 \\ 0 \\ -0.94006 \\ -0.48988 \\ 0.00074192 \end{bmatrix}$$

The member local end forces can now be obtained by using the member local stiffness matrix $\mathbf{k}_1$ and fixed-end force vector $\mathbf{Q}_{f1}$, from Example 6.6, as

$$\mathbf{Q}_1 = \mathbf{k}_1\mathbf{u}_1 + \mathbf{Q}_{f1} = \begin{bmatrix} 98.441 \text{ k} \\ 20.919 \text{ k} \\ 1{,}431.7 \text{ k-in.} \\ -17.943 \text{ k} \\ 19.331 \text{ k} \\ -1{,}218.6 \text{ k-in.} \end{bmatrix} \qquad \textbf{Ans}$$

Member 2 The global and local end displacements for this horizontal member are

$$\mathbf{u}_1 = \mathbf{v}_1 = \begin{bmatrix} v_1 \\ v_2 \\ v_3 \\ v_4 \\ v_5 \\ v_6 \end{bmatrix} \begin{matrix} 1 \\ 2 \\ 3 \\ 7 \\ 8 \\ 9 \end{matrix} = \begin{bmatrix} d_1^* \\ d_2^* \\ d_3^* \\ d_7^* \\ d_8^* \\ d_9^* \end{bmatrix} = \begin{bmatrix} 0.017762 \\ -1.0599 \\ 0.00074192 \\ 0 \\ 0 \\ 0 \end{bmatrix}$$

By using $\mathbf{k}_2$ and $\mathbf{Q}_{f2}$ from Example 6.6, we compute the member local end forces to be

$$\mathbf{Q}_2 = \mathbf{k}_2\mathbf{u}_2 + \mathbf{Q}_{f2} = \begin{bmatrix} 25.325 \text{ k} \\ 7.4235 \text{ k} \\ -281.39 \text{ k-in.} \\ -25.325 \text{ k} \\ 22.576 \text{ k} \\ -1{,}537 \text{ k-in.} \end{bmatrix} \quad \textbf{Ans}$$

As expected, the foregoing member local end force vectors $\mathbf{Q}_1$ and $\mathbf{Q}_2$ are identical to those calculated in Example 7.4.

9.2 APPROXIMATE MATRIX ANALYSIS OF RECTANGULAR BUILDING FRAMES

In building frames of low to medium height, the axial deformations of members are generally much smaller than the bending deformations. Therefore, the number of degrees of freedom of such frames can be reduced, without significantly compromising the accuracy of the analysis results, by neglecting the axial deformations of members, or by assuming that the members are *inextensible*. In this section, we consider the analysis of rectangular plane frames composed of horizontal and vertical members which are assumed to be inextensible (i.e., they cannot undergo any axial elongation or shortening).

Consider, for example, the portal frame shown in Fig. 9.2. Recall from Chapter 6 that the frame actually has six degrees of freedom, when both axial

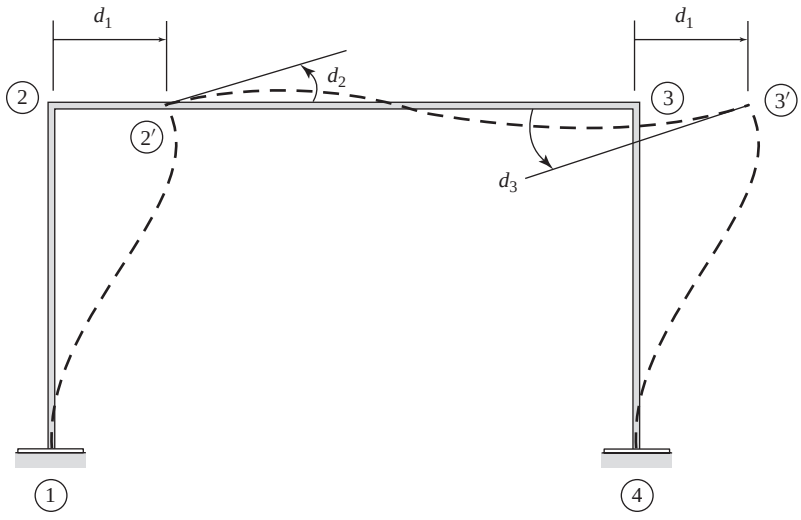

Fig. 9.2 *Portal Frame with Inextensible Members* (*Three Degrees of Freedom*)

and bending deformations of members are taken into account in the analysis. However, if the members of the frame are assumed to be inextensible, then the number of degrees of freedom is reduced to only three. From the deformed shape of the arbitrarily loaded frame given in Fig. 9.2, we can see that fixed joints 1 and 4 can neither rotate nor translate, whereas joints 2 and 3 can rotate and translate in the horizontal direction, but not in the vertical direction because their vertical translations are prevented by the left and right columns, respectively, which are assumed to be inextensible. Furthermore, since the girder (i.e., the horizontal member) of the frame is assumed to be inextensible, the horizontal translations of joints 2 and 3 must be equal. Thus, the portal frame has three degrees of freedom, namely d_1, d_2, and d_3, as shown in the figure.

As another example, consider the two-story three-bay building frame shown in Fig. 9.3. The frame actually has 24 degrees of freedom when both axial and bending deformations are included in the analysis. However, if the members are assumed to be inextensible, then the number of degrees of freedom is reduced to 10, as shown in the figure. As this example indicates, the assumption of member inextensibility provides a means for a significant reduction in the number of degrees of freedom of large structures. Needless to say, this approximate approach is appropriate only for frames in which the member axial deformations are small enough to have a negligible effect on their response. As the axial deformations in the columns of tall building frames can have a significant effect on the structural response, the approximate method under consideration is usually not considered suitable for the analysis of such structures.

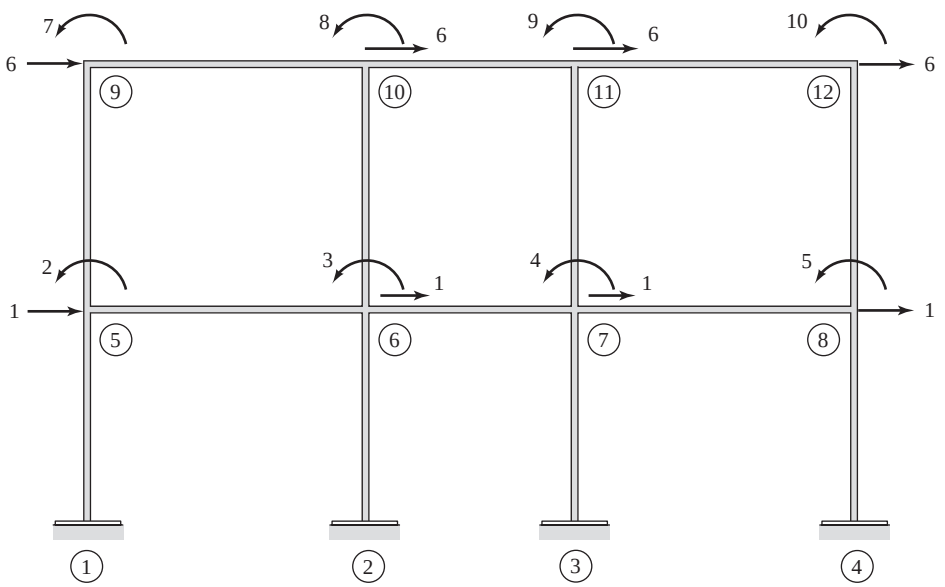

Fig. 9.3 *Inextensible Building Frame* (*Ten Degrees of Freedom*)

The overall procedure for the approximate analysis of rectangular plane frames remains the same as that for general plane frames, developed in Chapter 6—provided that the member stiffness relations are modified to exclude the axial effects. As the frame is composed of only horizontal and vertical members, each member now has four degrees of freedom in both the local and global coordinate systems. The local and global end forces and end displacements for the girders (i.e., horizontal members), and the columns (i.e., vertical members), of the frame, are given in Fig. 9.4. To simplify the analysis, the member local x axis is oriented positive to the right for girders (Fig. 9.4(a)) and positive upward for columns (Fig. 9.4(b)). With the axial effects neglected, the relationship between the member local end forces, $\mathbf{Q}$, and end displacements, $\mathbf{u}$, is expressed by the local stiffness matrix $\mathbf{k}$ and fixed-end force vector $\mathbf{Q}_f$ for

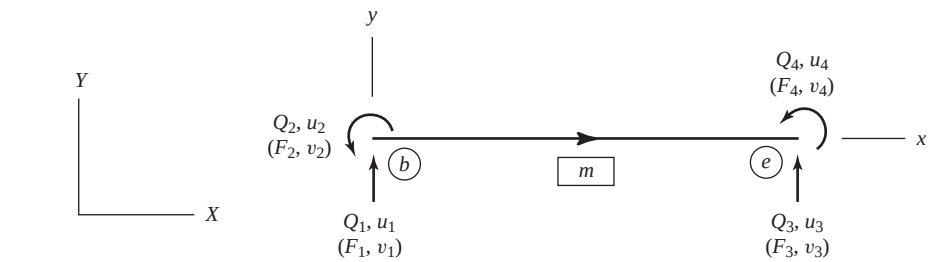

(a) Girder End Forces and End Displacements in Local and Global Coordinate Systems

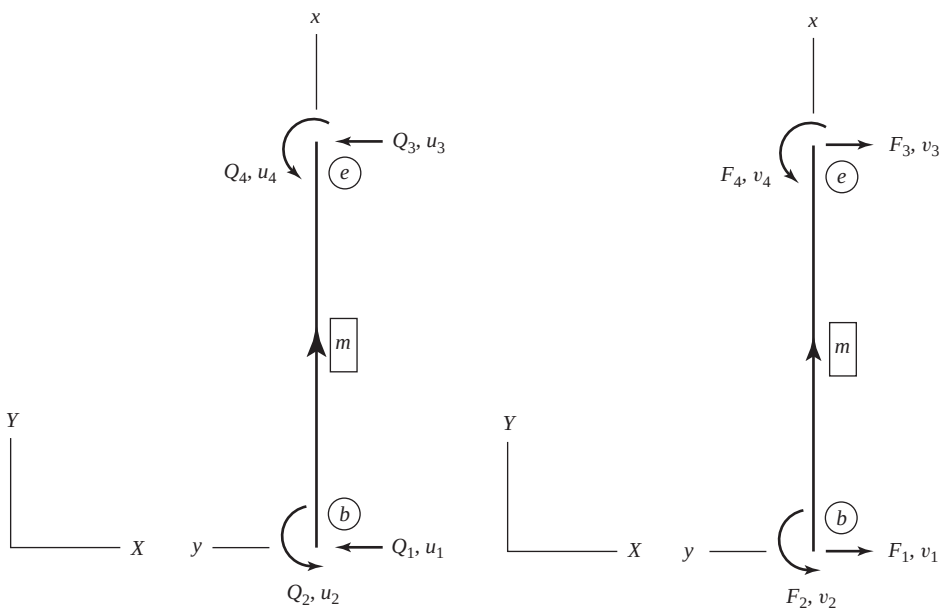

(b) Column End Forces and End Displacements in the Local Coordinate System

(c) Column End Forces and End Displacements in the Global Coordinate System

Fig. 9.4

beam members, derived in Chapter 5 (Eqs. (5.53) and (5.99)). Thus, $\mathbf{Q} = \mathbf{ku} + \mathbf{Q}_f$, with

$$\mathbf{k} = \frac{EI}{L^3}\begin{bmatrix} 12 & 6L & -12 & 6L \\ 6L & 4L^2 & -6L & 2L^2 \\ -12 & -6L & 12 & -6L \\ 6L & 2L^2 & -6L & 4L^2 \end{bmatrix} \tag{9.7}$$

and

$$\mathbf{Q}_f = \begin{bmatrix} FS_b \\ FM_b \\ FS_e \\ FM_e \end{bmatrix} \tag{9.8}$$

As for the member stiffness relations in the global coordinate system, for girders (Fig. 9.4(a)) no coordinate transformations are needed; that is, $\mathbf{K}$ (girder) $= \mathbf{k}$ and $\mathbf{F}_f$ (girder) $= \mathbf{Q}_f$. For columns, the transformation matrix, $\mathbf{T}$ (column), can be established via the following relationships between the local end forces $\mathbf{Q}$ and the global end forces $\mathbf{F}$ (see Figs. 9.4(b) and (c)):

$$Q_1 = -F_1 \qquad Q_2 = F_2 \qquad Q_3 = -F_3 \qquad Q_4 = F_4$$

or

$$\begin{bmatrix} Q_1 \\ Q_2 \\ Q_3 \\ Q_4 \end{bmatrix} = \begin{bmatrix} -1 & 0 & 0 & 0 \\ 0 & 1 & 0 & 0 \\ 0 & 0 & -1 & 0 \\ 0 & 0 & 0 & 1 \end{bmatrix} \begin{bmatrix} F_1 \\ F_2 \\ F_3 \\ F_4 \end{bmatrix}$$

from which,

$$\mathbf{T}\text{ (column)} = \begin{bmatrix} -1 & 0 & 0 & 0 \\ 0 & 1 & 0 & 0 \\ 0 & 0 & -1 & 0 \\ 0 & 0 & 0 & 1 \end{bmatrix} \tag{9.9}$$

The expression of the global stiffness matrix for columns, $\mathbf{K}$ (column), can now be obtained by applying the relationship $\mathbf{K} = \mathbf{T}^T\mathbf{kT}$, which yields

$$\mathbf{K}\text{ (column)} = \frac{EI}{L^3}\begin{bmatrix} 12 & -6L & -12 & -6L \\ -6L & 4L^2 & 6L & 2L^2 \\ -12 & 6L & 12 & 6L \\ -6L & 2L^2 & 6L & 4L^2 \end{bmatrix} \tag{9.10}$$

It is important to realize that the assumption of negligibly small axial deformations, as used herein, does not imply that the member axial forces are also negligibly small. As the axial forces do not appear in the member stiffness relations, the application of the matrix stiffness method yields only member end shears and end moments. Once the member end shears are known, the member axial forces can be evaluated by considering the equilibrium of the free bodies of the joints and members of the structure.

EXAMPLE 9.2 Determine the approximate joint displacements, member local end forces, and support reactions for the portal frame shown in Fig. 9.5(a), assuming the members to be inextensible.

SOLUTION *Analytical Model:* See Fig. 9.5(b). The frame has three degrees of freedom—the translation of the girder in the X direction, and the rotations of joints 2 and 3. The six restrained coordinates of the frame are identified by numbers 4 through 9 as usual, as shown in Fig. 9.5(b).

Structure Stiffness Matrix and Fixed-Joint Force Vector: By applying Eq. (9.10) for members 1 and 3, and Eq. (9.7) for member 2, we obtain the following member global stiffness matrices (in units of kips and inches):

$$\begin{array}{l} \text{Member 3} \longrightarrow \quad 7 \quad\quad 9 \quad\quad 1 \quad\quad 3 \\ \text{Member 1} \longrightarrow \quad 4 \quad\quad 6 \quad\quad 1 \quad\quad 2 \end{array}$$

$$\mathbf{K}_1 = \mathbf{K}_3 = \begin{bmatrix} 5.3107 & -955.93 & -5.3107 & -955.93 \\ -955.93 & 229{,}422 & 955.93 & 114{,}711 \\ -5.3107 & 955.93 & 5.3107 & 955.93 \\ -955.93 & 114{,}711 & 955.93 & 229{,}422 \end{bmatrix} \begin{matrix} 4 \\ 6 \\ 1 \\ 2 \end{matrix} \quad \begin{matrix} 7 \\ 9 \\ 1 \\ 3 \end{matrix}$$

$$\mathbf{K}_2 = \mathbf{k}_2 = \mathbf{k}_1 = \mathbf{k}_3 = \begin{array}{c} \begin{matrix} 0 & 2 & 0 & 3 \end{matrix} \\ \begin{bmatrix} 5.3107 & 955.93 & -5.3107 & 955.93 \\ 955.93 & 229{,}422 & -955.93 & 114{,}711 \\ -5.3107 & -955.93 & 5.3107 & -955.93 \\ 955.93 & 114{,}711 & -955.93 & 229{,}422 \end{bmatrix} \end{array} \begin{matrix} 0 \\ 2 \\ 0 \\ 3 \end{matrix} \qquad \textbf{(1)}$$

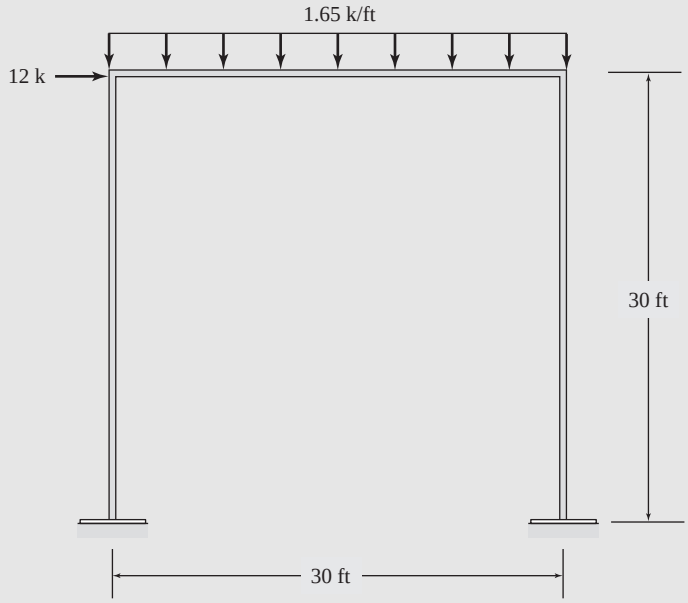

$E, I =$ constant
$E = 29{,}000$ ksi
$I = 712$ in.^{4}

(a) Frame

Fig. 9.5

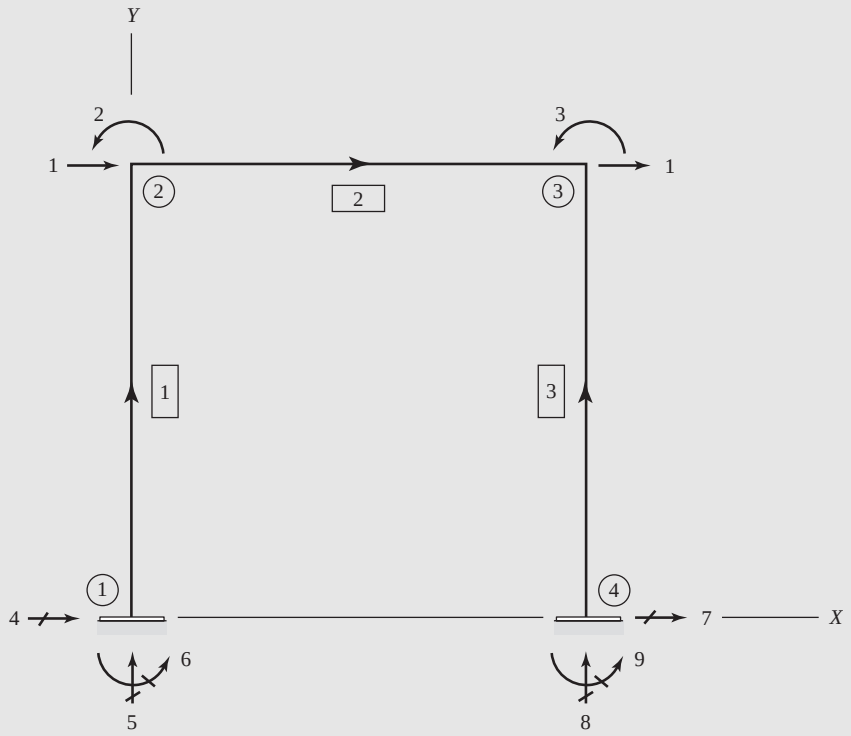

(b) Analytical Model

Fig. 9.5 (*continued*)

From Fig. 9.5(b), we can see that for member 1, the structure coordinates in the directions of the member end shears and end moments are numbered 4, 6, 1, and 2. Thus, the code numbers for this member are 4, 6, 1, 2. Similarly, the code numbers for member 3 are 7, 9, 1, 3. Since the structure coordinates corresponding to the end shears of member 2 are not defined (because the corresponding joint displacements are 0), we use 0s for the corresponding member code numbers. Thus, the code numbers for member 1 are 0, 2, 0, 3. By using the foregoing member code numbers, the relevant elements of $\mathbf{K}_1$, $\mathbf{K}_2$, and $\mathbf{K}_3$ are stored in the 3×3 structure stiffness matrix $\mathbf{S}$. Note that the elements of $\mathbf{K}_2$ that correspond to 0 code numbers are simply disregarded. The structure stiffness matrix thus obtained is

$$\mathbf{S} = \begin{array}{c} \begin{matrix} \quad 1 \quad & \quad 2 \quad & \quad 3 \quad \end{matrix} \\ \begin{bmatrix} 10.621 & 955.93 & 955.93 \\ 955.93 & 458{,}844 & 114{,}711 \\ 955.93 & 114{,}711 & 458{,}844 \end{bmatrix} \end{array} \begin{matrix} 1 \\ 2 \\ 3 \end{matrix} \qquad \textbf{(2)}$$

The fixed-end shears and moments due to the 0.1375 k/in. (= 1.65 k/ft) uniformly distributed load applied to member 2 are calculated as

$$FS_b = FS_e = \frac{wL}{2} = \frac{0.1375(360)}{2} = 24.75 \text{ k}$$

$$FM_b = -FM_e = \frac{wL^2}{12} = \frac{0.1375(360)^2}{12} = 1{,}485 \text{ k-in.}$$

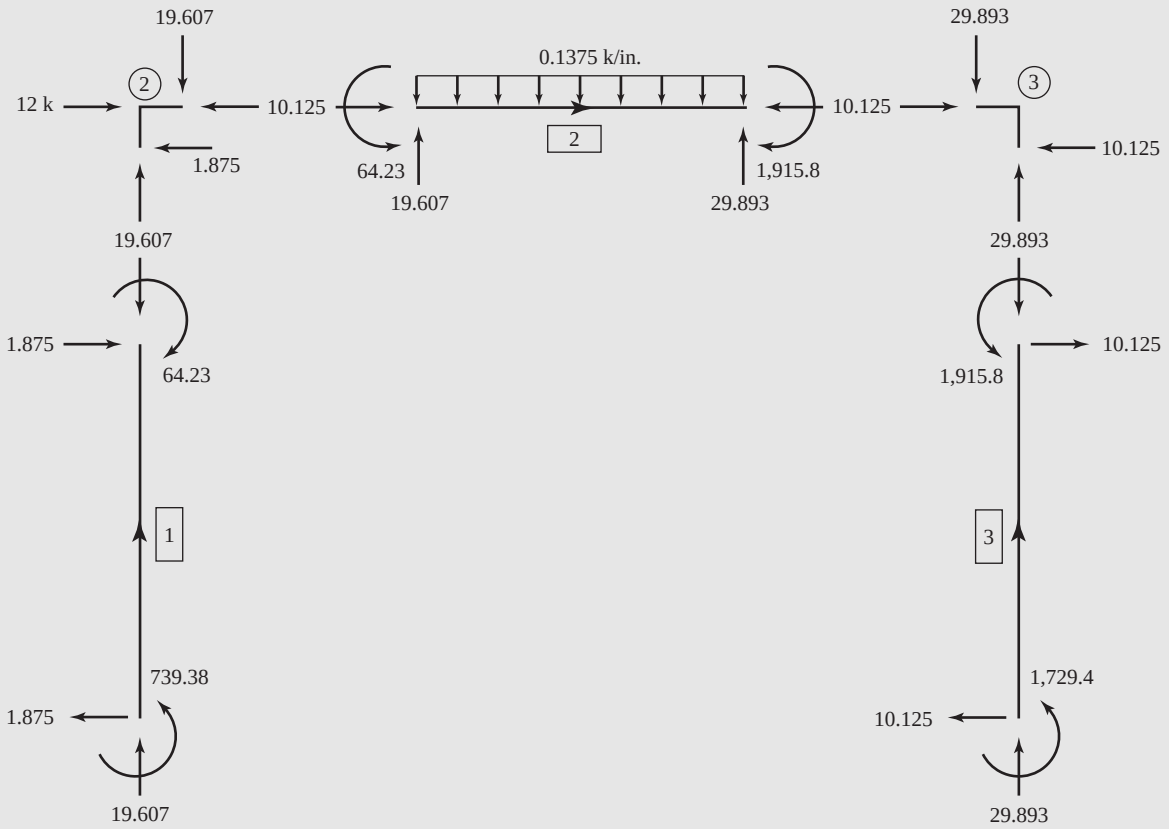

(c) Member End Forces

Fig. 9.5 (*continued*)

Using Eq. (9.8), we obtain

$$\mathbf{F}_{f2} = \mathbf{Q}_{f2} = \begin{bmatrix} 24.75 \\ 1{,}485 \\ 24.75 \\ -1{,}485 \end{bmatrix} \begin{matrix} 0 \\ 2 \\ 0 \\ 3 \end{matrix} \tag{3}$$

Thus, the structure fixed-joint force vector $\mathbf{P}_f$ is given by

$$\mathbf{P}_f = \begin{bmatrix} 0 \\ 1{,}485 \\ -1{,}485 \end{bmatrix} \begin{matrix} 1 \\ 2 \\ 3 \end{matrix} \tag{4}$$

Joint Load Vector:

$$\mathbf{P} = \begin{bmatrix} 12 \\ 0 \\ 0 \end{bmatrix} \begin{matrix} 1 \\ 2 \\ 3 \end{matrix} \tag{5}$$

Joint Displacements: By substituting the numerical values of **S** (Eq. (2)), $\mathbf{P}_f$ (Eq. (4)), and **P** (Eq. (5)) into the structure stiffness relationship $\mathbf{P} - \mathbf{P}_f = \mathbf{Sd}$, and solving

the resulting system of simultaneous equations, we obtain the following joint displacements.

$$\mathbf{d} = \begin{bmatrix} 1.6141 \text{ in.} \\ -0.0070053 \text{ rad} \\ 0.001625 \text{ rad} \end{bmatrix} \begin{matrix} 1 \\ 2 \\ 3 \end{matrix} \quad \textbf{Ans}$$

Member End Shears and End Moments:

Member 1

$$\mathbf{v}_1 = \begin{bmatrix} v_1 \\ v_2 \\ v_3 \\ v_4 \end{bmatrix} \begin{matrix} 4 \\ 6 \\ 1 \\ 2 \end{matrix} = \begin{bmatrix} 0 \\ 0 \\ d_1 \\ d_2 \end{bmatrix} = \begin{bmatrix} 0 \\ 0 \\ 1.6141 \\ -0.0070053 \end{bmatrix}$$

From Eq. (9.9):

$$\mathbf{T}_1 = \mathbf{T}_3 = \begin{bmatrix} -1 & 0 & 0 & 0 \\ 0 & 1 & 0 & 0 \\ 0 & 0 & -1 & 0 \\ 0 & 0 & 0 & 1 \end{bmatrix} \quad \textbf{(6)}$$

$$\mathbf{u}_1 = \mathbf{T}_1\mathbf{v}_1 = \begin{bmatrix} 0 \\ 0 \\ -1.6141 \\ -0.0070053 \end{bmatrix}$$

By using $\mathbf{k}_1$ from Eq. (1) and $\mathbf{Q}_{f1} = \mathbf{0}$, we obtain

$$\mathbf{Q}_1 = \mathbf{k}_1\mathbf{u}_1 = \begin{bmatrix} 1.875 \text{ k} \\ 739.38 \text{ k-in.} \\ -1.875 \text{ k} \\ -64.23 \text{ k-in.} \end{bmatrix} \quad \textbf{Ans}$$

Member 2

$$\mathbf{u}_2 = \mathbf{v}_2 = \begin{bmatrix} 0 \\ -0.0070053 \\ 0 \\ 0.001625 \end{bmatrix} \begin{matrix} 0 \\ 2 \\ 0 \\ 3 \end{matrix}$$

By using $\mathbf{k}_2$ from Eq. (1) and $\mathbf{Q}_{f2}$ from Eq. (3), we calculate

$$\mathbf{Q}_2 = \mathbf{k}_2\mathbf{u}_2 + \mathbf{Q}_{f2} = \begin{bmatrix} 19.607 \text{ k} \\ 64.23 \text{ k-in.} \\ 29.893 \text{ k} \\ -1{,}915.8 \text{ k-in.} \end{bmatrix} \quad \textbf{Ans}$$

Member 3

$$\mathbf{v}_3 = \begin{bmatrix} 0 \\ 0 \\ 1.6141 \\ 0.001625 \end{bmatrix} \begin{matrix} 7 \\ 9 \\ 1 \\ 3 \end{matrix}$$

Using $\mathbf{T}_3$ from Eq. (6), we obtain

$$\mathbf{u}_3 = \mathbf{T}_3\mathbf{v}_3 = \begin{bmatrix} 0 \\ 0 \\ -1.6141 \\ 0.001625 \end{bmatrix}$$

Using $\mathbf{k}_3$ from Eq. (1) and $\mathbf{Q}_{f3} = \mathbf{0}$, we calculate

$$\mathbf{Q}_3 = \mathbf{k}_3\mathbf{u}_3 + \mathbf{Q}_{f3} = \begin{bmatrix} 10.125 \text{ k} \\ 1{,}729.4 \text{ k-in.} \\ -10.125 \text{ k} \\ 1{,}915.8 \text{ k-in.} \end{bmatrix} \quad \textbf{Ans}$$

The member end shears and end moments, as given by the foregoing local end force vectors $\mathbf{Q}_1$, $\mathbf{Q}_2$, and $\mathbf{Q}_3$, are depicted in Fig. 9.5(c).

Member Axial Forces: With the member end shears now known, we can calculate the axial forces for the three members of the frame by applying the equations of equilibrium, $\sum F_X = 0$ and $\sum F_Y = 0$, to the free bodies of joints 2 and 3. The member axial forces thus obtained are shown in Fig. 9.5(c). **Ans**

Support Reactions: By comparing Figs. 9.5(b) and (c), we realize that the forces at the lower ends of the columns of the frame represent its support reactions; that is,

$$\mathbf{R} = \begin{bmatrix} -1.875 \text{ k} \\ 19.607 \text{ k} \\ 739.38 \text{ k-in.} \\ -10.125 \text{ k} \\ 29.893 \text{ k} \\ 1{,}729.4 \text{ k-in.} \end{bmatrix} \begin{matrix} 4 \\ 5 \\ 6 \\ 7 \\ 8 \\ 9 \end{matrix} \quad \textbf{Ans}$$

9.3 CONDENSATION OF DEGREES OF FREEDOM, AND SUBSTRUCTURING

A problem that can arise during computer analysis of large structures is that the computer may not have sufficient memory to store and process information about the entire structure. A commonly used approach to circumvent this problem is to *condense* (or reduce the number of) the structure's stiffness equations that are to be solved simultaneously, by suppressing some of the degrees of freedom. This process is referred to as *condensation* (also called *static condensation*). For very large structures, it may become necessary to combine condensation with another process called *substructuring,* in which the structure is divided into parts called *substructures,* with the condensed stiffness relations for each substructure generated separately; these are then combined to obtain the stiffness relations for the entire structure. In this section, we consider the basic concepts of condensation of degrees of freedom, and analysis using substructures.

Condensation

The objective of condensation is to reduce the number of independent degrees of freedom of a structure (or substructure, or member). This is achieved by treating some of the degrees of freedom as dependent variables and expressing them in terms of the remaining independent degrees of freedom. The relationship between the dependent and independent degrees of freedom is then substituted into the original stiffness relations to obtain a condensed system of stiffness equations, which contains only the independent degrees of freedom as unknowns. From a theoretical viewpoint, the dependent degrees of freedom can be chosen arbitrarily. However, for computational purposes, it is usually convenient to select those degrees of freedom that are internal to the structure (or substructure, or member) as the dependent degrees of freedom. Hence, the dependent degrees of freedom are commonly referred to as the *internal degrees of freedom;* whereas, the independent degrees of freedom are called the *external degrees of freedom*.

As discussed in the preceding chapters, the stiffness relations for a general framed structure can be expressed as (see, for example, Eq. (6.42))

$$\overline{\mathbf{P}} = \mathbf{S}\mathbf{d} \tag{9.11}$$

with

$$\overline{\mathbf{P}} = \mathbf{P} - \mathbf{P}_f \tag{9.12}$$

When using the condensation process, it is usually convenient to assign numbers to the degrees of freedom so that the external and internal degrees of freedom are separated into two groups. The structure stiffness relations (Eq. (9.11)) can then be written in partitioned-matrix form:

$$\left[\begin{array}{c} \overline{\mathbf{P}}_E \\ \hdashline \overline{\mathbf{P}}_I \end{array}\right] = \left[\begin{array}{c:c} \mathbf{S}_{EE} & \mathbf{S}_{EI} \\ \hdashline \mathbf{S}_{IE} & \mathbf{S}_{II} \end{array}\right] \left[\begin{array}{c} \mathbf{d}_E \\ \hdashline \mathbf{d}_I \end{array}\right] \tag{9.13}$$

in which the subscripts E and I refer to quantities related to the external and internal degrees of freedom, respectively. By multiplying the two partitioned matrices on the right side of Eq. (9.13), we obtain the two matrix equations,

$$\overline{\mathbf{P}}_E = \mathbf{S}_{EE}\mathbf{d}_E + \mathbf{S}_{EI}\mathbf{d}_I \tag{9.14}$$

$$\overline{\mathbf{P}}_I = \mathbf{S}_{IE}\mathbf{d}_E + \mathbf{S}_{II}\mathbf{d}_I \tag{9.15}$$

To express the internal degrees of freedom $\mathbf{d}_I$ in terms of the external degrees of freedom $\mathbf{d}_E$, we solve Eq. (9.15) for $\mathbf{d}_I$, as

$$\boxed{\mathbf{d}_I = \mathbf{S}_{II}^{-1}(\overline{\mathbf{P}}_I - \mathbf{S}_{IE}\mathbf{d}_E)} \tag{9.16}$$

Finally, by substituting Eq. (9.16) into Eq. (9.14), we obtain the condensed stiffness equations

$$\overline{\mathbf{P}}_E - \mathbf{S}_{EI}\mathbf{S}_{II}^{-1}\overline{\mathbf{P}}_I = (\mathbf{S}_{EE} - \mathbf{S}_{EI}\mathbf{S}_{II}^{-1}\mathbf{S}_{IE})\mathbf{d}_E \tag{9.17}$$

Note that the external degrees of freedom $\mathbf{d}_E$ are the only unknowns in Eq. (9.17). Equation (9.17) can be rewritten in a compact form as

$$\boxed{\mathbf{P}_E^* = \mathbf{S}_{EE}^* \mathbf{d}_E} \tag{9.18}$$

in which,

$$\boxed{\mathbf{P}_E^* = \overline{\mathbf{P}}_E - \mathbf{S}_{EI}\mathbf{S}_{II}^{-1}\overline{\mathbf{P}}_I} \tag{9.19}$$

and

$$\boxed{\mathbf{S}_{EE}^* = \mathbf{S}_{EE} - \mathbf{S}_{EI}\mathbf{S}_{II}^{-1}\mathbf{S}_{IE}} \tag{9.20}$$

As the foregoing equations indicate, the solution of the structure stiffness equations is carried out in two parts. In the first part, $\mathbf{P}_E^*$ and $\mathbf{S}_{EE}^*$ are evaluated using Eqs. (9.19) and (9.20), respectively, and the external joint displacements $\mathbf{d}_E$ are determined by solving Eq. (9.18). In the second part, the now-known $\mathbf{d}_E$ is substituted into Eq. (9.16) to obtain the internal joint displacements $\mathbf{d}_I$. Once all the joint displacements have been evaluated, the member end displacements and end forces, and support reactions, can be calculated using the procedures described in the previous chapters.

It should be realized that analysis involving condensation generally requires more computational effort than the standard formulation in which all of the structure's stiffness equations are solved simultaneously. However, condensation provides a useful means of analyzing large structures whose full stiffness matrices and load vectors exceed the available computer memory. This is because, when employing condensation, only parts of $\mathbf{S}$ and $\overline{\mathbf{P}}$ need to be assembled and processed in the computer memory at a given time. The basic concept of condensation is illustrated by the following relatively simple example.

EXAMPLE 9.3 Analyze the plane frame shown in Fig. 9.6(a) using condensation, by treating the rotation of the free joint as the internal degree of freedom.

SOLUTION This frame was analyzed in Example 6.6 using the standard formulation. The analytical model of the structure is given in Fig. 9.6(b).

Condensed Structure Stiffness Matrix: The full (3×3) stiffness matrix, $\mathbf{S}$, for the frame, as determined in Example 6.6, is given by (in units of kips and inches):

$$\mathbf{S} = \begin{array}{c} \begin{matrix} \quad 1 \quad & \quad 2 \quad & \quad 3 \quad \end{matrix} \\ \left[\begin{array}{ccc:c} 1{,}685.3 & 507.89 & 670.08 & 1 \\ 507.89 & 1{,}029.2 & 601.42 & 2 \\ \hdashline 670.08 & 601.42 & 283{,}848 & 3 \end{array}\right] \end{array} \tag{1}$$

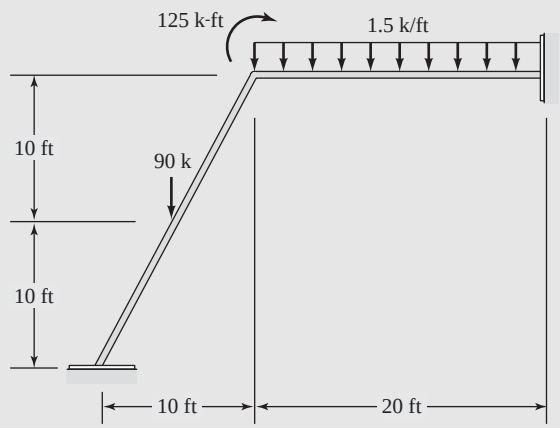

E, A, I = constant
$E = 29{,}000$ ksi
$A = 11.8$ in.^{2}
$I = 310$ in.^{4}

(a) Frame

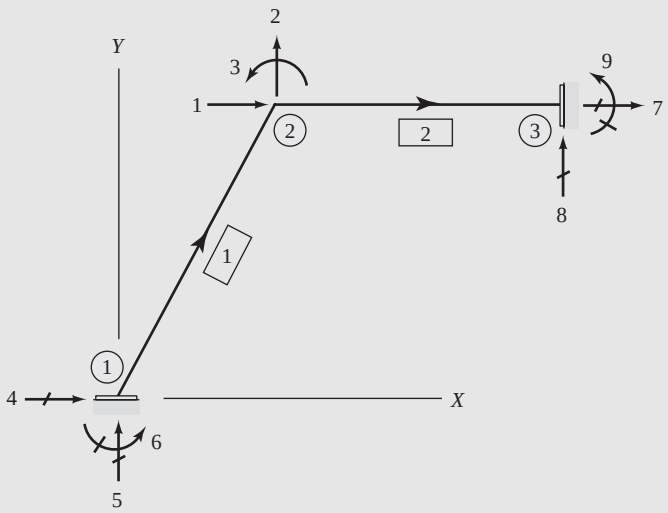

(b) Analytical Model

Fig. 9.6

in which **S** is partitioned to separate the external degrees of freedom, 1 and 2, from the internal degree of freedom, 3. From Eq. (1), we obtain

$$\mathbf{S}_{EE} = \begin{matrix} \\ 1 \\ 2 \end{matrix} \begin{matrix} \begin{matrix} 1 & 2 \end{matrix} \\ \begin{bmatrix} 1{,}685.3 & 507.89 \\ 507.89 & 1{,}029.2 \end{bmatrix} \end{matrix} \quad \textbf{(2)}$$

$$\mathbf{S}_{IE} = \begin{matrix} \begin{matrix} 1 & 2 \end{matrix} \\ \begin{bmatrix} 670.08 & 601.42 \end{bmatrix} \end{matrix} \begin{matrix} \\ 3 \end{matrix} \quad \textbf{(3)}$$

$$\mathbf{S}_{EI} = \begin{matrix} \\ \\ \end{matrix}\begin{matrix} 3 \\ \left[\begin{matrix} 670.08 \\ 601.42 \end{matrix}\right] \end{matrix}\begin{matrix} \\ 1 \\ 2 \end{matrix} \tag{4}$$

$$\mathbf{S}_{II} = \begin{matrix} 3 \\ [283{,}848] \end{matrix}\begin{matrix} \\ 3 \end{matrix} \tag{5}$$

with the inverse of $\mathbf{S}_{II}$ given by

$$\mathbf{S}_{II}^{-1} = \left[\frac{1}{283{,}848}\right] \tag{6}$$

By substituting Eqs. (2), (3), (4), and (6) into Eq. (9.20), we obtain the condensed structure stiffness matrix:

$$\mathbf{S}_{EE}^{*} = \mathbf{S}_{EE} - \mathbf{S}_{EI}\mathbf{S}_{II}^{-1}\mathbf{S}_{IE} = \begin{bmatrix} 1{,}683.7 & 506.47 \\ 506.47 & 1{,}027.9 \end{bmatrix} \text{ k/in.} \tag{7}$$

Condensed Joint Load Vector: Recall from Example 6.6 that

$$\overline{\mathbf{P}} = \mathbf{P} - \mathbf{P}_f = \begin{matrix} \left[\begin{matrix} 0 \\ -60 \\ \hdashline -750 \end{matrix}\right] \end{matrix}\begin{matrix} \\ 1 \\ 2 \\ \\ 3 \end{matrix} \tag{8}$$

from which,

$$\overline{\mathbf{P}}_E = \begin{matrix} \left[\begin{matrix} 0 \\ -60 \end{matrix}\right] \end{matrix}\begin{matrix} \\ 1 \\ 2 \end{matrix} \tag{9}$$

and

$$\overline{\mathbf{P}}_I = \begin{matrix} [-750] \end{matrix}\begin{matrix} \\ 3 \end{matrix} \tag{10}$$

Substitution of Eqs. (4), (6), (9), and (10) into Eq. (9.19) yields the following condensed joint load vector.

$$\mathbf{P}_E^{*} = \overline{\mathbf{P}}_E - \mathbf{S}_{EI}\mathbf{S}_{II}^{-1}\overline{\mathbf{P}}_I = \begin{bmatrix} 1.7705 \\ -58.411 \end{bmatrix} \text{ k} \tag{11}$$

Joint Displacements: By substituting Eqs. (7) and (11) into the condensed structure stiffness relationship, $\mathbf{P}_E^{*} = \mathbf{S}_{EE}^{*}\mathbf{d}_E$ (Eq. (9.18)), and solving the resulting 2×2 system of simultaneous equations, we obtain the external joint displacements (corresponding to degrees of freedom 1 and 2), as

$$\mathbf{d}_E = \begin{matrix} \left[\begin{matrix} 0.021302 \\ -0.06732 \end{matrix}\right] \end{matrix}\begin{matrix} \\ 1 \\ 2 \end{matrix} \text{ in.} \tag{12}$$

The internal joint displacement (i.e., the rotation corresponding to degree of freedom 3), can now be determined by applying Eq. (9.16). Thus,

$$\mathbf{d}_I = \mathbf{S}_{II}^{-1}(\overline{\mathbf{P}}_I - \mathbf{S}_{IE}\mathbf{d}_E) = [-0.0025499]3 \text{ rad} \tag{13}$$

By combining Eqs. (12) and (13), we obtain the full joint displacement vector,

$$\mathbf{d} = \begin{bmatrix} \mathbf{d}_E \\ \hdashline \mathbf{d}_I \end{bmatrix} = \begin{matrix} \left[\begin{matrix} 0.021302 \text{ in.} \\ -0.06732 \text{ in.} \\ \hdashline -0.0025499 \text{ rad} \end{matrix}\right] \end{matrix}\begin{matrix} \\ 1 \\ 2 \\ \\ 3 \end{matrix} \quad \textbf{Ans}$$

Note that the foregoing joint displacements are identical to those determined in Example 6.6 by solving the structure's three stiffness equations simultaneously.

Member End Displacements and End Forces: See Example 6.6.

It is important to realize that, in this example, the submatrices of $\mathbf{S}$ and $\overline{\mathbf{P}}$ were obtained from the corresponding full matrices, for convenience only. In actual computer analysis, to save memory space, the individual parts of $\mathbf{S}$ and $\overline{\mathbf{P}}$ are assembled directly from the corresponding member matrices as they are needed in the analysis.

In the foregoing paragraphs, we have discussed the application of condensation to reduce the number of independent degrees of freedom of an entire structure. The condensation process is also frequently used to establish the stiffness relationships for substructures, which are defined as groups of members with known stiffness relations. In this case, condensation is used to eliminate the degrees of freedom of those joints that are internal to the substructure, thereby producing a condensed system of stiffness relations expressed solely in terms of the degrees of freedom of those (external) joints through which the substructure is connected to the rest of the structure and/or supports.

The procedure for condensing the internal degrees of freedom of a substructure is analogous to that just discussed for the case of a whole structure. The stiffness relations involving both the internal and external degrees of freedom of a substructure can be symbolically expressed as

$$\overline{\mathbf{F}} = \overline{\mathbf{K}}\bar{\mathbf{v}} + \overline{\mathbf{F}}_f \tag{9.21}$$

in which $\overline{\mathbf{F}}$ and $\bar{\mathbf{v}}$ represent, respectively, the joint forces and displacements for the substructure; $\overline{\mathbf{K}}$ denotes the substructure stiffness matrix; and $\overline{\mathbf{F}}_f$ represents the fixed-joint forces for the substructure. The matrix $\overline{\mathbf{K}}$ and the vector $\overline{\mathbf{F}}_f$ can be assembled from the member stiffness matrices and fixed-end force vectors in the usual way. To apply condensation, we rewrite Eq. (9.21) in partitioned-matrix form as

$$\left[\begin{array}{c} \overline{\mathbf{F}}_E \\ \hdashline \overline{\mathbf{F}}_I \end{array}\right] = \left[\begin{array}{c:c} \overline{\mathbf{K}}_{EE} & \overline{\mathbf{K}}_{EI} \\ \hdashline \overline{\mathbf{K}}_{IE} & \overline{\mathbf{K}}_{II} \end{array}\right] \left[\begin{array}{c} \bar{\mathbf{v}}_E \\ \hdashline \bar{\mathbf{v}}_I \end{array}\right] + \left[\begin{array}{c} \overline{\mathbf{F}}_{fE} \\ \hdashline \overline{\mathbf{F}}_{fI} \end{array}\right] \tag{9.22}$$

The multiplication of the two partitioned matrices on the right-hand side of Eq. (9.22) yields the matrix equations

$$\overline{\mathbf{F}}_E = \overline{\mathbf{K}}_{EE}\bar{\mathbf{v}}_E + \overline{\mathbf{K}}_{EI}\bar{\mathbf{v}}_I + \overline{\mathbf{F}}_{fE} \tag{9.23}$$

$$\overline{\mathbf{F}}_I = \overline{\mathbf{K}}_{IE}\bar{\mathbf{v}}_E + \overline{\mathbf{K}}_{II}\bar{\mathbf{v}}_I + \overline{\mathbf{F}}_{fI} \tag{9.24}$$

Solving Eq. (9.24) for $\bar{\mathbf{v}}_I$, we obtain

$$\boxed{\bar{\mathbf{v}}_I = \overline{\mathbf{K}}_{II}^{-1}(\overline{\mathbf{F}}_I - \overline{\mathbf{F}}_{fI} - \overline{\mathbf{K}}_{IE}\bar{\mathbf{v}}_E)} \tag{9.25}$$

and, substituting Eq. (9.25) into Eq. (9.23), we determine the condensed stiffness relations for the substructure to be

$$\boxed{\overline{\mathbf{F}}_E = \overline{\mathbf{K}}_{EE}^{*}\bar{\mathbf{v}}_E + \overline{\mathbf{F}}_{fE}^{*}} \tag{9.26}$$

in which,

$$\overline{\mathbf{K}}^{*}_{EE} = \overline{\mathbf{K}}_{EE} - \overline{\mathbf{K}}_{EI}\overline{\mathbf{K}}^{-1}_{II}\overline{\mathbf{K}}_{IE} \tag{9.27}$$

and

$$\overline{\mathbf{F}}^{*}_{fE} = \overline{\mathbf{F}}_{fE} + \overline{\mathbf{K}}_{EI}\overline{\mathbf{K}}^{-1}_{II}\left(\overline{\mathbf{F}}_{I} - \overline{\mathbf{F}}_{fI}\right) \tag{9.28}$$

EXAMPLE 9.4 Determine the stiffness matrix and the fixed-joint force vector for the substructure of a beam shown in Fig. 9.7(a), in terms of its external degrees of freedom only. The substructure is composed of two members connected together by a hinged joint, as shown in the figure.

SOLUTION *Analytical Model:* The analytical model of the substructure is depicted in Fig. 9.7(b). For member 1, $MT = 2$, because the end of this member is hinged; $MT = 1$ for member 2, which is hinged at its beginning. Joint 3 is modeled as a hinged joint with its rotation restrained by an imaginary clamp. Thus, the substructure has a total of five degrees of freedom, of which four are external (identified by numbers 1 through 4) and one is internal (identified by number 5).

Substructure Stiffness Matrix: We will first assemble the full (5×5) stiffness matrix $\overline{\mathbf{K}}$ from the member stiffness matrices $\mathbf{k}$, and then apply Eq. (9.27) to determine the condensed stiffness matrix $\overline{\mathbf{K}}^{*}_{EE}$.

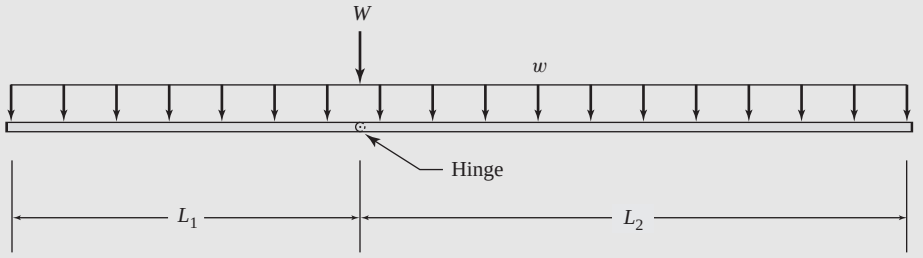

$E, I =$ constant

(a) Substructure

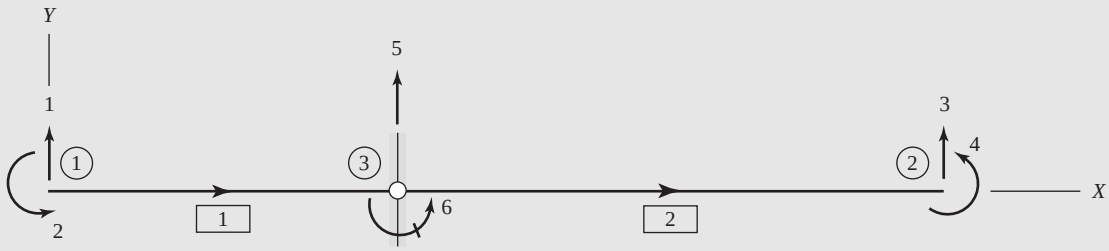

(b) Analytical Model

Fig. 9.7

$$\overline{\mathbf{K}} = \left[\begin{array}{c|c} \overline{\mathbf{K}}_{EE} & \overline{\mathbf{K}}_{EI} \\ \hline \overline{\mathbf{K}}_{IE} & \overline{\mathbf{K}}_{II} \end{array}\right] = 3EI \begin{array}{c} \\ \\ \\ \\ \\ \end{array} \begin{array}{c} \begin{array}{ccccc} 1 & 2 & 3 & 4 & 5 \end{array} \\ \left[\begin{array}{cccc:c} \frac{1}{L_1^3} & \frac{1}{L_1^2} & 0 & 0 & -\frac{1}{L_1^3} \\ \frac{1}{L_1^2} & \frac{1}{L_1} & 0 & 0 & -\frac{1}{L_1^2} \\ 0 & 0 & \frac{1}{L_2^3} & -\frac{1}{L_2^2} & -\frac{1}{L_2^3} \\ 0 & 0 & -\frac{1}{L_2^2} & \frac{1}{L_2} & \frac{1}{L_2^2} \\ \hdashline -\frac{1}{L_1^3} & -\frac{1}{L_1^2} & -\frac{1}{L_2^3} & \frac{1}{L_2^2} & \frac{1}{L_1^3}+\frac{1}{L_2^3} \end{array}\right] \begin{array}{c} 1 \\ 2 \\ 3 \\ 4 \\ 5 \end{array} \end{array}$$

(c) Full (Uncondensed) Stiffness Matrix for Substructure

$$\overline{\mathbf{F}}_f = \left[\begin{array}{c} \overline{\mathbf{F}}_{fE} \\ \hdashline \overline{\mathbf{F}}_{fI} \end{array}\right] = \frac{w}{8} \begin{array}{c} \left[\begin{array}{c} 5L_1 \\ L_1^2 \\ 5L_2 \\ -L_2^2 \\ \hdashline 3L_1+3L_2 \end{array}\right] \begin{array}{c} 1 \\ 2 \\ 3 \\ 4 \\ 5 \end{array} \end{array}$$

(d) Full (Uncondensed) Fixed-Joint Force Vector For Substructure

Fig. 9.7 (*continued*)

Member 1 ($MT = 2$) Using Eq. (7.18), we obtain

$$\mathbf{k}_1 = \frac{3EI}{L_1^3} \begin{array}{c} \begin{array}{cccc} 1 & 2 & 5 & 6 \end{array} \\ \left[\begin{array}{cccc} 1 & L_1 & -1 & 0 \\ L_1 & L_1^2 & -L_1 & 0 \\ -1 & -L_1 & 1 & 0 \\ 0 & 0 & 0 & 0 \end{array}\right] \begin{array}{c} 1 \\ 2 \\ 5 \\ 6 \end{array} \end{array}$$

Member 2 ($MT = 1$) Application of Eq. (7.15) yields

$$\mathbf{k}_2 = \frac{3EI}{L_2^3} \begin{array}{c} \begin{array}{cccc} 5 & 6 & 3 & 4 \end{array} \\ \left[\begin{array}{cccc} 1 & 0 & -1 & L_2 \\ 0 & 0 & 0 & 0 \\ -1 & 0 & 1 & -L_2 \\ L_2 & 0 & -L_2 & L_2^2 \end{array}\right] \begin{array}{c} 5 \\ 6 \\ 3 \\ 4 \end{array} \end{array}$$

Using the code numbers of the members, we store the pertinent elements of $\mathbf{k}_1$ and $\mathbf{k}_2$ in the full 5×5 stiffness matrix $\overline{\mathbf{K}}$ of the substructure, as shown in Fig. 9.7(c).

Substituting into Eq. (9.27) the appropriate submatrices of $\overline{\mathbf{K}}$ from Fig. 9.7(c) and

$$\overline{\mathbf{K}}_{II}^{-1} = \left[\frac{L_1^3 L_2^3}{3EI(L_1^3 + L_2^3)}\right] \tag{1}$$

we obtain the condensed stiffness matrix for the substructure:

$$\overline{\mathbf{K}}_{EE}^{*} = \overline{\mathbf{K}}_{EE} - \overline{\mathbf{K}}_{EI}\overline{\mathbf{K}}_{II}^{-1}\overline{\mathbf{K}}_{IE} = \frac{3EI}{L_1^3 + L_2^3} \left[\begin{array}{cccc} 1 & L_1 & -1 & L_2 \\ L_1 & L_1^2 & -L_1 & L_1L_2 \\ -1 & -L_1 & 1 & -L_2 \\ L_2 & L_1L_2 & -L_2 & L_2^2 \end{array}\right] \tag{2}$$

Ans

Substructure Fixed-Joint Force Vector:

Member 1 ($MT = 2$) Using Eq. (7.19), we obtain

$$\mathbf{Q}_{f1} = \frac{wL_1}{8} \begin{array}{c} \left[\begin{array}{c} 5 \\ L_1 \\ 3 \\ 0 \end{array}\right] \begin{array}{c} 1 \\ 2 \\ 5 \\ 6 \end{array} \end{array}$$

Member 2 ($MT = 1$) Using Eq. (7.16), we write

$$\mathbf{Q}_{f2} = \frac{wL_2}{8}\begin{bmatrix} 3 \\ 0 \\ 5 \\ -L_2 \end{bmatrix}\begin{matrix} 5 \\ 6 \\ 3 \\ 4 \end{matrix}$$

The relevant elements of $\mathbf{Q}_{f1}$ and $\mathbf{Q}_{f2}$ are stored in the full 5×1 fixed-joint force vector $\overline{\mathbf{F}}_f$ of the substructure, as shown in Fig. 9.7(d).

A comparison of Figs. 9.7(a) and (b) indicates that $\overline{F}_5 = -W$; that is,

$$\overline{\mathbf{F}}_I = [\overline{F}_5] = [-W] \tag{3}$$

Finally, the application of Eq. (9.28) yields the following condensed fixed-joint force vector for the substructure.

$$\overline{\mathbf{F}}^*_{fE} = \overline{\mathbf{F}}_{fE} + \overline{\mathbf{K}}_{EI}\overline{\mathbf{K}}^{-1}_{II}(\overline{\mathbf{F}}_I - \overline{\mathbf{F}}_{fI})$$

$$= \frac{w}{8(L_1^3 + L_2^3)}\begin{bmatrix} 5L_1^4 + 8L_1L_2^3 + 3L_2^4 \\ L_1^5 + 4L_1^2L_2^3 + 3L_1L_2^4 \\ 3L_1^4 + 8L_1^3L_2 + 5L_2^4 \\ -(3L_1^4L_2 + 4L_1^3L_2^2 + L_2^5) \end{bmatrix} - \frac{W}{L_1^3 + L_2^3}\begin{bmatrix} -L_2^3 \\ -L_1L_2^3 \\ -L_1^3 \\ L_1^3L_2 \end{bmatrix} \tag{4}$$ **Ans**

Analysis Using Substructures

The procedure for the analysis of (large) structures, divided into substructures, is essentially the same as the standard stiffness method developed in previous chapters. However, each substructure is treated as an ordinary member of the structure, and the degrees of freedom of only those joints through which the substructures are connected to each other and/or to supports are considered to be the structure's degrees of freedom **d**. The structure's stiffness matrix **S** and fixed-joint force vector $\mathbf{P}_f$, are assembled, respectively, from the substructure stiffness matrices $\overline{\mathbf{K}}^*_{EE}$ and fixed-joint force vectors $\overline{\mathbf{F}}^*_{fE}$, which are expressed in terms of the external coordinates of the substructures only. The structure stiffness equations, $\mathbf{P} - \mathbf{P}_f = \mathbf{Sd}$, thus obtained, can then be solved for the joint displacements **d**.

Consider, for example, the nine-story plane frame shown in Fig. 9.8(a). The frame actually has 20 joints and 54 degrees of freedom; that is, if we were to analyze the frame using the standard stiffness method for plane frames as developed in Chapter 6, we would have to assemble and solve 54 structure stiffness equations simultaneously. Now, suppose that we wish to analyze the frame by dividing it into three substructures, each consisting of three stories of the frame, as depicted in Fig. 9.8(b). As this figure indicates, for analysis purposes, the frame is now modeled as having only six joints, at which the three substructures are connected to each other and to external supports. Thus, the analytical model of the frame has 12 degrees of freedom and six restrained coordinates.

To develop the stiffness matrix **S** and the fixed-joint force vector $\mathbf{P}_f$ for the frame, we first determine the substructure stiffness matrices $\overline{\mathbf{K}}^*_{EE}$ and fixed-joint

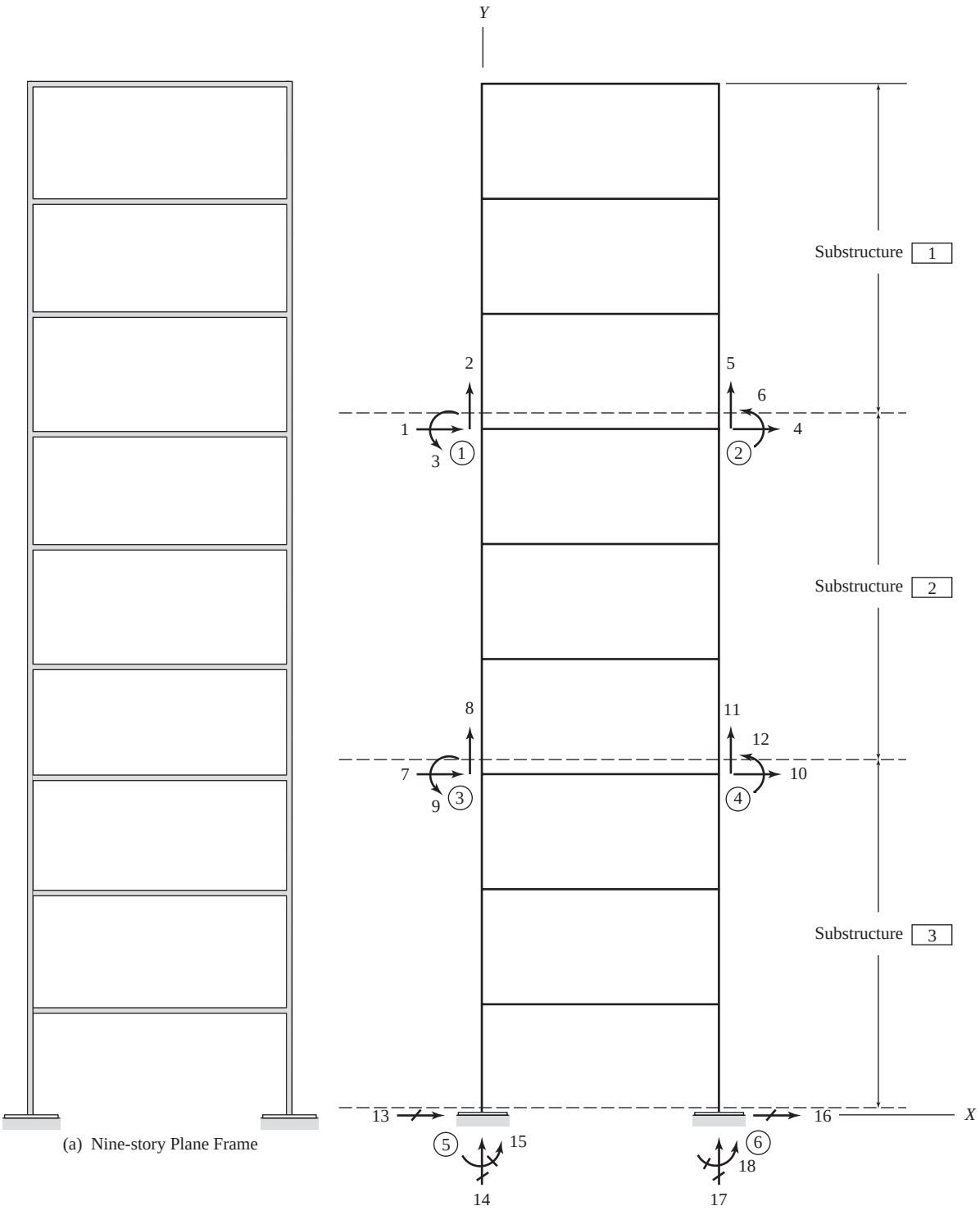

(a) Nine-story Plane Frame

(b) Analytical Model of Frame Divided into Three Substructures

Fig. 9.8

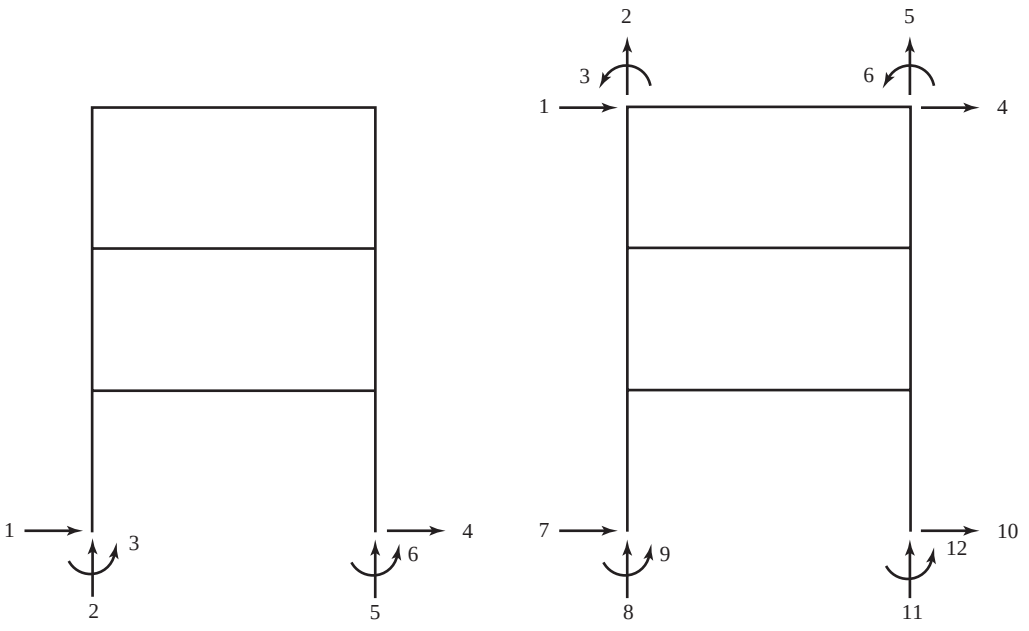

(c) External Degrees of Freedom of Substructures

Fig. 9.8 (*continued*)

force vectors $\overline{\mathbf{F}}^*_{fE}$, in terms of the external degrees of freedom of the substructures, using condensation as described earlier in this section. As shown in Fig. 9.8(c), substructure 1 has six external degrees of freedom; whereas, substructures 2 and 3 each have 12 external degrees of freedom. The pertinent elements of $\overline{\mathbf{K}}^*_{EE}$ matrices and $\overline{\mathbf{F}}^*_{fE}$ vectors are then stored in $\mathbf{S}$ and $\mathbf{P}_f$, respectively, using the substructure code numbers in the usual manner. By comparing Figs. 9.8(b) and (c), we can see that the code numbers for substructure 1 are 1, 2, 3, 4, 5, 6; whereas, the code numbers for substructure 2 are 1, 2, 3, 4, 5, 6, 7, 8, 9, 10, 11, 12. Similarly, for substructure 3, the code numbers are 7, 8, 9, 10, 11, 12, 13, 14, 15, 16, 17, 18.

Once the structure stiffness matrix $\mathbf{S}$ (12×12) and the fixed-joint force vector $\mathbf{P}_f$ (12×1) have been assembled, the structure stiffness equations, $\mathbf{P} - \mathbf{P}_f = \mathbf{Sd}$, are solved to calculate the joint displacement vector $\mathbf{d}$. With $\mathbf{d}$ known, the external joint displacements, $\bar{\mathbf{v}}_E$, for each substructure are obtained from $\mathbf{d}$ using the substructure's code numbers, and then the substructure's internal joint displacements, $\bar{\mathbf{v}}_I$, are calculated using Eq. (9.25). After the joint displacement vector $\bar{\mathbf{v}}$ of a substructure has been determined, the end displacements and forces for its individual members, and support reactions, can be evaluated using the standard procedure described in previous chapters. The basic concept of analysis using substructures is illustrated by the following relatively simple example.

EXAMPLE 9.5 Analyze the two-span continuous beam shown in Fig. 9.9(a), treating each span as a substructure.

SOLUTION *Analytical Model:* The structure is modeled as being composed of two substructures and three joints, as shown in Fig. 9.9(b). It has one degree of freedom and five restrained coordinates. As each substructure consists of two beam members connected together by a hinged joint, we will use the expressions of stiffnesses and fixed-joint forces for such substructures, derived in Example 9.4, in the present example.

Structure Stiffness Matrix, **S***:* Substituting $E = 70(10^6)$ kN/m^2, $I = 200(10^{-6})$ m^4, and $L_1 = L_2 = 5$ m into Eq. (2) of Example 9.4, we obtain the following condensed stiffness matrix for the two substructures.

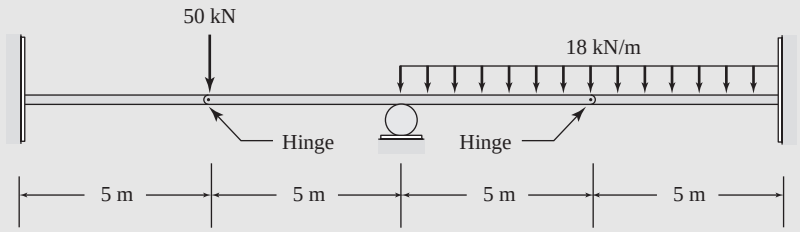

EI = constant
$E = 70$ GPa
$I = 200(10^6)\,\text{mm}^4$

(a) Beam

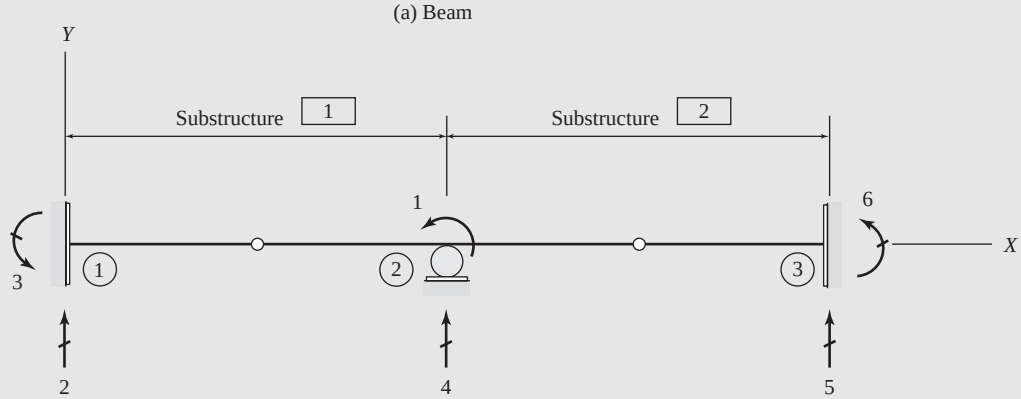

(b) Analytical Model of Beam Divided into Two Substructures

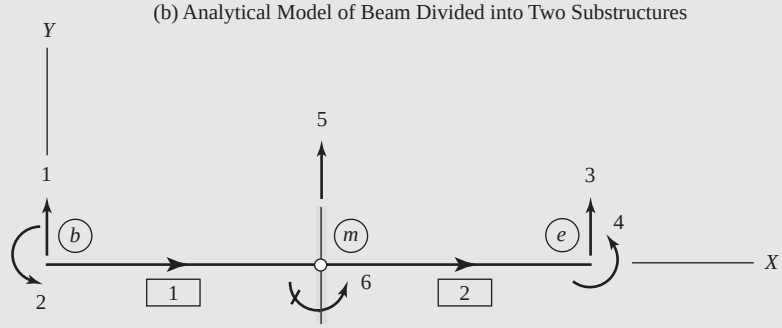

(c) Analytical Model of a Substructure Composed of Two Beam Members

Fig. 9.9

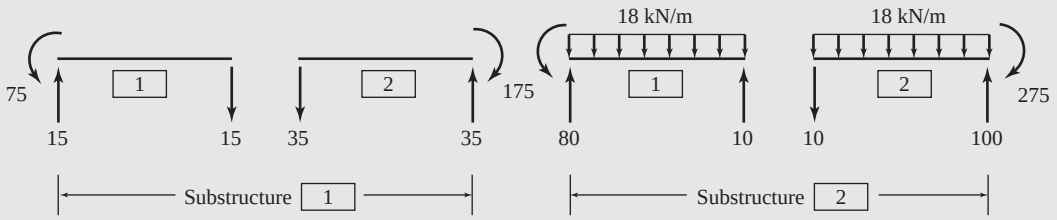

(d) Member End Forces

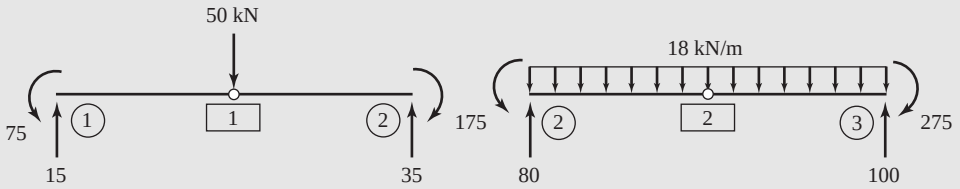

(e) Substructure Forces

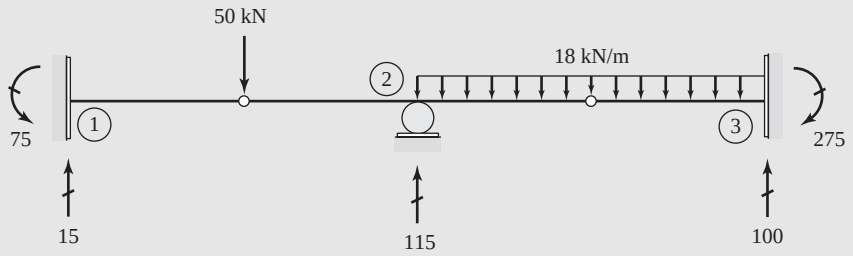

(f) Support Reactions

Fig. 9.9 (*continued*)

$$\begin{array}{l}\text{Substructure 2} \longrightarrow \quad 4 \quad 1 \quad 5 \quad 6 \\ \text{Substructure 1} \longrightarrow \quad 2 \quad 3 \quad 4 \quad 1\end{array}$$

$$\overline{\mathbf{K}}^*_{EE1} = \overline{\mathbf{K}}^*_{EE2} = \left[\begin{array}{cccc|cc} 168 & 840 & -168 & 840 & 2 & 4 \\ 840 & 4{,}200 & -840 & 4{,}200 & 3 & 1 \\ -168 & -840 & 168 & -840 & 4 & 5 \\ 840 & 4{,}200 & -840 & 4{,}200 & 1 & 6 \end{array}\right]$$

By comparing the numbers of the external degrees of freedom of a substructure (Fig. 9.9(c)) to those of the structure degrees of freedom (Fig. 9.9(b)), we obtain code numbers 2, 3, 4, 1 for substructure 1, and 4, 1, 5, 6 for substructure 2. By adding the pertinent elements of $\overline{\mathbf{K}}^*_{EE1}$ and $\overline{\mathbf{K}}^*_{EE2}$, we determine the structure stiffness matrix **S** to be

$$\begin{array}{c} \quad 1 \\ \mathbf{S} = [8{,}400] \begin{array}{l} 1 \end{array} \end{array} \text{ kN} \cdot \text{m/rad}$$

Structure Fixed-Joint Force Vector $\mathbf{P}_f$ *:*

Substructure 1 By substituting $w = 0$, $W = 50$ kN, and $L_1 = L_2 = 5$ m into Eq. (4) of Example 9.4, we obtain the following condensed fixed-joint force vector for substructure 1.

$$\overline{\mathbf{F}}^*_{fE1} = \left[\begin{array}{c|c} 25 & 2 \\ 125 & 3 \\ 25 & 4 \\ -125 & 1 \end{array}\right]$$

Substructure 2 By substituting $w = 18$ kN/m, $W = 0$, and $L_1 = L_2 = 5$ m into Eq. (4) of Example 9.4, we obtain

$$\overline{\mathbf{F}}^*_{fE2} = \begin{bmatrix} 90 \\ 225 \\ 90 \\ -225 \end{bmatrix} \begin{matrix} 4 \\ 1 \\ 5 \\ 6 \end{matrix}$$

Thus, the fixed-joint force vector for the whole structure is given by

$$\mathbf{P}_f = [100] \text{ 1 kN} \cdot \text{m}$$

Joint Displacements: By substituting $\mathbf{P} = \mathbf{0}$ and the numerical values of $\mathbf{S}$ and $\mathbf{P}_f$ into the structure stiffness relation, $\mathbf{P} - \mathbf{P}_f = \mathbf{Sd}$, we write

$$[-100] = [8{,}400]\,[d_1]$$

from which,

$$\mathbf{d} = [d_1] = [-0.011905] \text{ rad}$$

Substructure Joint Displacements, and Member End Displacements and End Forces:

Substructure 1 The substructure's external joint displacements $\bar{\mathbf{v}}_E$ can be obtained by simply comparing the substructure's external degree of freedom numbers with its code numbers, as follows.

$$\bar{\mathbf{v}}_{E1} = \begin{bmatrix} \bar{v}_1 \\ \bar{v}_2 \\ \bar{v}_3 \\ \bar{v}_4 \end{bmatrix} \begin{matrix} 2 \\ 3 \\ 4 \\ 1 \end{matrix} = \begin{bmatrix} 0 \\ 0 \\ 0 \\ d_1 \end{bmatrix} = \begin{bmatrix} 0 \\ 0 \\ 0 \\ -0.011905 \end{bmatrix}$$

The substructure's internal joint displacements can now be calculated, using the relationship (Eq. (9.25)) $\bar{\mathbf{v}}_I = \overline{\mathbf{K}}^{-1}_{II}(\overline{\mathbf{F}}_I - \overline{\mathbf{F}}_{fI} - \overline{\mathbf{K}}_{IE}\bar{\mathbf{v}}_E)$. Substitution of the numerical values of E, I, L_1, L_2, and W into Eqs. (1) and (3) of Example 9.4 yields

$$\overline{\mathbf{K}}^{-1}_{II1} = [0.0014881]$$

and

$$\overline{\mathbf{F}}_{I1} = [-50]$$

Similarly, by substituting the appropriate numerical values into the expressions of $\overline{\mathbf{K}}_{IE}$ and $\overline{\mathbf{F}}_{fI}$ given in Figs. 9.7(c) and (d), respectively, of Example 9.4, we obtain

$$\overline{\mathbf{K}}_{IE1} = [\,-336 \quad -1{,}680 \quad -336 \quad 1{,}680\,]$$

and

$$\overline{\mathbf{F}}_{fI1} = \mathbf{0}$$

By substituting the numerical values of the foregoing submatrices and subvectors into Eq. (9.25), we determine the internal joint displacements for substructure 1 to be

$$\bar{\mathbf{v}}_{I1} = \overline{\mathbf{K}}^{-1}_{II1}(\overline{\mathbf{F}}_{I1} - \overline{\mathbf{F}}_{fI1} - \overline{\mathbf{K}}_{IE1}\bar{\mathbf{v}}_{E1}) = [-0.044643]$$

Thus, the complete joint displacement vector for substructure 1 is

$$\bar{\mathbf{v}}_1 = \begin{bmatrix} \bar{\mathbf{v}}_{E1} \\ \hline \bar{\mathbf{v}}_{I1} \end{bmatrix} = \begin{bmatrix} 0 \\ 0 \\ 0 \\ -0.011905 \text{ rad} \\ -0.044643 \text{ m} \end{bmatrix} \begin{matrix} 1 \\ 2 \\ 3 \\ 4 \\ 5 \end{matrix} \qquad \textbf{Ans}$$

With the displacements of all the joints of substructure 1 now known, we can determine the end displacements **u**, and end forces **Q**, for its two members (Fig. 9.9(c)) in the usual manner.

Member 1 ($MT = 2$) From Fig. 9.9(c), we can see that the code numbers for member 1 are 1, 2, 5, 6. Thus,

$$\mathbf{u}_1 = \begin{bmatrix} u_1 \\ u_2 \\ u_3 \\ u_4 \end{bmatrix} \begin{matrix} 1 \\ 2 \\ 5 \\ 6 \end{matrix} = \begin{bmatrix} 0 \\ 0 \\ \bar{v}_5 \\ 0 \end{bmatrix} = \begin{bmatrix} 0 \\ 0 \\ -0.044643 \\ 0 \end{bmatrix}$$

Substituting the numerical values of E and I and $L = 5$ m into Eq. (7.18), we obtain the member stiffness matrix,

$$\mathbf{k}_1 = \begin{bmatrix} 336 & 1{,}680 & -336 & 0 \\ 1{,}680 & 8{,}400 & -1{,}680 & 0 \\ -336 & -1{,}680 & 336 & 0 \\ 0 & 0 & 0 & 0 \end{bmatrix}$$

Substitution of $\mathbf{k}_1$ and $\mathbf{Q}_{f1} = \mathbf{0}$ into the member stiffness relationship, $\mathbf{Q} = \mathbf{ku} + \mathbf{Q}_f$, yields the following end forces for member 1 of substructure 1.

$$\mathbf{Q}_1 = \mathbf{k}_1\mathbf{u}_1 + \mathbf{Q}_{f1} = \begin{bmatrix} 15 \text{ kN} \\ 75 \text{ kN} \cdot \text{m} \\ -15 \text{ kN} \\ 0 \end{bmatrix} \quad \textbf{Ans}$$

Member 2 ($MT = 1$)

$$\mathbf{u}_2 = \begin{bmatrix} -0.044643 \\ 0 \\ 0 \\ -0.011905 \end{bmatrix} \begin{matrix} 5 \\ 6 \\ 3 \\ 4 \end{matrix}$$

Applying Eq. (7.15),

$$\mathbf{k}_2 = \begin{bmatrix} 336 & 0 & -336 & 1{,}680 \\ 0 & 0 & 0 & 0 \\ -336 & 0 & 336 & -1{,}680 \\ 1{,}680 & 0 & -1{,}680 & 8{,}400 \end{bmatrix}$$

$$\mathbf{Q}_{f2} = \mathbf{0}$$

$$\mathbf{Q}_2 = \mathbf{k}_2\mathbf{u}_2 + \mathbf{Q}_{f2} = \begin{bmatrix} -35 \text{ kN} \\ 0 \\ 35 \text{ kN} \\ -175 \text{ kN} \cdot \text{m} \end{bmatrix} \quad \textbf{Ans}$$

Substructure 2

$$\bar{\mathbf{v}}_{E2} = \begin{bmatrix} 0 \\ -0.011905 \\ 0 \\ 0 \end{bmatrix} \begin{matrix} 4 \\ 1 \\ 5 \\ 6 \end{matrix}$$

From Fig. 9.7(d) of Example 9.4, we obtain

$$\overline{\mathbf{F}}_{fI2} = [67.5]$$

The submatrices $\overline{\mathbf{K}}_{II}^{-1}$ and $\overline{\mathbf{K}}_{IE}$ remain the same as for substructure 1, and $\overline{\mathbf{F}}_{I2} = \mathbf{0}$. Thus, the application of Eq. (9.25) yields

$$\bar{\mathbf{v}}_{I2} = [-0.13021]$$

and, therefore,

$$\bar{\mathbf{v}}_2 = \begin{bmatrix} \bar{\mathbf{v}}_{E2} \\ \hline \bar{\mathbf{v}}_{I2} \end{bmatrix} = \begin{bmatrix} 0 \\ -0.011905 \text{ rad} \\ 0 \\ 0 \\ -0.13021 \text{ m} \end{bmatrix} \begin{matrix} 1 \\ 2 \\ 3 \\ 4 \\ 5 \end{matrix} \quad \textbf{Ans}$$

Member 1 ($MT = 2$)

$$\mathbf{u}_1 = \begin{bmatrix} 0 \\ -0.011905 \\ -0.13021 \\ 0 \end{bmatrix} \begin{matrix} 1 \\ 2 \\ 5 \\ 6 \end{matrix}$$

The $\mathbf{k}$ matrix for member 1 of substructure 2 is the same as that for the corresponding member of substructure 1. Using Eq. (7.19), we calculate

$$\mathbf{Q}_{f1} = \begin{bmatrix} 56.25 \\ 56.25 \\ 33.75 \\ 0 \end{bmatrix}$$

Thus,

$$\mathbf{Q}_1 = \mathbf{k}_1\mathbf{u}_1 + \mathbf{Q}_{f1} = \begin{bmatrix} 80 \text{ kN} \\ 175 \text{ kN} \cdot \text{m} \\ 10 \text{ kN} \\ 0 \end{bmatrix} \quad \textbf{Ans}$$

Member 2 ($MT = 1$)

$$\mathbf{u}_2 = \begin{bmatrix} -0.13021 \\ 0 \\ 0 \\ 0 \end{bmatrix} \begin{matrix} 5 \\ 6 \\ 3 \\ 4 \end{matrix}$$

The $\mathbf{k}$ matrix for this member is the same as that for member 2 of substructure 1. Applying Eq. (7.16),

$$\mathbf{Q}_{f2} = \begin{bmatrix} 33.75 \\ 0 \\ 56.25 \\ -56.25 \end{bmatrix}$$

Thus,

$$\mathbf{Q}_2 = \mathbf{k}_2\mathbf{u}_2 + \mathbf{Q}_{f2} = \begin{bmatrix} -10 \text{ kN} \\ 0 \\ 100 \text{ kN} \\ -275 \text{ kN} \cdot \text{m} \end{bmatrix} \quad \textbf{Ans}$$

The end forces for the individual members of the structure are shown in Fig. 9.9(d).

Support Reactions: The reaction vector **R** can be assembled either directly from the member end force vectors **Q**, or from the external joint force vectors, $\overline{\mathbf{F}}_E$, of the substructures. To use the latter option, we first apply Eq. (9.26) to calculate $\overline{\mathbf{F}}_E$. Thus, by substituting the previously calculated numerical values of $\overline{\mathbf{K}}^*_{EE}$, $\overline{\mathbf{F}}^*_{fE}$, and $\bar{\mathbf{v}}_E$ into Eq. (9.26), we obtain

$$\overline{\mathbf{F}}_{E1} = \overline{\mathbf{K}}^*_{EE1}\bar{\mathbf{v}}_{E1} + \overline{\mathbf{F}}^*_{fE1} = \begin{bmatrix} 15 \\ 75 \\ 35 \\ -175 \end{bmatrix} \begin{matrix} 2 \\ 3 \\ 4 \\ 1 \end{matrix}$$

and

$$\overline{\mathbf{F}}_{E2} = \overline{\mathbf{K}}^*_{EE2}\bar{\mathbf{v}}_{E2} + \overline{\mathbf{F}}^*_{fE2} = \begin{bmatrix} 80 \\ 175 \\ 100 \\ -275 \end{bmatrix} \begin{matrix} 4 \\ 1 \\ 5 \\ 6 \end{matrix}$$

The foregoing substructure forces are depicted in Fig. 9.9(e). Finally, we calculate the support reaction vector **R** by storing the pertinent elements of $\overline{\mathbf{F}}_{E1}$ and $\overline{\mathbf{F}}_{E2}$ in their proper positions in **R**, using the substructure code numbers. This yields,

$$\mathbf{R} = \begin{bmatrix} 15\ \text{kN} \\ 75\ \text{kN} \cdot \text{m} \\ 115\ \text{kN} \\ 100\ \text{kN} \\ -275\ \text{kN} \cdot \text{m} \end{bmatrix} \begin{matrix} 2 \\ 3 \\ 4 \\ 5 \\ 6 \end{matrix} \qquad \textbf{Ans}$$

The support reactions are shown in Fig. 9.9(f).

9.4 INCLINED ROLLER SUPPORTS

The structures that we have considered thus far in this text have been supported such that the joint displacements prevented by the supports are in the directions of the global coordinate axes oriented in the horizontal and vertical directions. Because an inclined roller support prevents translation of a joint in an inclined direction (normal to the incline), while permitting translation in the perpendicular direction, it exerts a reaction force on the joint in that inclined, nonglobal, direction. Thus, the effect of an inclined roller support cannot be included in analysis by simply eliminating one of the structure's degrees of freedom; that is, by treating one of the structure's coordinates, which are defined in the directions of the global coordinate axes, as a restrained coordinate.

An obvious approach to alleviate this problem would be to orient the global coordinate system so that its axes are parallel and perpendicular to the inclined plane upon which the roller moves. However, this approach generally proves to be quite cumbersome, as it requires that the joint coordinates and loads, which are usually specified in the horizontal and vertical directions, be calculated with respect to the inclined global coordinate system. Furthermore, the foregoing

approach cannot be used if the structure is supported by two or more rollers inclined in different (i.e., neither parallel nor perpendicular) directions.

A theoretically exact solution of the problem of inclined rollers usually involves first defining the reaction force and the support displacements with reference to a *local joint coordinate system,* with axes parallel and perpendicular to the incline; and then introducing these restraint conditions in the structure's global stiffness relations via a special transformation matrix [26]. While this approach is exact in the sense that it yields exactly 0 displacement of the support joint perpendicular to the incline, it is generally not considered to be the most convenient because its computer implementation requires a significant amount of programming effort.

Perhaps the most convenient and commonly used technique for modeling an inclined roller support is to replace it with an imaginary axial force member with very large axial stiffness, and oriented in the direction perpendicular to the incline, as shown in Figs. 9.10 and 9.11 (on the next page). As depicted there, one end of the imaginary member is connected to the original support joint by a hinged connection, while the other end is attached to an imaginary hinged support, to ensure that only axial force (i.e., no bending moment) develops in the member when the structure is loaded. In order for the imaginary member to accurately represent the effect of the roller support, its axial stiffness must be made sufficiently large so that its axial deformation is negligibly small. This is usually achieved by specifying a very large value for the cross-sectional area of

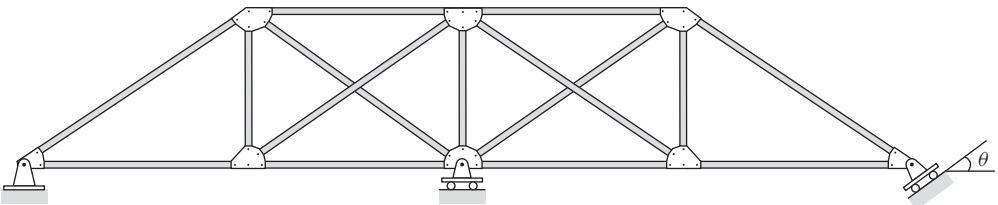

(a) Plane Truss with Inclined Roller Support

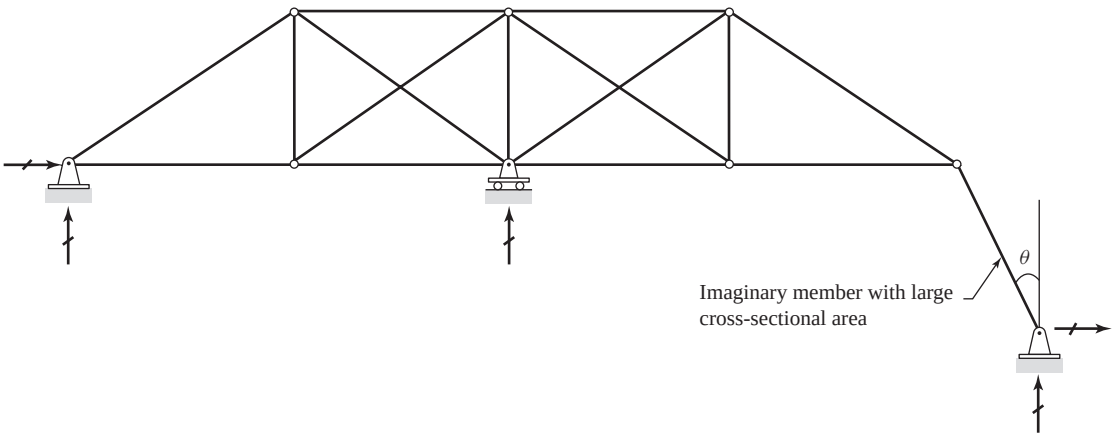

(b) Analytical Model

Fig. 9.10

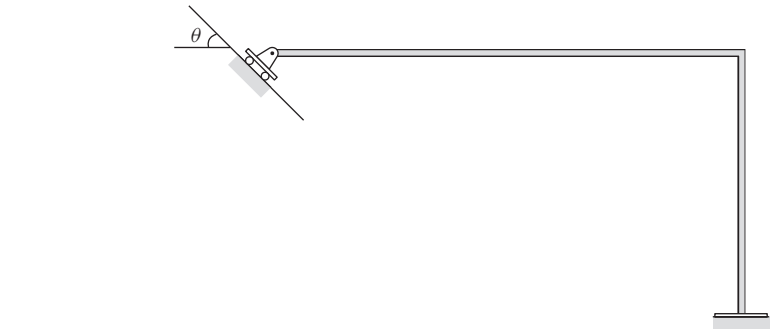

(a) Plane Frame with Inclined Roller Support

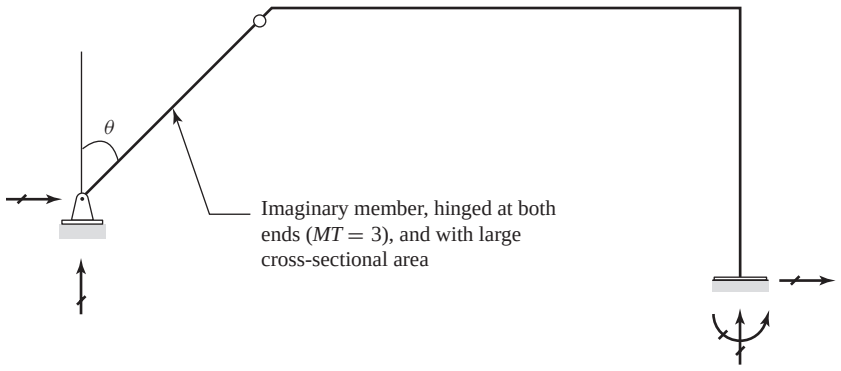

(b) Analytical Model

Fig. 9.11

the imaginary member in the analysis, while keeping its length of the same order of magnitude as the other (real) structural members, to ensure that the imaginary member undergoes only small rotations. Provided that the foregoing conditions are satisfied, the axial force in the imaginary member represents the reaction of the actual inclined roller support.

The main advantage of modeling inclined roller supports with imaginary members is that computer programs for standard supports, such as those developed in previous chapters, can be used, without any modifications, to analyze structures supported on inclined rollers. When analyzing trusses, ordinary truss members with large cross-sectional areas can be used to model inclined roller supports (Fig. 9.10). In the case of frames, however, the members used to model inclined rollers, in addition to having large cross-sectional areas, must be of type 3 ($MT = 3$); that is, they must be hinged at both ends, as shown in Fig. 9.11. As noted before, the cross-sectional area of the imaginary member, used to model the inclined roller support, should be sufficiently large so that the member's axial deformations are negligibly small. However, using an extremely large value for the cross-sectional area of the imaginary member can cause some off-diagonal elements of the structure stiffness matrix to become so large, as compared to the other elements, that they introduce numerical errors, or cause numerical instability, during the solution of the structure's stiffness equations.

9.5 OFFSET CONNECTIONS

In formulating the stiffness method of analysis, we have ignored the size of joints or connections, assuming them to be of infinitesimal size. While this assumption proves to be adequate for most framed structures, the dimensions of moment-resisting connections in some structures may be large enough, relative to member lengths, that ignoring their effect in the analysis can lead to erroneous results. In this section, we discuss procedures for including the effect of finite sizes of connections or joints in the analysis.

Consider an arbitrary girder of a typical plane building frame, as shown in Fig. 9.12(a) on the next page. The girder is connected at its ends, to columns and adjacent girders, by means of rigid or moment-resisting connections. As indicated in the figure, the dimensions of connections usually (but not always) equal the cross-sectional depths of the connected members. If the connection dimensions are small, as compared to the member lengths, then their effect is ignored in the analysis. In such a case, it would be assumed for analysis purposes that the girder under consideration extends in length from one column centerline to the next, and is connected at its ends to other members through rigid connections of infinitesimal size, as depicted in Fig. 9.12(b).

However, if the connection dimensions are not small, then their effect must be considered in the analysis. As shown in Fig. 9.12(c), rigid connections of finite size can be conveniently modeled by using rigid *offsets*, with each offset being a rigid body of length equal to the distance between the center of the connection and its edge which is adjacent to the member under consideration. Thus, from Fig. 9.12(c), we can see that the girder under consideration has offset connections of lengths d_b and d_e at its left and right ends, respectively.

Two approaches are commonly used to include the effect of offset connections in analysis. In the first approach, each offset is treated as a small member with very large stiffness. For example, in [13] it is suggested that the cross-sectional properties of an offset member be chosen so that its stiffness is 1,000 times that of the connected member. The main advantage of this approach is that computer programs, such as those developed in previous chapters, can be used without any modification. The disadvantage of this approach is that each offset increases, by one, the number of members and joints to be analyzed. For example, the girder of Fig. 9.12(c) would have to be divided into three members of lengths d_b, L, and d_e, in order to include the effect of offset connections at its two ends in the analysis.

An alternate approach that can be used to handle the effect of offset connections involves modifying the member stiffness relationships to include the effect of offsets at member ends. The main advantage of this approach is that a natural member (e.g., a girder or a column), together with its end offsets, can be treated as a single member for the purpose of analysis. For example, the whole girder of Fig. 9.12(c), including its end offsets, would be treated as a single member when using this approach. However, the disadvantage of this approach is that it requires rewriting of some parts of the computer programs developed in previous chapters.

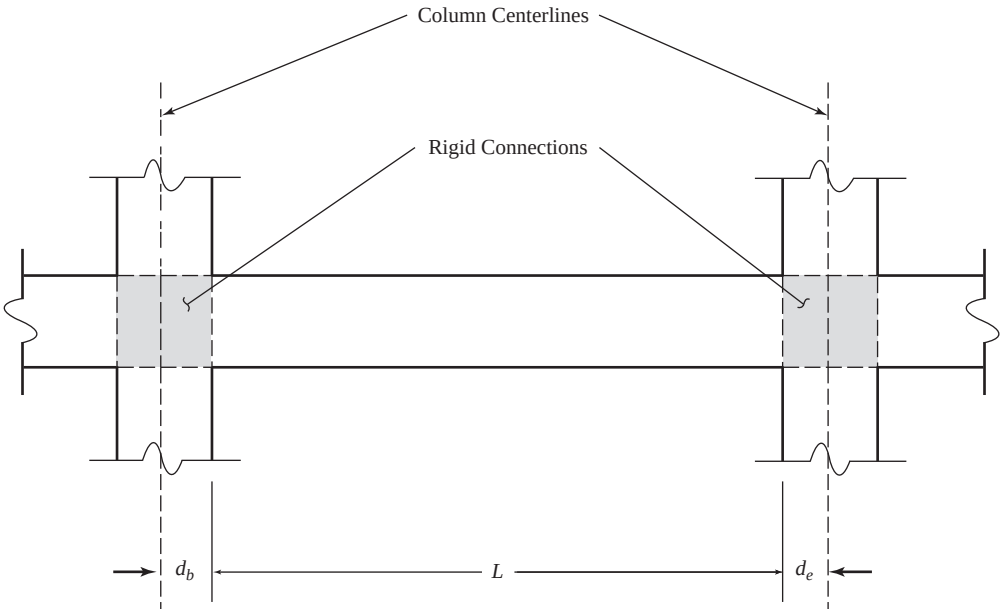

(a) Girder

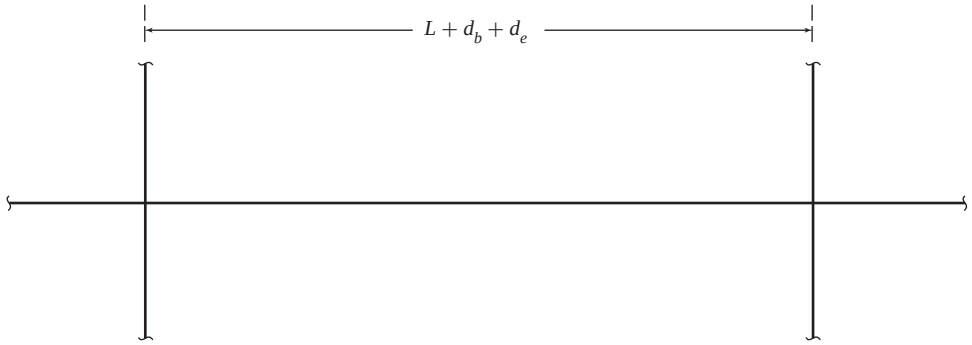

(b) Analytical Model Neglecting Connection Sizes

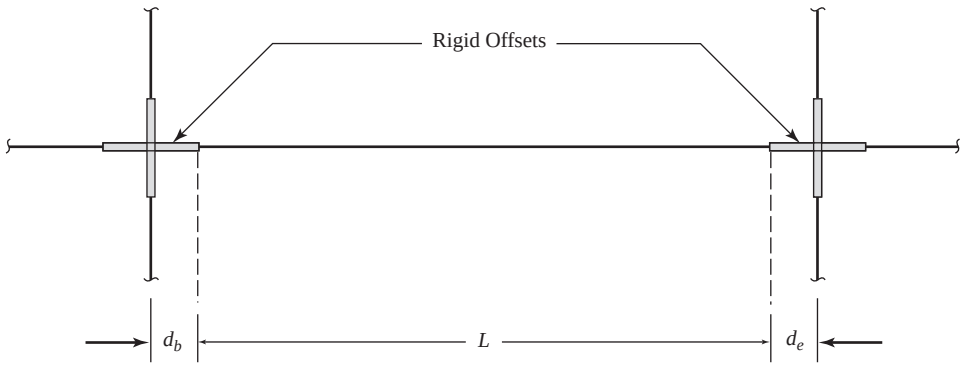

(c) Analytical Model Considering Connection Sizes

Fig. 9.12

In the following, we modify the stiffness relations for the members of plane frames to include the effect of rigid end offsets. Similar procedures can be employed to derive modified stiffness relations for the members of other types of framed structures.

Consider an arbitrary member of length L of a plane frame, and let $\overline{\mathbf{Q}}$ and $\bar{\mathbf{u}}$ denote the local end forces and end displacements, respectively, at the exterior ends of its offsets, as shown in Fig. 9.13(a). Our objective is to express $\overline{\mathbf{Q}}$ in terms of $\bar{\mathbf{u}}$ and any external loading applied to the member between its actual ends b and e. Recall from Chapter 6 that the relationship between the end forces $\mathbf{Q}$ and the end displacement $\mathbf{u}$, which are defined at the ends b and e of the member, is of the form $\mathbf{Q} = \mathbf{ku} + \mathbf{Q}_f$, with $\mathbf{k}$ and $\mathbf{Q}_f$ given by Eqs. (6.6) and (6.15), respectively.

To express $\overline{\mathbf{Q}}$ in terms of $\mathbf{Q}$, we consider the equilibrium of the rigid bodies of the two offsets. This yields (see Fig. 9.13(b))

$$\overline{Q}_1 = Q_1 \qquad \overline{Q}_2 = Q_2 \qquad \overline{Q}_3 = d_b\ Q_2 + Q_3$$
$$\overline{Q}_4 = Q_4 \qquad \overline{Q}_5 = Q_5 \qquad \overline{Q}_6 = -d_e\ Q_5 + Q_6$$

which can be written in matrix form as

$$\overline{\mathbf{Q}} = \overline{\mathbf{T}}\mathbf{Q} \tag{9.29}$$

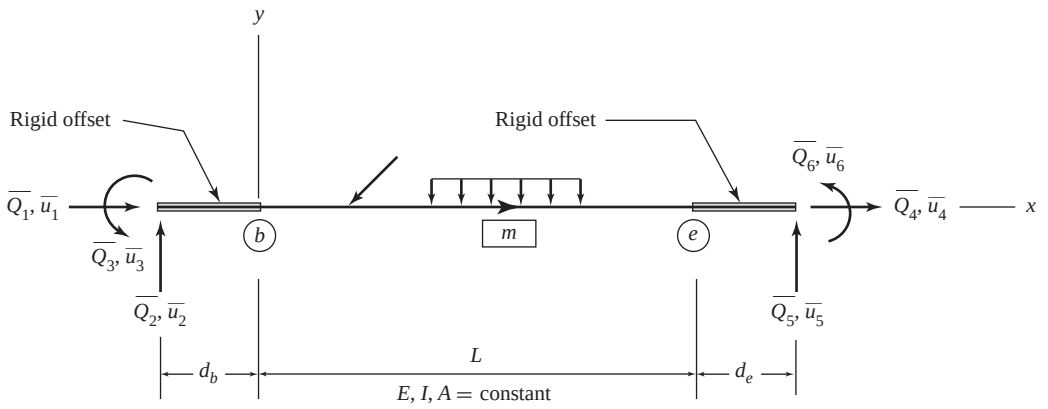

(a) Plane Frame Member with Rigid End Offsets

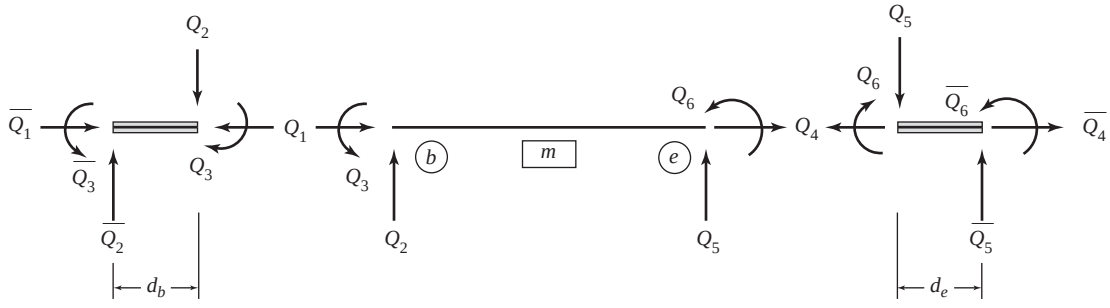

(b) Member Forces

Fig. 9.13

with

$$\overline{\mathbf{T}} = \begin{bmatrix} 1 & 0 & 0 & 0 & 0 & 0 \\ 0 & 1 & 0 & 0 & 0 & 0 \\ 0 & d_b & 1 & 0 & 0 & 0 \\ 0 & 0 & 0 & 1 & 0 & 0 \\ 0 & 0 & 0 & 0 & 1 & 0 \\ 0 & 0 & 0 & 0 & -d_e & 1 \end{bmatrix} \tag{9.30}$$

in which $\overline{\mathbf{T}}$ can be considered to be a transformation matrix which translates the member's end forces from its actual ends *b* and *e*, to the exterior ends of its rigid offsets.

From geometrical considerations, it can be shown that the relationship between the end displacements $\mathbf{u}$ and $\bar{\mathbf{u}}$ can be written as

$$\mathbf{u} = \overline{\mathbf{T}}^T \bar{\mathbf{u}} \tag{9.31}$$

By substituting Eq. (9.31) into Eq. (6.4), and substituting the resulting expression into Eq. (9.29), we obtain the desired stiffness relationship:

$$\boxed{\overline{\mathbf{Q}} = \bar{\mathbf{k}}\bar{\mathbf{u}} + \overline{\mathbf{Q}}_f} \tag{9.32}$$

with

$$\boxed{\bar{\mathbf{k}} = \overline{\mathbf{T}}\mathbf{k}\overline{\mathbf{T}}^T} \tag{9.33}$$

$$\boxed{\overline{\mathbf{Q}}_f = \overline{\mathbf{T}}\mathbf{Q}_f} \tag{9.34}$$

in which $\bar{\mathbf{k}}$ and $\overline{\mathbf{Q}}_f$ represent the modified member stiffness matrix and fixed-end force vector, respectively, in the local coordinate system. Note that $\bar{\mathbf{k}}$ and $\overline{\mathbf{Q}}_f$ include the effect of rigid offsets at the ends of the member. The explicit forms of $\bar{\mathbf{k}}$ and $\overline{\mathbf{Q}}_f$, respectively, can be obtained by substituting Eqs. (6.6) and (9.30) into Eq. (9.33), and Eqs. (6.15) and (9.30) into Eq. (9.34). These are given in Eqs. (9.35) and (9.36).

$$\bar{\mathbf{k}} = \frac{EI}{L^3}\begin{bmatrix} \frac{AL^2}{I} & 0 & 0 & -\frac{AL^2}{I} & 0 & 0 \\ 0 & 12 & (6L+12d_b) & 0 & -12 & (6L+12d_e) \\ 0 & (6L+12d_b) & (4L^2+12Ld_b+12d_b^2) & 0 & (-6L-12d_b) & (2L^2+6Ld_b+6Ld_e+12d_bd_e) \\ -\frac{AL^2}{I} & 0 & 0 & \frac{AL^2}{I} & 0 & 0 \\ 0 & -12 & (-6L-12d_b) & 0 & 12 & (-6L-12d_e) \\ 0 & (6L+12d_e) & (2L^2+6Ld_b+6Ld_e+12d_bd_e) & 0 & (-6L-12d_e) & (4L^2+12Ld_e+12d_e^2) \end{bmatrix} \tag{9.35}$$

$$\overline{\mathbf{Q}}_f = \begin{bmatrix} FA_b \\ FS_b \\ d_b FS_b + FM_b \\ FA_e \\ FS_e \\ -d_e FS_e + FM_e \end{bmatrix} \tag{9.36}$$

The procedure for analysis essentially remains the same as developed previously, except that the modified expressions for the stiffness matrices $\bar{\mathbf{k}}$ (Eq. (9.35)) and fixed-end force vectors $\overline{\mathbf{Q}}_f$ (Eq. (9.36)) are used (instead of $\mathbf{k}$ and $\mathbf{Q}_f$, respectively), for members with offset connections.

9.6 SEMIRIGID CONNECTIONS

While rigid and hinged types of connections, as considered thus far in this text, are the most commonly used in structural designs, a third type of connection, termed the *semirigid connection*, is also recognized by some design codes, and can be used for designing such structures as structural steel building frames. Recall that the rotation of a rigidly connected member end equals the rotation of the adjacent joint, whereas the rotation of a hinged end of a member must be such that the moment at the hinged end is 0. A connection is considered to be semirigid if its rotational restraint is less than that of a perfectly rigid connection, but more than that of a frictionless hinged connection. In other words, the moment transmitted by a semirigid connection is greater than 0, but less than that transmitted by a rigid connection. For the purpose of analysis, a semirigid connection can be conveniently modeled by a rotational (torsional) spring with stiffness equal to that of the actual connection. In this section, we derive the stiffness relations for members of beams with semirigid connections at their ends. Such relationships for other types of framed structures can be determined by using a similar procedure.

Consider an arbitrary member of a beam, as shown in Fig. 9.14(a) on the next page. The member is connected to the joints adjacent to its ends *b* and *e*, by means of rotational springs of infinitesimal size representing the semirigid connections of stiffnesses k_b and k_e, respectively. As shown in this figure, $\overline{\mathbf{Q}}$ and $\bar{\mathbf{u}}$ represent the local end forces and end displacements, respectively, at the exterior ends of the rotational springs. Our objective is to express $\overline{\mathbf{Q}}$ in terms of $\bar{\mathbf{u}}$ and any external loading applied to the member.

We begin by writing, in explicit form, the previously derived relationship $\mathbf{Q} = \mathbf{ku} + \mathbf{Q}_f$, between the end forces $\mathbf{Q}$ and the end displacements $\mathbf{u}$, which are defined at the actual ends *b* and *e* of the member. By using the expressions for $\mathbf{k}$ and $\mathbf{Q}_f$ from Eqs. (5.53) and (5.99), respectively, we write

$$\begin{bmatrix} Q_1 \\ Q_2 \\ Q_3 \\ Q_4 \end{bmatrix} = \frac{EI}{L^3} \begin{bmatrix} 12 & 6L & -12 & 6L \\ 6L & 4L^2 & -6L & 2L^2 \\ -12 & -6L & 12 & -6L \\ 6L & 2L^2 & -6L & 4L^2 \end{bmatrix} \begin{bmatrix} u_1 \\ u_2 \\ u_3 \\ u_4 \end{bmatrix} + \begin{bmatrix} FS_b \\ FM_b \\ FS_e \\ FM_e \end{bmatrix} \tag{9.37}$$

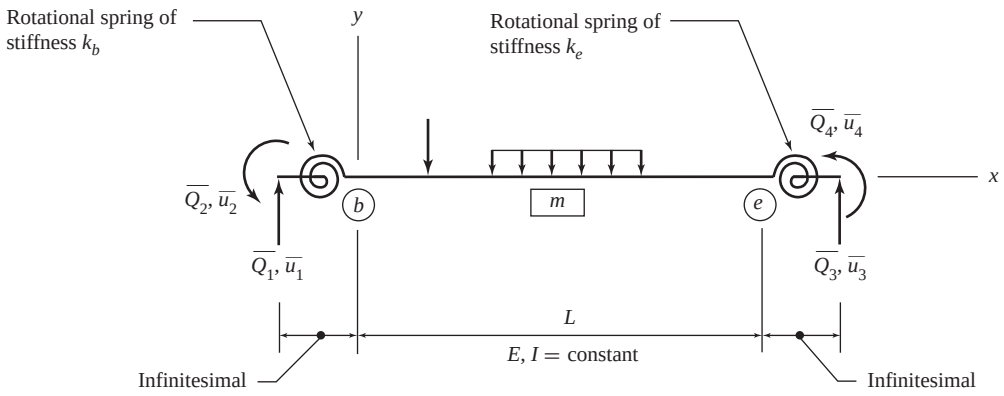

(a) Beam Member with Semirigid Connections

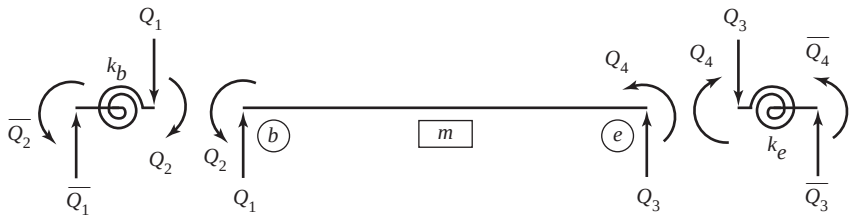

(b) Member Forces

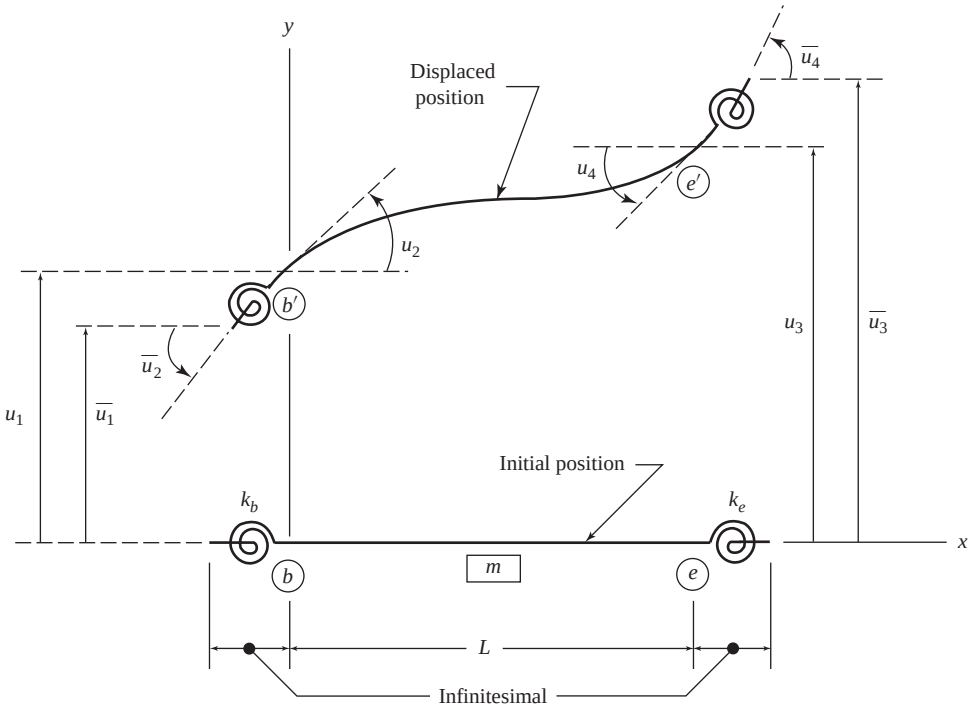

(c) Member Displacements

Fig. 9.14

Figure 9.14(b) shows the forces $\overline{\mathbf{Q}}$ and $\mathbf{Q}$ acting at the exterior and interior ends, respectively, of the member's rotational springs. As the lengths of these springs are infinitesimal, equilibrium equations for the free bodies of the springs yield

$$\mathbf{Q} = \overline{\mathbf{Q}} \tag{9.38}$$

The displacements $\mathbf{u}$ and $\bar{\mathbf{u}}$ are depicted in Fig. 9.14(c) using an exaggerated scale. Because of the infinitesimal size of the springs, the translations of the spring ends are equal; that is,

$$u_1 = \bar{u}_1 \tag{9.39a}$$

$$u_3 = \bar{u}_3 \tag{9.39b}$$

The relationship between the rotations (u_2 and $\bar{u}_2$) of the two ends of the spring, at member end b, can be established by applying the spring stiffness relation:

$$\overline{Q}_2 = k_b\,(\bar{u}_2 - u_2)$$

from which,

$$u_2 = \bar{u}_2 - \frac{\overline{Q}_2}{k_b} \tag{9.39c}$$

Similarly, by using the stiffness relation for the spring attached to member end e, we obtain

$$u_4 = \bar{u}_4 - \frac{\overline{Q}_4}{k_e} \tag{9.39d}$$

To obtain the desired relationship between $\overline{\mathbf{Q}}$ and $\bar{\mathbf{u}}$, we now substitute Eqs. (9.38) and (9.39) into Eq. (9.37) to obtain the following equations.

$$\overline{Q}_1 = \frac{EI}{L^3}\left[12\bar{u}_1 + 6L\left(\bar{u}_2 - \frac{\overline{Q}_2}{k_b}\right) - 12\bar{u}_3 + 6L\left(\bar{u}_4 - \frac{\overline{Q}_4}{k_e}\right)\right] + FS_b \tag{9.40a}$$

$$\overline{Q}_2 = \frac{EI}{L^3}\left[6L\bar{u}_1 + 4L^2\left(\bar{u}_2 - \frac{\overline{Q}_2}{k_b}\right) - 6L\bar{u}_3 + 2L^2\left(\bar{u}_4 - \frac{\overline{Q}_4}{k_e}\right)\right] + FM_b \tag{9.40b}$$

$$\overline{Q}_3 = \frac{EI}{L^3}\left[-12\bar{u}_1 - 6L\left(\bar{u}_2 - \frac{\overline{Q}_2}{k_b}\right) + 12\bar{u}_3 - 6L\left(\bar{u}_4 - \frac{\overline{Q}_4}{k_e}\right)\right] + FS_e \tag{9.40c}$$

$$\overline{Q}_4 = \frac{EI}{L^3}\left[6L\bar{u}_1 + 2L^2\left(\bar{u}_2 - \frac{\overline{Q}_2}{k_b}\right) - 6L\bar{u}_3 + 4L^2\left(\bar{u}_4 - \frac{\overline{Q}_4}{k_e}\right)\right] + FM_e \tag{9.40d}$$

Next, we solve Eqs. (9.40b) and (9.40d) simultaneously, to express $\overline{Q}_2$ and $\overline{Q}_4$ in terms of $\bar{u}_1$ through $\bar{u}_4$. This yields

$$\overline{Q}_2 = \frac{EIr_b}{L^3R}[6L(2-r_e)\bar{u}_1 + 4L^2(3-2r_e)\bar{u}_2 - 6L(2-r_e)\bar{u}_3 + 2L^2r_e\bar{u}_4] + \frac{r_b}{R}[(4-3r_e)FM_b - 2(1-r_e)FM_e] \quad \textbf{(9.41a)}$$

$$\overline{Q}_4 = \frac{EIr_e}{L^3R}[6L(2-r_b)\bar{u}_1 + 2L^2r_b\bar{u}_2 - 6L(2-r_b)\bar{u}_3 + 4L^2(3-2r_b)\bar{u}_4] + \frac{r_e}{R}[(4-3r_b)FM_e - 2(1-r_b)FM_b] \quad \textbf{(9.41b)}$$

in which r_b and r_e denote the dimensionless rigidity parameters defined as

$$\boxed{r_i = \frac{k_i L}{EI + k_i L} \qquad i = b,\ e} \quad \textbf{(9.42)}$$

and

$$\boxed{R = 12 - 8r_b - 8r_e + 5r_br_e} \quad \textbf{(9.43)}$$

Finally, by substituting Eqs. (9.41) into Eqs. (9.40a) and (9.40c), we determine expressions for $\overline{Q}_1$ and $\overline{Q}_3$ in terms of $\bar{u}_1$ through $\bar{u}_4$. Thus,

$$\overline{Q}_1 = \frac{EI}{L^3R}[12(r_b + r_e - r_br_e)\bar{u}_1 + 6Lr_b(2-r_e)\bar{u}_2 - 12(r_b + r_e - r_br_e)\bar{u}_3 + 6Lr_e(2-r_b)\bar{u}_4] + FS_b - \frac{6}{LR}[(1-r_b)(2-r_e)FM_b + (1-r_e)(2-r_b)FM_e] \quad \textbf{(9.44a)}$$

$$\overline{Q}_3 = \frac{EI}{L^3R}[-12(r_b + r_e - r_br_e)\bar{u}_1 - 6Lr_b(2-r_e)\bar{u}_2 + 12(r_b + r_e - r_br_e)\bar{u}_3 - 6Lr_e(2-r_b)\bar{u}_4] + FS_e + \frac{6}{LR}[(1-r_b)(2-r_e)FM_b + (1-r_e)(2-r_b)FM_e] \quad \textbf{(9.44b)}$$

Equations (9.41) and (9.44), which represent the modified stiffness relations for beam members with semirigid connections at both ends, can be expressed in matrix form:

$$\boxed{\overline{\mathbf{Q}} = \bar{\mathbf{k}}\bar{\mathbf{u}} + \overline{\mathbf{Q}}_f} \quad \textbf{(9.45)}$$

with

$$\bar{\mathbf{k}} = \frac{EI}{L^3 R}\begin{bmatrix} 12(r_b + r_e - r_b r_e) & 6Lr_b(2 - r_e) & -12(r_b + r_e - r_b r_e) & 6Lr_e(2 - r_b) \\ 6Lr_b(2 - r_e) & 4L^2 r_b(3 - 2r_e) & -6Lr_b(2 - r_e) & 2L^2 r_b r_e \\ -12(r_b + r_e - r_b r_e) & -6Lr_b(2 - r_e) & 12(r_b + r_e - r_b r_e) & -6Lr_e(2 - r_b) \\ 6Lr_e(2 - r_b) & 2L^2 r_b r_e & -6Lr_e(2 - r_b) & 4L^2 r_e(3 - 2r_b) \end{bmatrix} \tag{9.46}$$

and

$$\overline{\mathbf{Q}}_f = \begin{bmatrix} FS_b - \dfrac{6}{LR}[(1 - r_b)(2 - r_e)FM_b + (1 - r_e)(2 - r_b)FM_e] \\ \dfrac{r_b}{R}[(4 - 3r_e)FM_b - 2(1 - r_e)FM_e] \\ FS_e + \dfrac{6}{LR}[(1 - r_b)(2 - r_e)FM_b + (1 - r_e)(2 - r_b)FM_e] \\ \dfrac{r_e}{R}[-2(1 - r_b)FM_b + (4 - 3r_b)FM_e] \end{bmatrix} \tag{9.47}$$

The $\bar{\mathbf{k}}$ matrix in Eq. (9.46) and the $\overline{\mathbf{Q}}_f$ vector in Eq. (9.47) represent the modified stiffness matrix and fixed-end force vector, respectively, for the members of beams with semirigid connections. It should be noted that these expressions for $\bar{\mathbf{k}}$ and $\overline{\mathbf{Q}}_f$ are valid for the values of the spring stiffness k_i ($i = b$ or e) ranging from 0, which represents a hinged connection, to infinity, which represents a rigid connection. From Eq. (9.42), we can see that as k_i varies from 0 to infinity, the value of the corresponding rigidity parameter r_i varies from 0 to 1. Thus, $r_i = 0$ represents a frictionless hinged connection, whereas $r_i = 1$ represents a perfectly rigid connection. The reader is encouraged to verify that when both r_b and r_e are set equal to 1, then $\bar{\mathbf{k}}$ (Eq. (9.46)) and $\overline{\mathbf{Q}}_f$ (Eq. (9.47)) reduce the $\mathbf{k}$ (Eq. (5.53)) and $\mathbf{Q}_f$ (Eq. (5.99)) for a beam member rigidly connected at both ends. Similarly, the expressions of $\mathbf{k}$ and $\mathbf{Q}_f$, derived in Chapter 7 for beam members with three combinations of rigid and hinged connections (i.e., $MT = 1$, 2, and 3), can be obtained from Eqs. (9.46) and (9.47), respectively, by setting r_b and r_e to 0 or 1, as appropriate.

The procedure for analysis of beams with rigid and hinged connections, developed previously, can be applied to beams with semirigid connections—provided that the modified member stiffness matrix $\bar{\mathbf{k}}$ (Eq. (9.46)) and fixed-end force vector $\overline{\mathbf{Q}}_f$ (Eq. (9.47)) are used in the analysis.

9.7 SHEAR DEFORMATIONS

The stiffness relations that have been developed thus far for beams, grids, and frames, do not include the effect of shear deformations of members. Such structures are generally composed of members with relatively large length-to-depth ratios, so that their shear deformations are usually negligibly small as compared to the bending deformations. However, in the case of beams, grids

and rigid frames consisting of members with length-to-depth ratios of 10 or less, and/or built-up (fabricated) members, the magnitudes of shear deformations can be considerable; therefore, the effect of shear deformations should be included in the analyses of such structures. In this section, we consider a procedure for including the effect of shear deformations in the member stiffness relations, and present the modified stiffness matrix for the members of beams. This matrix, which contains the effects of both the shear and bending deformations, can be easily extended to obtain the corresponding modified member stiffness matrices for grids, and plane and space frames.

The relationship between the shearing strain at a cross-section of a beam member and the slope of the elastic curve due to shear can be obtained by considering the shear deformation of a differential element of length *dx* of the member, as shown in Fig. 9.15. From this figure, we can see that

$$\gamma = -\frac{d\bar{u}_{yS}}{dx} \tag{9.48}$$

in which γ denotes the shear strain, and $\bar{u}_{yS}$ represents the deflection, due to shear, of the member's centroidal axis in the *y* direction. The negative sign in Eq. (9.48) indicates that the positive shear force *S* causes deflection in the negative *y* direction, as shown in the figure. Substitutions of Hooke's law for shear, $\gamma = \tau/G$, and the stress-force relation, $\tau = f_S S/A$, into Eq. (9.48), yield the following expression for the slope of the elastic curve due to shear.

$$\boxed{\frac{d\bar{u}_{yS}}{dx} = -\left(\frac{f_S}{GA}\right) S} \tag{9.49}$$

in which f_S represents the *shape factor for shear*. The dimensionless shape factor f_S depends on the shape of the member cross-section, and takes into account

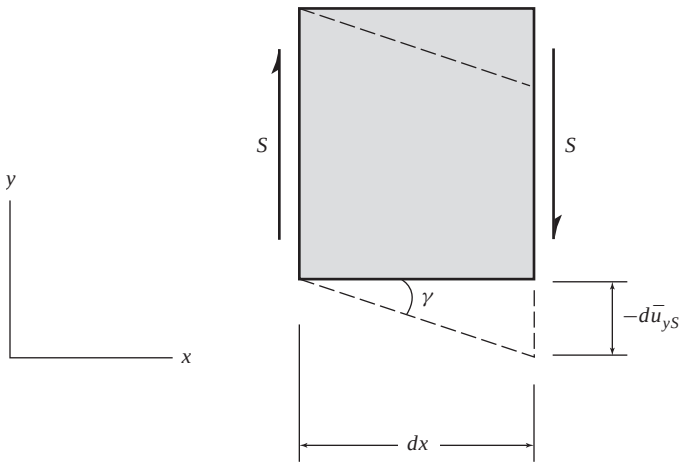

Fig. 9.15

the nonuniform distribution of shear stress on the member cross-section. The values of f_S for some common cross-sectional shapes are as follows.

$f_S = 1.2$ for rectangular cross-sections

$f_S = 10/9$ for circular cross-sections

$f_S = 1$ for wide-flange beams bent about the major axis, provided that the area of the web is used for A in Eq. (9.49)

Integration of Eq. (9.49) yields the expression for deflection due to shear; the total deflection (or slope) of the member due to the combined effect of shear and bending can be determined via superposition of the deflections (or slopes) caused by shear and by bending. As discussed in Chapter 5, the equations for the slope and deflection, due to bending, can be obtained by integrating the moment–curvature relationship:

$$\frac{d^2\bar{u}_{yB}}{dx^2} = \frac{M}{EI} \tag{9.50}$$

in which $\bar{u}_{yB}$ represents the deflection of the member due to bending.

The expressions for the elements of the modified stiffness matrix **k** for a beam member, due to the combined effect of the bending and shear deformations, can be derived using the direct integration approach. To obtain the expressions for the stiffness coefficients k_{i1} ($i = 1$ through 4) in the first column of **k**, we subject a prismatic beam member of length L to a unit value of the end displacement u_1 at end b, as shown in Fig. 9.16. Note that all other member end displacements are 0, and the member is in equilibrium under the action of two end moments k_{21} and k_{41}, and two end shears k_{11} and k_{31}. From the figure, we

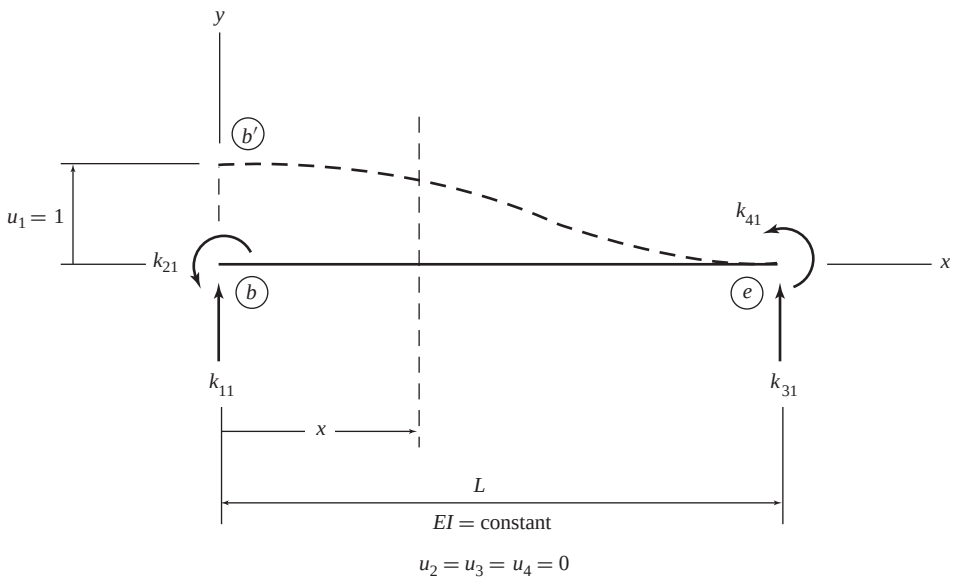

Fig. 9.16

can see that the shear and bending moment at a distance x from end b of the member are:

$$S = k_{11} \tag{9.51}$$

$$M = -k_{21} + k_{11}x \tag{9.52}$$

By substituting Eq. (9.51) into Eq. (9.49), and integrating the resulting equation, we obtain the equation for deflection, due to shear, as

$$\bar{u}_{yS} = -\left(\frac{f_S}{GA}\right) k_{11}x + C_1 \tag{9.53}$$

in which C_1 denotes a constant of integration. By substituting Eq. (9.52) into Eq. (9.50), and integrating the resulting equation twice, we obtain the equations for the slope and deflection of the member, due to bending:

$$\frac{d\bar{u}_{yB}}{dx} = \frac{1}{EI}\left(-k_{21}x + k_{11}\frac{x^2}{2}\right) + C_2 \tag{9.54}$$

$$\bar{u}_{yB} = \frac{1}{EI}\left(-k_{21}\frac{x^2}{2} + k_{11}\frac{x^3}{6}\right) + C_2x + C_3 \tag{9.55}$$

As the shear deformation does not cause any rotation of the member cross-section (see Fig. 9.15), the rotation of the cross-section, θ, results entirely from bending deformation, and is given by (see Eq. (9.54))

$$\theta = \frac{d\bar{u}_{yB}}{dx} = \frac{1}{EI}\left(-k_{21}x + k_{11}\frac{x^2}{2}\right) + C_2 \tag{9.56}$$

By combining Eqs. (9.53) and (9.55), we obtain the equation for the total deflection, $\bar{u}_y$, due to the combined effect of the shear and bending deformations:

$$\bar{u}_y = \bar{u}_{yS} + \bar{u}_{yB} = -\left(\frac{f_S}{GA}\right) k_{11}x + \frac{1}{EI}\left(-k_{21}\frac{x^2}{2} + k_{11}\frac{x^3}{6}\right) + C_2x + C_4 \tag{9.57}$$

in which the constant $C_4 = C_1 + C_3$.

The four unknowns in Eqs. (9.56) and (9.57)—that is, two constants C_2 and C_4 and two stiffness coefficients k_{11} and k_{21}—can now be evaluated by applying the following four boundary conditions:

at end b,	$x = 0$	$\theta = 0$
	$x = 0$	$\bar{u}_y = 1$
at end e,	$x = L$	$\theta = 0$
	$x = L$	$\bar{u}_y = 0$

By applying these boundary conditions, we obtain $C_2 = 0$, $C_4 = 1$, and

$$k_{11} = \frac{12EI}{L^3}\left(\frac{1}{1+\beta_S}\right) \tag{9.58}$$

$$k_{21} = \frac{6EI}{L^2}\left(\frac{1}{1+\beta_S}\right) \tag{9.59}$$

with

$$\boxed{\beta_S = \frac{12EIf_S}{GAL^2}} \tag{9.60}$$

The dimensionless parameter β_S is called the *shear deformation constant*.

The two remaining stiffness coefficients, k_{31} and k_{41}, can now be determined by applying the equations of equilibrium to the free body of the member (Fig. 9.16). Thus,

$$k_{31} = -\frac{12EI}{L^3}\left(\frac{1}{1+\beta_S}\right) \tag{9.61}$$

$$k_{41} = \frac{6EI}{L^2}\left(\frac{1}{1+\beta_S}\right) \tag{9.62}$$

The expressions for elements in the remaining three columns of the **k** matrix can be derived in a similar manner, and the complete modified stiffness matrix for rigidly-connected members of beams, thus obtained, is

$$\mathbf{k} = \frac{EI}{L^3(1+\beta_S)}\begin{bmatrix} 12 & 6L & -12 & 6L \\ 6L & L^2(4+\beta_S) & -6L & L^2(2-\beta_S) \\ -12 & -6L & 12 & -6L \\ 6L & L^2(2-\beta_S) & -6L & L^2(4+\beta_S) \end{bmatrix} \tag{9.63}$$

From Eq. (9.63), we can see that when the shear deformation constant β_S is set equal to 0, then **k** of Eq. (9.63) is reduced to that of Eq. (5.53). It should be realized that the expressions for fixed-end forces due to member loads, given inside the front cover, do not include the effects of shear deformations. If modified fixed-end force expressions including shear deformations are desired, they can be derived using the procedure described in this section.

9.8 NONPRISMATIC MEMBERS

Thus far in this text, we have considered the analysis of structures composed of prismatic members. A member is considered to be prismatic if its axial and flexural rigidities (*EA* and *EI*), or its cross-sectional properties, are constant along its length. In some structures, for aesthetic reasons and/or to save material, it may become necessary to design members with variable cross sections. In this section, we consider the analysis of structures composed of such nonprismatic members.

Perhaps the simplest (albeit approximate) way to handle a nonprismatic natural member, such as a girder or a column, is to subdivide it into a sufficient number of segments, and model each segment by a prismatic member (or element) with cross-sectional properties equal to the average of the cross-sectional properties at the two ends of the segment (Fig. 9.17 on the next page). The main advantage of this approach is that computer programs such as those

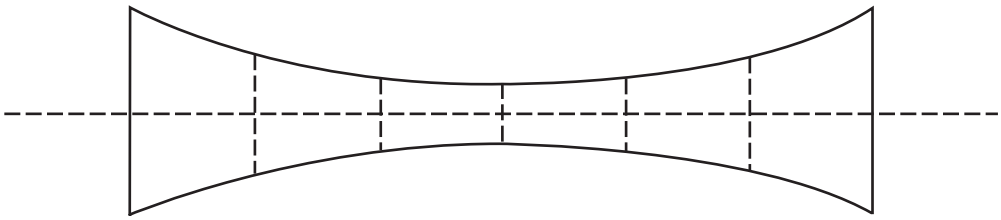

(a) Nonprismatic Member

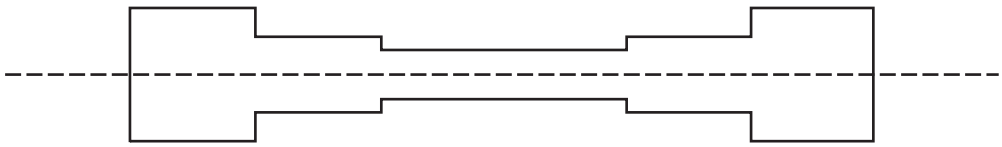

(b) Analytical Model of Nonprismatic Member

Fig. 9.17

developed in previous chapters can be used without any modifications. The main disadvantage of this approach is that the accuracy of the analytical results depends on the number of prismatic members (or elements) used to model each nonprismatic member, and an inordinate number of prismatic members may be required to achieve an acceptable level of accuracy.

An alternate approach that can be used to handle nonprismatic members involves formulation of the nonprismatic member's stiffness relations while taking into account the exact variation of the member's cross-sectional properties. The main advantage of this exact approach is that a natural nonprismatic member (e.g., a girder or a column) can be treated as a single member for the purpose of analysis. However, as will become apparent later in this section, the exact expressions for the stiffness coefficients for nonprismatic members can be quite complicated [43]. In the following, we illustrate the exact approach via derivation of the local stiffness matrix **k** for a tapered plane truss member [26].

Consider a tapered member of a plane truss, as shown in Fig. 9.18(a). The cross-sectional area of the member varies linearly along its length in accordance with the relationship

$$A_x = A_b \left(1 - \frac{r_A x}{L}\right) \tag{9.64}$$

in which A_b and A_x denote, respectively, the member's cross-sectional areas at its end b, and at a distance x from end b; and r_A represents the *area ratio* given by

$$r_A = \frac{A_b - A_e}{A_b} \tag{9.65}$$

with A_e denoting the member's cross-sectional area at end e, as shown in the figure.

To derive the first column of the tapered member's local stiffness matrix **k**, we subject the member to a unit end displacement $u_1 = 1$ (with $u_2 = u_3 = u_4 = 0$), as shown in Fig. 9.18(b). The expressions for the member axial forces required

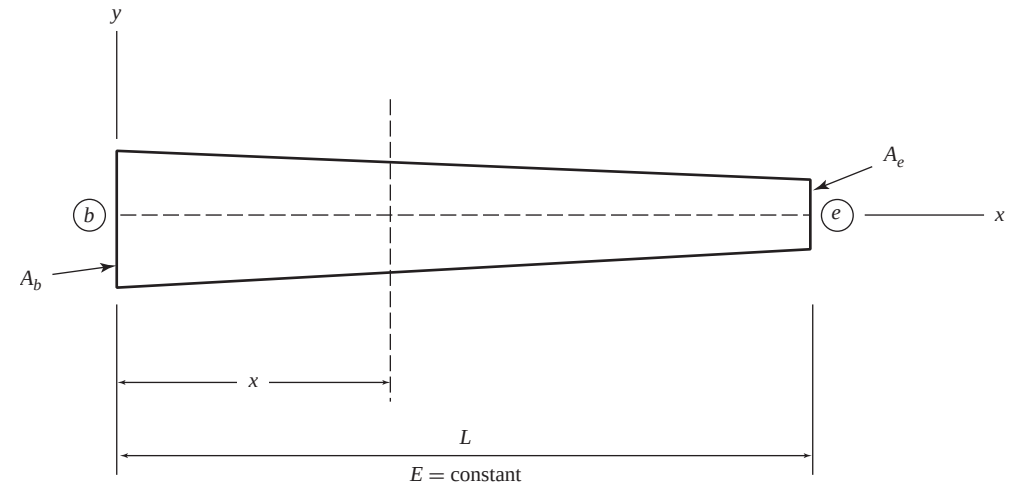

(a) Tapered Plane Truss Member

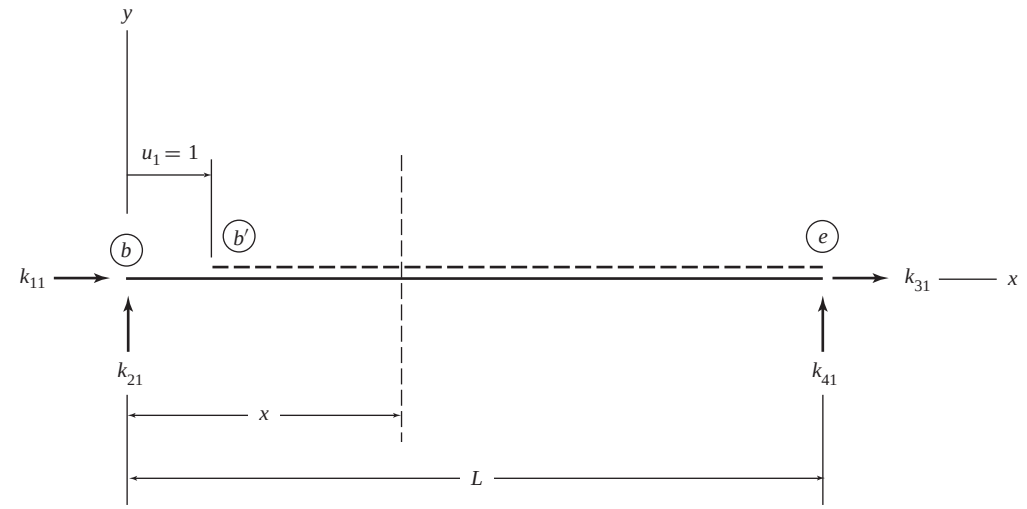

(b) $u_1 = 1$, $u_2 = u_3 = u_4 = 0$

Fig. 9.18

to cause this unit axial deformation can be determined by integrating the differential equation for member axial deformation that, for members with variable cross-sections, can be written as (see Eq. (6.7), Section 6.2)

$$\frac{d\bar{u}_x}{dx} = \frac{Q_a}{EA_x} \tag{9.66}$$

From Fig. 9.18(b), we can see that the axial force acting on the member cross-section at a distance x from its end b is

$$Q_a = -k_{11} \tag{9.67}$$

in which the negative sign indicates that k_{11} causes compression at the member cross-section. Substituting Eqs. (9.64) and (9.67) into Eq. (9.66), and integrating the resulting equation, we obtain

$$\bar{u}_x = \frac{k_{11}L}{EA_b r_A} \ln\left(1 - \frac{r_A x}{L}\right) + C \tag{9.68}$$

in which C is a constant of integration.

The two unknowns, C and k_{11}, in Eq. (9.68) can be evaluated by applying the boundary conditions:

at end b, $\quad x = 0 \quad \bar{u}_x = 1$
at end e, $\quad x = L \quad \bar{u}_x = 0$

Application of the foregoing boundary conditions yields $C = 1$, and

$$k_{11} = -\frac{EA_b r_A}{L \ln(1 - r_A)} \tag{9.69}$$

The three remaining stiffness coefficients can now be determined by applying the equations of equilibrium to the free body of the member (Fig. 9.18(b)). Thus,

$$k_{31} = \frac{EA_b r_A}{L \ln(1 - r_A)}, \quad k_{21} = k_{41} = 0 \tag{9.70}$$

The expressions for elements in the third column of the tapered member's local stiffness matrix **k** can be derived in a similar manner; and, as discussed in Section 3.3, all elements of the second and fourth columns of **k** are 0. The complete local stiffness matrix **k** for a tapered plane truss member, thus obtained, is

$$\mathbf{k} = \frac{EA_b r_A}{L \ln(1 - r_A)} \begin{bmatrix} -1 & 0 & 1 & 0 \\ 0 & 0 & 0 & 0 \\ 1 & 0 & -1 & 0 \\ 0 & 0 & 0 & 0 \end{bmatrix} \tag{9.71}$$

EXAMPLE 9.6 Using the direct integration approach, derive the expressions for the slope and deflection at the free end of the tapered cantilever beam shown in Fig. 9.19(a). The beam has a rectangular cross-section of constant width b, but its depth varies linearly from h_1 at the fixed end to h_2 at the free end.

SOLUTION The depth and moment of inertia of the beam at a distance $x (0 \le x \le L)$ from its free end can be expressed as

$$h_x = h_1\left(1 - \frac{r_h x}{L}\right)$$

$$I_x = I_1\left(1 - \frac{r_h x}{L}\right)^3$$

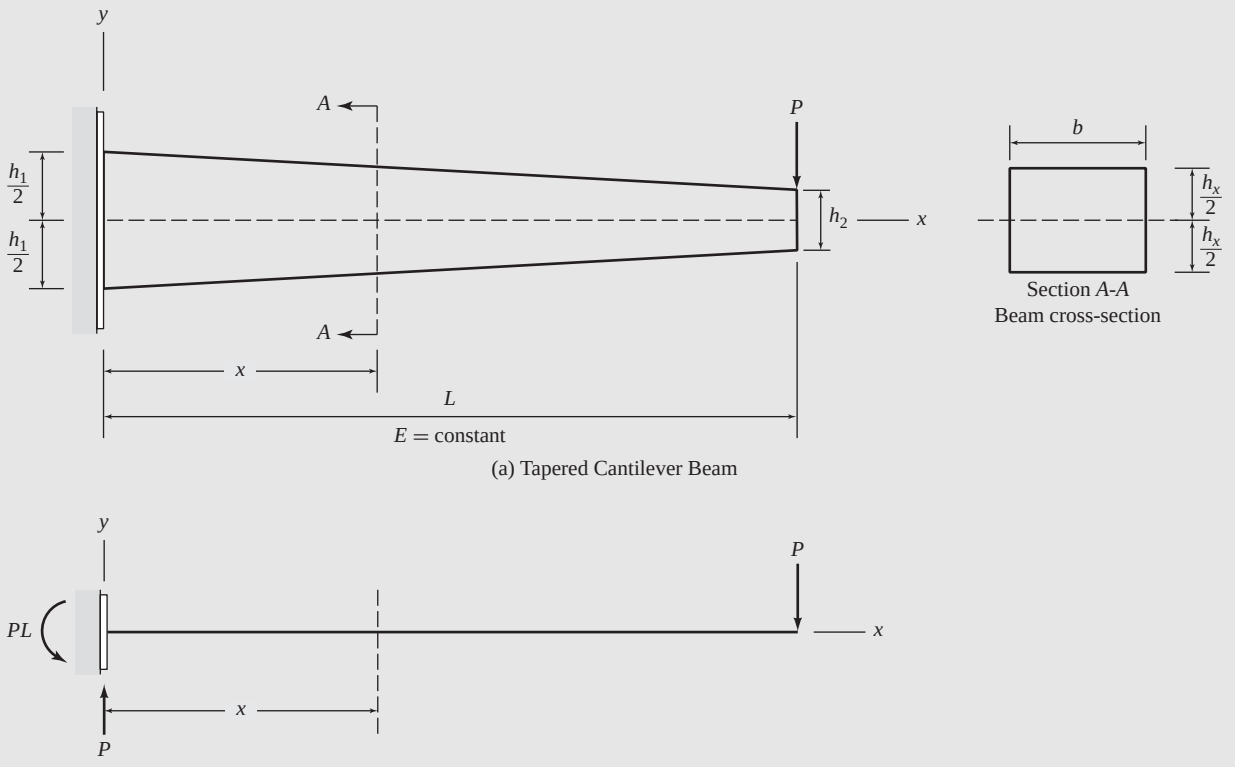

Fig. 9.19

in which r_h represents the *depth ratio* given by

$$r_h = \frac{h_1 - h_2}{h_1} \tag{1}$$

and $I_1 = bh_1^3/12 =$ beam's moment of inertia at its fixed end.

The equations for the slope and deflection can be derived by integrating the differential equation for bending of beams with variable cross-sections, which can be written as (see Eq. (5.5), Section 5.2)

$$\frac{d^2\bar{u}_y}{dx^2} = \frac{M}{EI_x} \tag{2}$$

From Fig. 9.19(b), we can see that the bending moment at the beam section at a distance x from its fixed end is

$$M = -P(L - x) \tag{3}$$

in which the negative sign indicates that the bending moment is negative in accordance with the *beam sign convention* (Fig. 5.4). Substituting Eq. (3) into Eq. (2) and integrating, we obtain the equation for slope as

$$\theta = -\frac{PL^3}{2EI_1}\left[\frac{L + r_h L - 2r_h x}{r_h^2(L - r_h x)^2}\right] + C_1 \tag{4}$$

Integrating once more, we obtain the equation for deflection as

$$\bar{u}_y = \frac{PL^3}{2EI_1 r_h^3}\left[\frac{1-r_h}{\left(1-\frac{r_h x}{L}\right)} + 2\ln\left(1-\frac{r_h x}{L}\right)\right] + C_1 x + C_2 \qquad \textbf{(5)}$$

The constants of integration, C_1 and C_2, are evaluated by applying the boundary conditions that at $x = 0$, $\theta = 0$ and $\bar{u}_y = 0$. Thus,

$$C_1 = \frac{PL^2}{2EI_1}\left(\frac{1+r_h}{r_h^2}\right)$$

$$C_2 = -\frac{PL^3(1-r_h)}{2EI_1 r_h^3}$$

By substituting these expressions for C_1 and C_2 into Eqs. (4) and (5) we determine the equations for slope and deflection of the beam as

$$\theta = \frac{Px}{2EI_1}\left[\frac{x-2L+r_h x}{\left(1-\frac{r_h x}{L}\right)^2}\right] \qquad \textbf{(6)}$$

$$\bar{u}_y = \frac{PL^3}{2EI_1 r_h^3\left(1-\frac{r_h x}{L}\right)}\left[\frac{2r_h x}{L} - \frac{r_h^2 x^2}{L^2}(1+r_h) + 2\left(1-\frac{r_h x}{L}\right)\ln\left(1-\frac{r_h x}{L}\right)\right] \qquad \textbf{(7)}$$

Finally, the expressions for slope and deflection at the free end of the tapered beam are obtained by setting $x = L$ in Eqs. (6) and (7), respectively. Thus,
Slope ($+\circlearrowleft$):

$$\theta_L = -\frac{PL^2}{2EI_1(1-r_h)} = -\frac{PL^2 h_1}{2EI_1 h_2} \qquad \textbf{Ans}$$

Deflection ($+\uparrow$):

$$\bar{u}_{yL} = -\frac{PL^3}{2EI_1 r_h^3(1-r_h)}[-2r_h + r_h^2(1+r_h) - 2(1-r_h)\ln(1-r_h)] \qquad \textbf{Ans}$$

EXAMPLE 9.7 Using a structural analysis computer program, determine the slope and deflection at the free end of the tapered cantilever beam shown in Fig. 9.20(a). The beam is of rectangular cross-section of width 150 mm, and its depth varies linearly from 400 mm at the fixed end to 100 mm at the free end, as shown in the figure. For analysis, divide the nonprismatic beam into smaller segments, and model each segment by a prismatic member (element) with a constant moment of inertia based on the average depth of the segment. Analyze several models of the beam with increasing number of members (elements) until the values of the desired displacements converge. Compare these numerical results with the exact analytical solutions for the tapered beam obtained from the expressions derived in Example 9.6.

SOLUTION Seven analytical models of the beam consisting of 1, 2, 3, 4, 6, 9, and 12 segments were analyzed using the computer program provided with this book. In these models, each tapered segment was approximated by a member of constant depth equal to the average depth of the segment. Figure 9.20(b) shows such a three-member model of the beam.

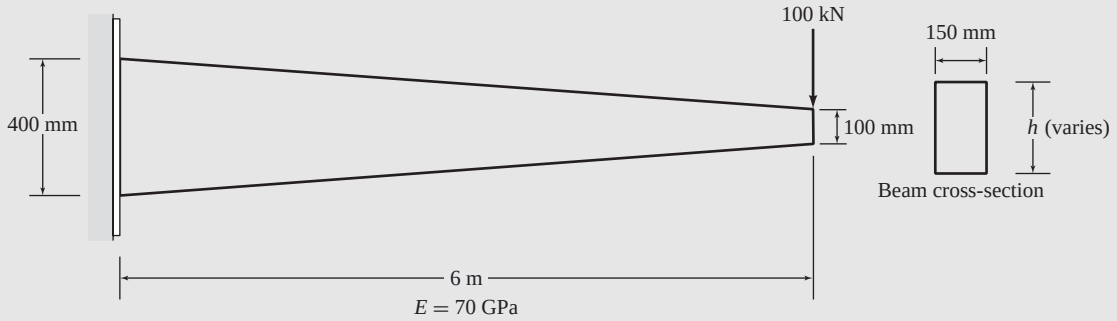

(a) Tapered Cantilever Beam

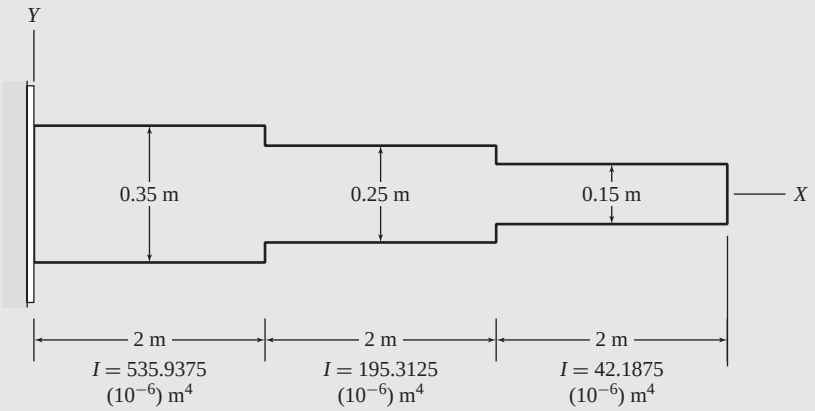

(b) Three-Member Analytical Model

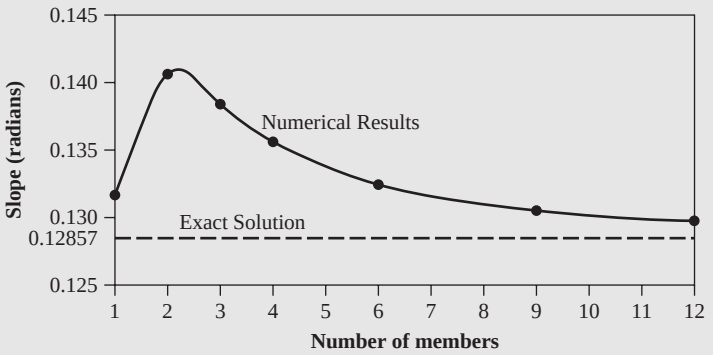

(c) Variation of Slope with Number of Members

Fig. 9.20

Numerical values of displacements at the free end of the beam obtained by using these analytical models are listed in Table 9.1, and plotted versus the number of members in Figs. 9.20(c) and (d).

The exact analytical solutions can be evaluated by substituting $P = 100$ kN, $L = 6$ m, $E = 70(10^6)$ kN/m^2, $h_1 = 0.4$ m, $h_2 = 0.1$ m, $I_1 = 0.15(0.4)^3/12 = 0.0008$ m^4, and $r_h = (0.4 - 0.1)/0.4 = 0.75$ into the expressions for slope and deflection at the cantilever's free end derived in Example 9.6. Thus,

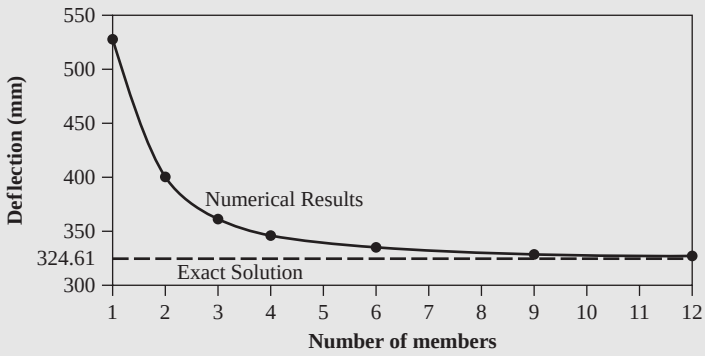

(d) Variation of Deflection with Number of Members

Fig. 9.20 (*continued*)

Table 9.1

Number of Member in Analytical Model	Slope		Deflection	
	(radians)	Error (%)	(mm)	Error (%)
1	0.13166	2.4034	526.63	62.235
2	0.14090	9.5901	401.66	23.736
3	0.13827	7.5445	361.89	11.485
4	0.13560	5.4678	345.91	6.5617
6	0.13246	3.0256	334.01	2.8958
9	0.13051	1.5089	328.73	1.2692
12	0.12973	0.90223	326.96	0.72395
Exact Solutions	0.12857		324.61	

Slope:

$$\theta_L = -\frac{PL^2 h_1}{2EI_1 h_2} = -0.12857\,\text{rad} = 0.12857\,\text{rad}\ \curvearrowright \qquad \textbf{Ans}$$

Deflection:

$$\bar{u}_{yL} = -\frac{PL^3}{2EI_1 r_h^3(1-r_h)}\left[-2r_h + r_h^2(1+r_h) - 2(1-r_h)\ln(1-r_h)\right]$$

$$= -\,0.32461\ \text{m} = 324.61\ \text{mm}\downarrow \qquad \textbf{Ans}$$

The exact values of slope and deflection are also given in Table 9.1, along with the percentage errors of the numerical results with respect to the exact solutions. We can see from this table and Figs. 9.20(c) and (d) that as the number of members in the computer model is increased, the numerical results tend to converge toward the exact solutions. **Ans**

9.9 SOLUTION OF LARGE SYSTEMS OF STIFFNESS EQUATIONS

In the computer programs for matrix stiffness analysis developed in previous chapters, we have stored the entire structure stiffness matrix **S** in computer memory, and have used Gauss–Jordan elimination to solve the structure stiffness equations, $\mathbf{Sd} = \overline{\mathbf{P}}$. While this approach provides a clear insight into the basic concept of the solution process and is easy to program, it is not efficient in the sense that it does not take advantage of the symmetry and other special features of the stiffness matrix **S**. In the case of large structures, a significant portion of the total memory and execution time required for analysis may be devoted to the storage and solution, respectively, of the structure stiffness equations. Accordingly, considerable research effort has been directed toward developing techniques and algorithms for efficiently generating, storing, and solving stiffness equations that arise in the analysis of large structures [2, 14, 26]. In this section, we discuss a commonly used procedure that takes advantage of the special features of the structure stiffness matrix to efficiently store and solve structural stiffness equations.

Half-Bandwidth of Structure Stiffness Matrices

The stiffness matrices **S** of large structures, in addition to being symmetric, are usually *sparse*, in the sense that they contain many 0 elements. Consider, for example, the analytical model of the six-degree-of-freedom continuous beam shown in Fig. 9.21(a) on the next page. The stiffness matrix **S** for this structure is also shown in the figure, in which all the nonzero elements are marked by $\times$s, and all the 0 elements are left blank. From this figure, we can see that, out of a total of 36 elements of **S**, 20 elements are 0s. Furthermore, this figure indicates that all the nonzero elements of **S** are located within a band centered on the main diagonal. Such a matrix, whose elements are all 0s, with the exception of those located within a band centered on the main diagonal, is referred to as a *banded matrix*. In general, a structure stiffness matrix is considered to be banded if

$$S_{ij} = 0 \quad \text{if} \quad |i - j| > NHB \tag{9.72}$$

where *NHB* is called the *half-bandwidth* of **S**, which is defined as *the number of elements in each row (or column) of the matrix, that are located within the band to the right of (or below) the diagonal element*. Thus, the half-bandwidth of the stiffness matrix of the continuous-beam analytical model of Fig. 9.21(a) is 1 (i.e., $NHB = 1$), as shown in the figure.

Although the total number of nonzero elements of a structure stiffness matrix remains the same, their locations depend on the order in which the structure's joints are numbered. Thus, the half-bandwidth of a structure stiffness matrix can be altered by renumbering the structure's joints. For example, if the numbers of two inner joints of the continuous beam of Fig. 9.21(a) are interchanged, the half-bandwidth of its stiffness matrix is increased to 2 (i.e., $NHB = 2$), as shown in Fig. 9.21(b). Note that the band of this **S** matrix contains both zero and nonzero elements.

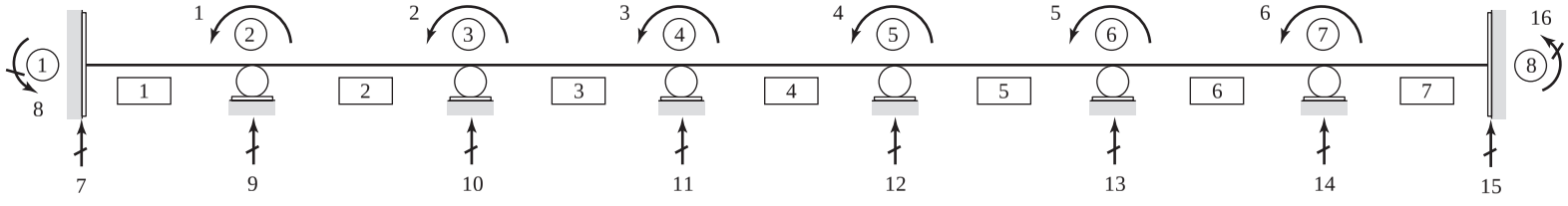

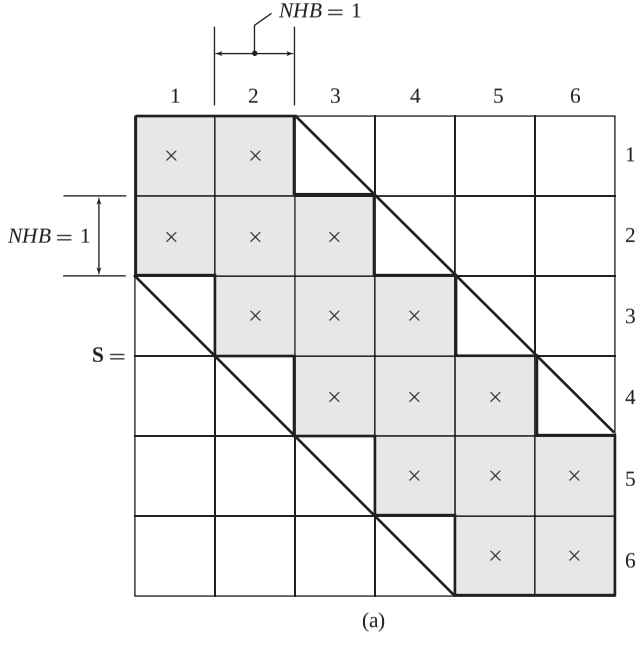

(a)

Fig. 9.21

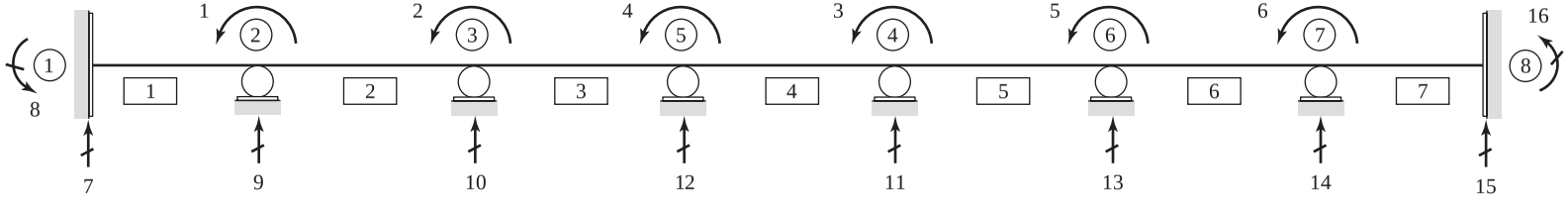

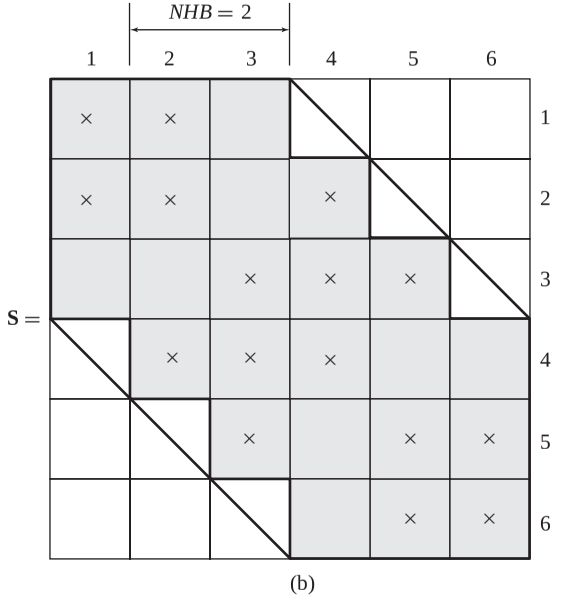

(b)

Fig. 9.21 (*continued*)

Since the structure stiffness matrices are assembled by storing the pertinent elements of the member stiffness matrices in their proper positions using member code numbers, the half-bandwidth of a structure stiffness matrix equals the maximum of the differences between the largest and smallest degree-of-freedom code numbers for the individual members of the structure; that is,

$$NHB = \max\{MCL_i - MCS_i\} \qquad i = 1, \ldots, NM \tag{9.73}$$

in which MCL_i and MCS_i denote, respectively, the largest and the smallest code numbers for member i, which correspond to the degrees of freedom (not the restrained coordinates) of the structure.

Considering again the analytical model of the continuous beam of Fig. 9.21(a), we can see that the code numbers for member 1 are 7, 8, 9, 1; of these, the first three numbers correspond to the restrained coordinates, and the fourth number represents a degree of freedom. Thus, the difference between the largest and smallest degree-of-freedom numbers for this member is $MCL_1 - MCS_1 = 1 - 1 = 0$. Similarly, we can see from the figure that for members 2 through 6, this difference is 1, and for member 7, it is 0. Thus, the half-bandwidth for the **S** matrix equals one. Note that when the numbers of two inner joints of the beam are interchanged as shown in Fig. 9.21(b), the difference in degree of freedom code numbers for members 3 and 5 increases by one, and as a result, the half-bandwidth of the **S** matrix widens by one element.

An important property of banded structure stiffness matrices is that the 0 elements outside the band remain 0 during the solution of the structure stiffness equations ($\mathbf{Sd} = \overline{\mathbf{P}}$); therefore, they need not be stored in computer memory for analysis. Furthermore, since the structure stiffness matrices are symmetric, only the diagonal elements, and the elements in the half band above (or below) the diagonal, need to be stored. As the stiffness matrices of large structures usually contain relatively few nonzero elements, significant savings in computer memory storage and execution time can be achieved, in the analysis of such structures, by numbering the joints to minimize the half-bandwidth of the stiffness matrix, and by storing and processing only the elements on the main diagonal, and within a half-bandwidth, of the stiffness matrix.

As discussed previously, the minimum possible half-bandwidth of a stiffness matrix can be obtained by numbering the joints of the structure in such an order that the largest difference between the joint numbers at the ends of any single member is as small as possible. For the configurations of the framed structures commonly encountered in practice, a relatively small (if not minimal) half-bandwidth of the stiffness matrix can usually be achieved by numbering joints consecutively across the dimension of the structure that has the least number of joints, as shown in Figs. 9.22 and 9.23 (on page 558).

The elements on the diagonal and in the upper half-bandwidth of **S** can be stored compactly in computer memory in a rectangular array $\hat{\mathbf{S}}$ of order $NDOF \times (NHB + 1)$, as illustrated in Fig. 9.24 on page 559 for a structure with $NDOF = 9$ and $NHB = 3$. As depicted in this figure, the elements in each row

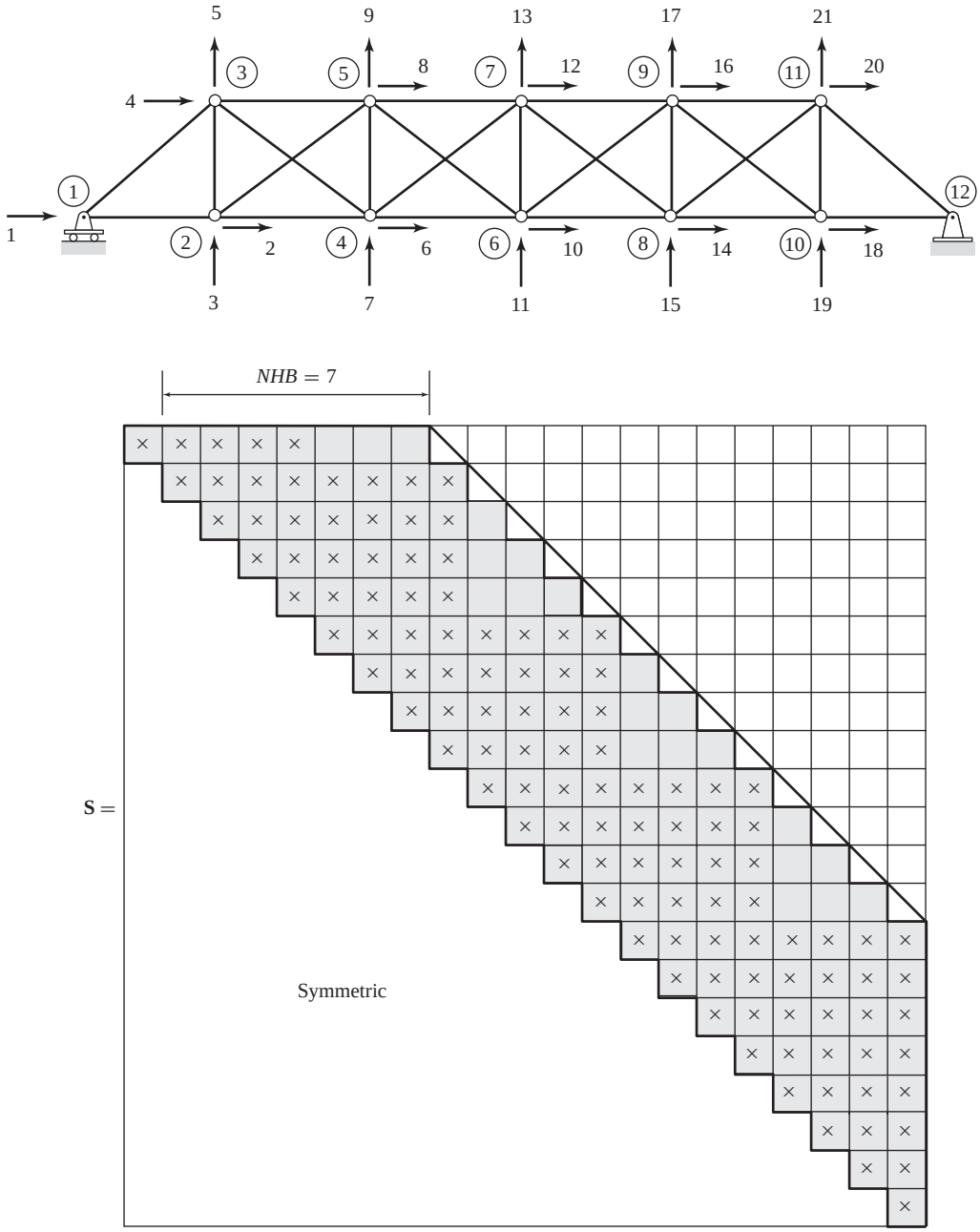

Fig. 9.22 *Joint Numbering for Minimum Half-Bandwidth* ($NDOF = 21$, $NHB = 7$)

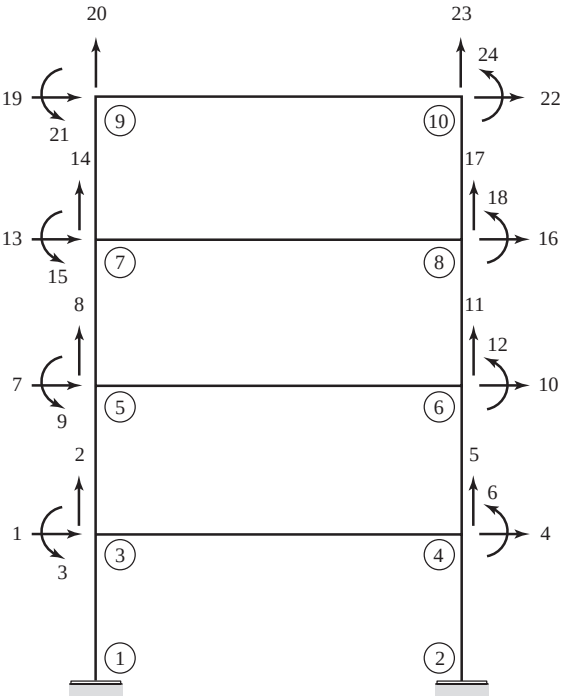

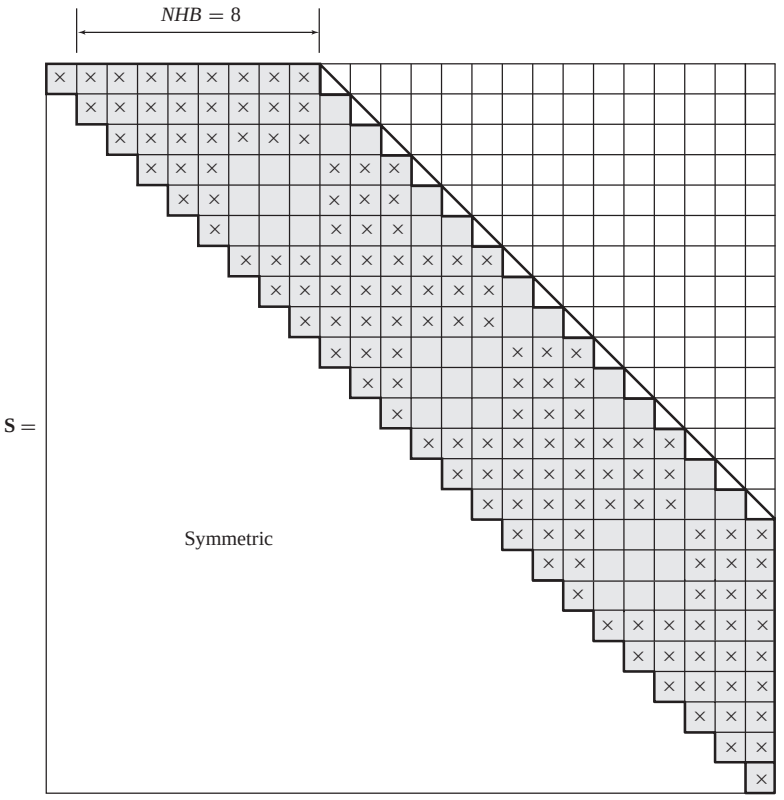

Fig. 9.23 *Joint Numbering for Minimum Half-Bandwidth* (*NDOF* = 24, *NHB* = 8)

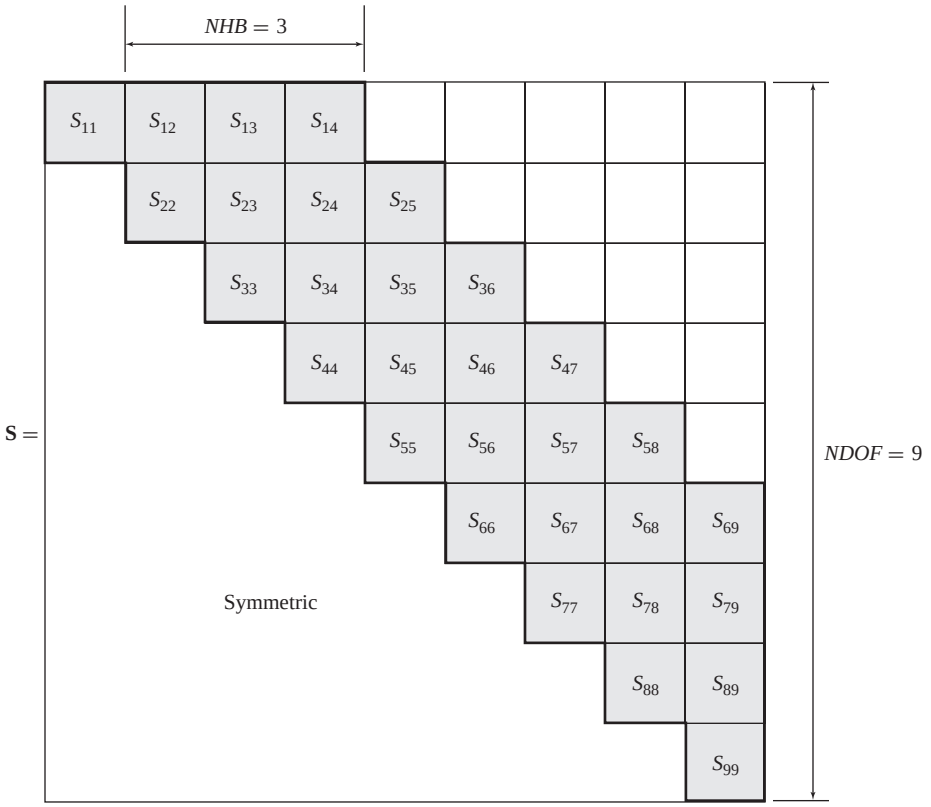

(a) Full Structure Stiffness Matrix **S** for $NDOF = 9$ and $NHB = 3$

Fig. 9.24

of **S** on the diagonal and in the half-bandwidth are stored in the same order in the corresponding row of the compact matrix $\hat{\mathbf{S}}$. The location of an element S_{ij} of **S** in the compact matrix $\hat{\mathbf{S}}$ is given by the relationship

$$S_{ij} = \hat{S}_{i,(1+j-i)} \qquad \begin{array}{l} \text{for } i = 1, 2, \ldots, NDOF; \\ \qquad j = i, i+1, \ldots, NHB + i \leq NDOF \end{array} \tag{9.74}$$

Solution of Banded Structure Stiffness Equations Using U^TDU Decomposition

Although Gauss–Jordan elimination, as discussed in Section 2.4, can be modified to take advantage of the symmetry and bandedness of structure stiffness equations, for the analysis of large structures, another type of elimination method, a *decomposition method*, is usually preferred. This is because, in decomposition methods, the solution is carried out in two distinct parts; namely, decomposition and substitution, with the decomposition part involving only the structure stiffness matrix **S**, but not the load vector $\overline{\mathbf{P}}$. Thus, the results

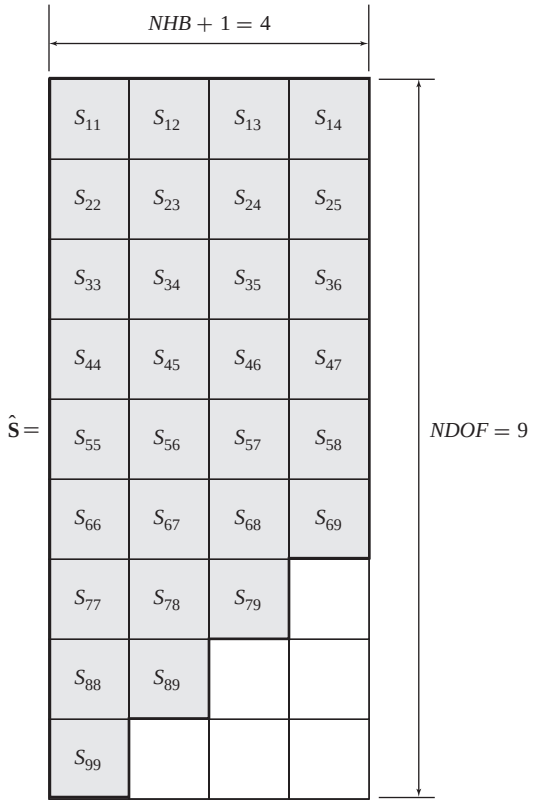

(b) Compact Structure Stiffness Matrix $\hat{\mathbf{S}}$ for $NDOF = 9$ and $NHB = 3$

Fig. 9.24 (*continued*)

of the time-consuming decomposition part can be stored for future use in case the structure needs to be reanalyzed for different loading conditions. In the following, we present a decomposition method, commonly used for solving large systems of structure stiffness equations, called the $\mathbf{U}^T\mathbf{D}\mathbf{U}$ *decomposition method*. The method is first formulated for the fully populated symmetric stiffness matrix **S**, and is then modified so that it can be used with the banded and compact forms of the structure stiffness matrix.

As stated previously, in the $\mathbf{U}^T\mathbf{D}\mathbf{U}$ decomposition method, the solution of the structure stiffness equations, $\mathbf{S}\mathbf{d} = \overline{\mathbf{P}}$, is carried out in two parts: decomposition and substitution. In decomposition, the structure stiffness matrix **S** is decomposed (or factored) into the matrix triple product,

$$\mathbf{S} = \mathbf{U}^T\mathbf{D}\mathbf{U} \tag{9.75}$$

in which **U** is a unit upper triangular matrix (i.e., an upper triangular matrix with diagonal elements equal to unity); and **D** is a diagonal matrix. For a general *n*-degree-of-freedom system, Eq. (9.75) can be written in expanded form as

$$\begin{bmatrix} S_{11} & S_{12} & S_{13} & \cdots & S_{1n} \\ & S_{22} & S_{23} & \cdots & S_{2n} \\ \text{(symmetric)} & & S_{33} & \cdots & S_{3n} \\ & & & \cdots & \cdots \\ & & & & S_{nn} \end{bmatrix} =$$

$$\begin{bmatrix} 1 & 0 & 0 & \cdots & 0 \\ U_{12} & 1 & 0 & \cdots & 0 \\ U_{13} & U_{23} & 1 & \cdots & 0 \\ \cdots & \cdots & \cdots & \cdots & \cdots \\ U_{1n} & U_{2n} & U_{3n} & \cdots & 1 \end{bmatrix} \begin{bmatrix} D_{11} & 0 & 0 & \cdots & 0 \\ 0 & D_{22} & 0 & \cdots & 0 \\ 0 & 0 & D_{33} & \cdots & 0 \\ \cdots & \cdots & \cdots & \cdots & \cdots \\ 0 & 0 & 0 & \cdots & D_{nn} \end{bmatrix} \begin{bmatrix} 1 & U_{12} & U_{13} & \cdots & U_{1n} \\ 0 & 1 & U_{23} & \cdots & U_{2n} \\ 0 & 0 & 1 & \cdots & U_{3n} \\ \cdots & \cdots & \cdots & \cdots & \cdots \\ 0 & 0 & 0 & \cdots & 1 \end{bmatrix} \tag{9.76}$$

Multiplying the three matrices on the right side of Eq. (9.76), we obtain

$$\begin{bmatrix} S_{11} & S_{12} & S_{13} & \cdots & S_{1n} \\ & S_{22} & S_{23} & \cdots & S_{2n} \\ \text{(symmetric)} & & S_{33} & \cdots & S_{3n} \\ & & & \cdots & \cdots \\ & & & & S_{nn} \end{bmatrix} =$$

$$\begin{bmatrix} D_{11} & D_{11}U_{12} & D_{11}U_{13} & \cdots & D_{11}U_{1n} \\ & D_{11}U_{12}^2 + D_{22} & D_{11}U_{12}U_{13} + D_{22}U_{23} & \cdots & D_{11}U_{12}U_{1n} + D_{22}U_{2n} \\ \text{(symmetric)} & & D_{11}U_{13}^2 + D_{22}U_{23}^2 + D_{33} & \cdots & D_{11}U_{13}U_{1n} + D_{22}U_{23}U_{2n} + D_{33}U_{3n} \\ & & & \cdots & \cdots \\ & & & & D_{11}U_{1n}^2 + D_{22}U_{2n}^2 + D_{33}U_{3n}^2 + \cdots + D_{nn} \end{bmatrix}$$

(9.77)

By comparing the corresponding elements of the matrices **S** and $\mathbf{U}^T\mathbf{D}\mathbf{U}$, on the left and right sides, respectively, of Eq. (9.77), we can develop an algorithm for evaluating the elements of matrices **D** and **U**. By comparing the elements in row 1 column 1 of the two matrices, we can see that $D_{11} = S_{11}$. With D_{11} known, the elements in the first row of **U** can be obtained by equating the remaining elements in the first rows of **S** and $\mathbf{U}^T\mathbf{D}\mathbf{U}$. This yields $U_{12} = S_{12}/D_{11}$, $U_{13} = S_{13}/D_{11}$, . . . , $U_{1n} = S_{1n}/D_{11}$. Next, we equate the corresponding elements in the second rows of **S** and $\mathbf{U}^T\mathbf{D}\mathbf{U}$ in Eq. (9.77) to obtain the second rows of **D** and **U**, and so on. The general recurrence relationships for computation of the elements of **D** and **U** can be expressed as follows.

$$D_{ii} = \begin{cases} S_{ii} & \text{for } i = 1 \\ S_{ii} - \sum_{k=1}^{i-1} D_{kk}U_{ki}^2 & \text{for } i = 2, 3, \ldots, NDOF \end{cases} \tag{9.78a}$$

$$U_{ij} = \begin{cases} \dfrac{S_{ij}}{D_{ii}} & \text{for } i = 1;\ j = i+1,\ i+2, \ldots, NDOF \\ \dfrac{1}{D_{ii}}\left(S_{ij} - \sum_{k=1}^{i-1} D_{kk}U_{ki}U_{kj}\right) & \text{for } i = 2, 3, \ldots, NDOF - 1; \\ & \quad j = i+1, i+2, \ldots, NDOF \end{cases} \tag{9.78b}$$

$$U_{ii} = 1 \qquad \text{for } i = 1, 2, \ldots, NDOF \tag{9.78c}$$

The nonzero elements of **D** and **U** are computed by starting at the first row number (i.e., $i = 1$), and proceeding sequentially to the last row number (i.e., $i = NDOF$). As implied by Eqs. 9.78(a) and (b), for each row number i, the diagonal element D_{ii} (Eq. (9.78a)) must be computed before the elements U_{ij} (Eq. (9.78b)) of the ith row of **U** can be calculated.

With the structure stiffness matrix **S** now decomposed into triangular and diagonal matrices, we can now begin the substitution part of the solution process. Substitution of $\mathbf{S} = \mathbf{U}^T\mathbf{D}\mathbf{U}$ into the structure stiffness equations, $\mathbf{S}\mathbf{d} = \overline{\mathbf{P}}$, yields

$$\mathbf{U}^T\mathbf{D}\mathbf{U}\,\mathbf{d} = \overline{\mathbf{P}} \tag{9.79}$$

The substitution part is carried out in two steps: forward substitution, and back substitution. In the forward substitution step, Eq. (9.79) is written as

$$\mathbf{U}^T\mathbf{D}\,\hat{\mathbf{d}} = \overline{\mathbf{P}} \tag{9.80}$$

with

$$\hat{\mathbf{d}} = \mathbf{U}\mathbf{d} \tag{9.81}$$

in which $\hat{\mathbf{d}}$ is an auxiliary vector of unknowns. Equation (9.80) can be written in expanded form as

$$\begin{bmatrix} D_{11} & 0 & 0 & \cdots & 0 \\ D_{11}U_{12} & D_{22} & 0 & \cdots & 0 \\ D_{11}U_{13} & D_{22}U_{23} & D_{33} & \cdots & 0 \\ \cdots & \cdots & \cdots & \cdots & \cdots \\ D_{11}U_{1n} & D_{22}U_{2n} & D_{33}U_{3n} & \cdots & D_{nn} \end{bmatrix} \begin{bmatrix} \hat{d}_1 \\ \hat{d}_2 \\ \hat{d}_3 \\ \cdots \\ \hat{d}_n \end{bmatrix} = \begin{bmatrix} \overline{P}_1 \\ \overline{P}_2 \\ \overline{P}_3 \\ \cdots \\ \overline{P}_n \end{bmatrix} \tag{9.82}$$

from which we can see that the auxiliary unknowns $\hat{\mathbf{d}}$ can be determined by the simple process of forward substitution, starting with the first row and proceeding sequentially to the last row. From the first row of Eq. (9.82), we can see that $\hat{d}_1 = \overline{P}_1/D_{11}$. With $\hat{d}_1$ known, the value of $\hat{d}_2$ can now be determined by solving the equation in the second row of Eq. (9.82); that is, $\hat{d}_2 = (\overline{P}_2 - D_{11}U_{12}\hat{d}_1)/D_{22}$. Next, we calculate $\hat{d}_3$ by solving the equation in the third row of Eq. (9.82), and so on. In general, the elements of $\hat{\mathbf{d}}$ can be computed as

$$\hat{d}_i = \begin{cases} \dfrac{\overline{P}_i}{D_{ii}} & \text{for } i = 1 \\ \dfrac{1}{D_{ii}}\left(\overline{P}_i - \displaystyle\sum_{k=1}^{i-1} D_{kk}U_{ki}\hat{d}_k\right) & \text{for } i = 2, 3, \ldots, NDOF \end{cases} \tag{9.83}$$

Once the auxiliary vector $\hat{\mathbf{d}}$ has been evaluated, the unknown joint displacement vector **d** can be calculated by solving Eq. (9.81), using back substitution. The expanded form of Eq. (9.81) can be expressed as

$$\begin{bmatrix} 1 & U_{12} & U_{13} & \cdots & U_{1,n-1} & U_{1n} \\ 0 & 1 & U_{23} & \cdots & U_{2,n-1} & U_{2n} \\ 0 & 0 & 1 & \cdots & U_{3,n-1} & U_{3n} \\ \cdots & \cdots & \cdots & \cdots & \cdots & \cdots \\ 0 & 0 & 0 & \cdots & 1 & U_{n-1,n} \\ 0 & 0 & 0 & \cdots & 0 & 1 \end{bmatrix} \begin{bmatrix} d_1 \\ d_2 \\ d_3 \\ \cdots \\ d_{n-1} \\ d_n \end{bmatrix} = \begin{bmatrix} \hat{d}_1 \\ \hat{d}_2 \\ \hat{d}_3 \\ \cdots \\ \hat{d}_{n-1} \\ \hat{d}_n \end{bmatrix} \tag{9.84}$$

From which we can see that the unknown joint displacements **d** can be determined by the simple process of back substitution, starting with the last row and proceeding sequentially to the first row. From the last row of Eq. (9.84), we can see that $d_n = \hat{d}_n$. With d_n known, the value of d_{n-1} can now be determined by solving the equation in the next to the last row of Eq. (9.84); that is, $d_{n-1} = \hat{d}_{n-1} - U_{n-1,n}\, d_n$. The back substitution is continued until all the joint displacements have been calculated. The back substitution process can be represented by the recurrence equation

$$d_i = \begin{cases} \hat{d}_i & \text{for } i = NDOF \\ \hat{d}_i - \sum_{k=i+1}^{NDOF} U_{ik} d_k & \text{for } i = NDOF - 1,\ NDOF - 2, \ldots, 1 \end{cases} \tag{9.85}$$

As discussed in the foregoing paragraphs, the $\mathbf{U}^T\mathbf{D}\mathbf{U}$ decomposition procedure for solving structure stiffness equations essentially consists of the following steps.

1. Decompose the structure stiffness matrix **S** into a diagonal matrix **D**, and a unit upper triangular matrix **U**, by applying Eqs. (9.78).
2. Calculate the auxiliary vector $\hat{\mathbf{d}}$ using forward substitution (Eq. (9.83)).
3. Determine the unknown joint displacements **d** by back substitution (Eq. (9.85)).

EXAMPLE 9.8 Use $\mathbf{U}^T\mathbf{D}\mathbf{U}$ decomposition to solve the following system of structural stiffness equations.

$$\begin{bmatrix} 5 & 2 & -1 & 0 \\ & 6 & -3 & 2 \\ \text{(symmetric)} & & 4 & 1 \\ & & & 7 \end{bmatrix} \begin{bmatrix} d_1 \\ d_2 \\ d_3 \\ d_4 \end{bmatrix} = \begin{bmatrix} -19 \\ -22 \\ 22 \\ -6 \end{bmatrix}$$

SOLUTION *Decomposition:* By applying Eqs. (9.78),

$$D_{11} = S_{11} = 5$$

$$U_{12} = \frac{S_{12}}{D_{11}} = \frac{2}{5} = 0.4$$

$$U_{13} = \frac{S_{13}}{D_{11}} = \frac{-1}{5} = -0.2$$

$$U_{14} = 0$$

$$U_{11} = U_{22} = U_{33} = U_{44} = 1$$

$$D_{22} = S_{22} - D_{11}U_{12}^2 = 6 - 5(0.4)^2 = 5.2$$

$$U_{23} = \frac{1}{D_{22}}(S_{23} - D_{11}U_{12}U_{13}) = \frac{1}{5.2}\,[-3 - 5(0.4)(-0.2)] = -0.5$$

$$U_{24} = \frac{1}{D_{22}}(S_{24} - D_{11}U_{12}U_{14}) = \frac{1}{5.2}\,[2 - 5(0.4)(0)] = 0.38462$$

$$D_{33} = S_{33} - D_{11}U_{13}^2 - D_{22}U_{23}^2 = 4 - 5(-0.2)^2 - 5.2(-0.5)^2 = 2.5$$

$$U_{34} = \frac{1}{D_{33}}(S_{34} - D_{11}U_{13}U_{14} - D_{22}U_{23}U_{24})$$
$$= \frac{1}{2.5}[1 - 5(-0.2)(0) - 5.2(-0.5)(0.38462)] = 0.8$$
$$D_{44} = S_{44} - D_{11}U_{14}^2 - D_{22}U_{24}^2 - D_{33}U_{34}^2$$
$$= 7 - 5(0)^2 - 5.2(0.38462)^2 - 2.5(0.8)^2 = 4.6308$$

Thus,

$$\mathbf{D} = \begin{bmatrix} 5 & 0 & 0 & 0 \\ 0 & 5.2 & 0 & 0 \\ 0 & 0 & 2.5 & 0 \\ 0 & 0 & 0 & 4.6308 \end{bmatrix} \qquad \mathbf{U} = \begin{bmatrix} 1 & 0.4 & -0.2 & 0 \\ 0 & 1 & -0.5 & 0.38462 \\ 0 & 0 & 1 & 0.8 \\ 0 & 0 & 0 & 1 \end{bmatrix}$$

Forward Substitution: Using Eq. (9.83),

$$\hat{d}_1 = \frac{\overline{P}_1}{D_{11}} = \frac{-19}{5} = -3.8$$

$$\hat{d}_2 = \frac{1}{D_{22}}(\overline{P}_2 - D_{11}U_{12}\hat{d}_1) = \frac{1}{5.2}[-22 - 5(0.4)(-3.8)] = -2.7692$$

$$\hat{d}_3 = \frac{1}{D_{33}}(\overline{P}_3 - D_{11}U_{13}\hat{d}_1 - D_{22}U_{23}\hat{d}_2)$$

$$= \frac{1}{2.5}[22 - 5(-0.2)(-3.8) - 5.2(-0.5)(-2.7692)] = 4.4$$

$$\hat{d}_4 = \frac{1}{D_{44}}(\overline{P}_4 - D_{11}U_{14}\hat{d}_1 - D_{22}U_{24}\hat{d}_2 - D_{33}U_{34}\hat{d}_3)$$

$$= \frac{1}{4.6308}[-6 - 5(0)(-3.8) - 5.2(0.38462)(-2.7692) - 2.5(0.8)(4.4)] = -2$$

Thus,

$$\hat{\mathbf{d}} = \begin{bmatrix} -3.8 \\ -2.7692 \\ 4.4 \\ -2 \end{bmatrix}$$

Back Substitution: Applying Eq. (9.85),

$$d_4 = \hat{d}_4 = -2$$
$$d_3 = \hat{d}_3 - U_{34}d_4 = 4.4 - 0.8(-2) = 6$$
$$d_2 = \hat{d}_2 - U_{23}d_3 - U_{24}d_4 = -2.7692 - (-0.5)6 - 0.38462(-2) = 1$$
$$d_1 = \hat{d}_1 - U_{12}d_2 - U_{13}d_3 - U_{14}d_4 = -3.8 - 0.4(1) - (-0.2)6 - 0(-2) = -3$$

Thus, the solution of the given system of equations is

$$\mathbf{d} = \begin{bmatrix} -3 \\ 1 \\ 6 \\ -2 \end{bmatrix}$$ **Ans**

If the structure stiffness matrix **S** is banded, then the corresponding **U** matrix contains nonzero elements only on its diagonal and within the upper half-bandwidth, as shown in Fig. 9.25(a) on the next page. In such cases, the computational effort required for solution can be significantly reduced by calculating only the elements in the upper half-bandwidth of **U**. From Fig. 9.25(a), we can see that, in any row number i of **U**, all the nonzero elements are located in column numbers i through $i + NHB \leq NDOF$. Similarly, in any column number j of **U**, the nonzero elements are located in row numbers $j - NHB \geq 1$ through j. Using the foregoing ranges for the indexing parameters in Eqs. (9.78), (9.83), and (9.85), we obtain the following modified recurrence formulas for solving the banded systems of structure stiffness equations by the $\mathbf{U}^T\mathbf{D}\mathbf{U}$ decomposition method.

Decomposition

$$D_{ii} = \begin{cases} S_{ii} & \text{for } i = 1 \\ S_{ii} - \sum_{k=m_1}^{i-1} D_{kk} U_{ki}^2 & \text{for } i = 2, 3, \ldots, NDOF \end{cases}$$

with $m_1 = i - NHB \geq 1$

$$U_{ij} = \begin{cases} \dfrac{S_{ij}}{D_{ii}} & \text{for } i = 1;\ j = i+1, i+2, \ldots, i + NHB \leq NDOF \\ \dfrac{1}{D_{ii}}(S_{ij} - B_{ij}) & \text{for } i = 2, 3, \ldots, NDOF - 1;\ j = i+1, i+2, \ldots, i + NHB \leq NDOF \end{cases}$$

with

$$B_{ij} = \begin{cases} \sum_{k=m_2}^{i-1} D_{kk} U_{ki} U_{kj} & \text{for } m_2 \leq i - 1 \\ 0 & \text{for } m_2 > i - 1 \end{cases}$$

in which, $m_2 = j - NHB \geq 1$

$$U_{ii} = 1 \qquad \text{for } i = 1, 2, \ldots, NDOF$$

(9.86)

Forward Substitution

$$\hat{d}_i = \begin{cases} \dfrac{\overline{P}_i}{D_{ii}} & \text{for } i = 1 \\ \dfrac{1}{D_{ii}} \left(\overline{P}_i - \sum_{k=m_1}^{i-1} D_{kk} U_{ki} \hat{d}_k \right) & \text{for } i = 2, 3, \ldots, NDOF \end{cases}$$

(9.87)

Back Substitution

$$d_i = \begin{cases} \hat{d}_i & \text{for } i = NDOF \\ \hat{d}_i - \sum_{k=i+1}^{m_3} U_{ik} d_k & \text{for } i = NDOF - 1, NDOF - 2, \ldots, 1 \end{cases}$$

with $m_3 = i + NHB \leq NDOF$

(9.88)

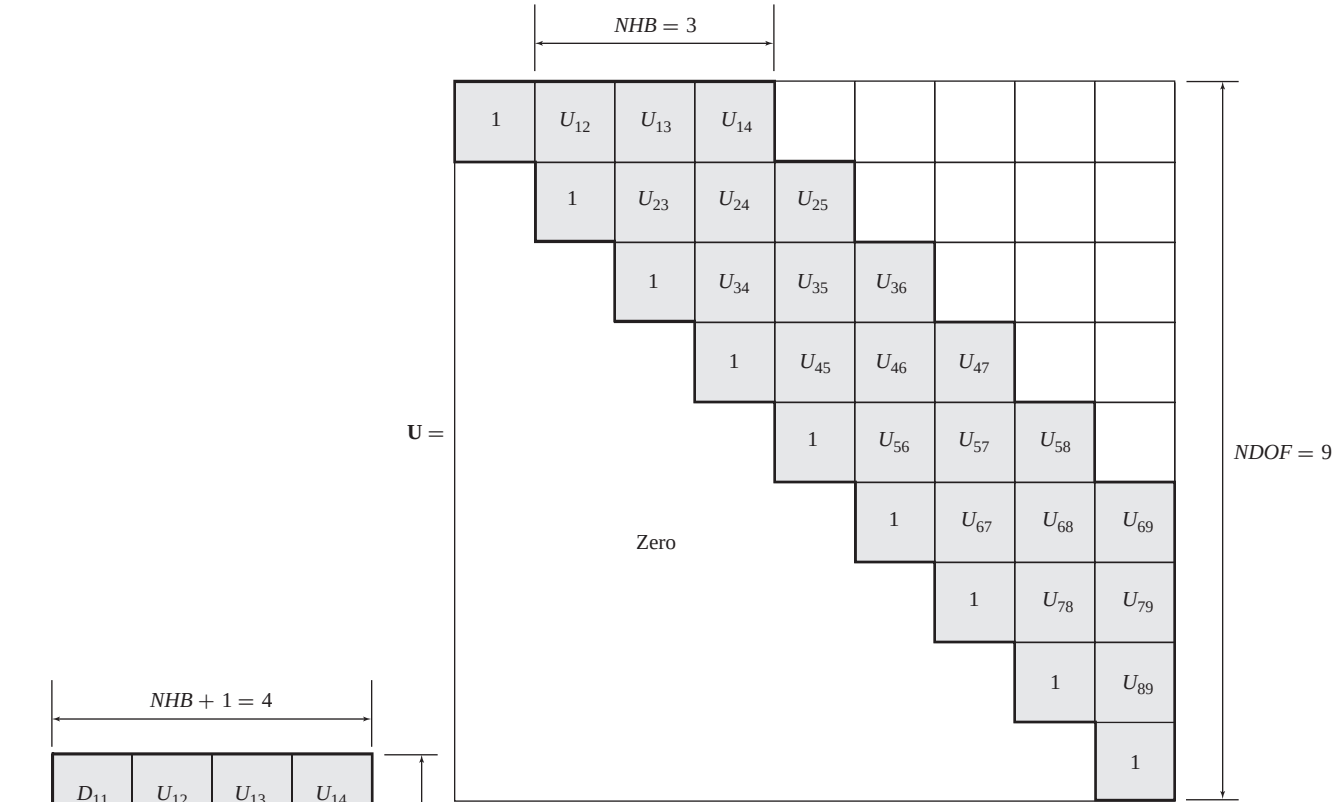

(a) Upper Unit Triangular Matrix **U** for a Structure Stiffness Matrix with $NDOF = 9$ and $NHB = 3$

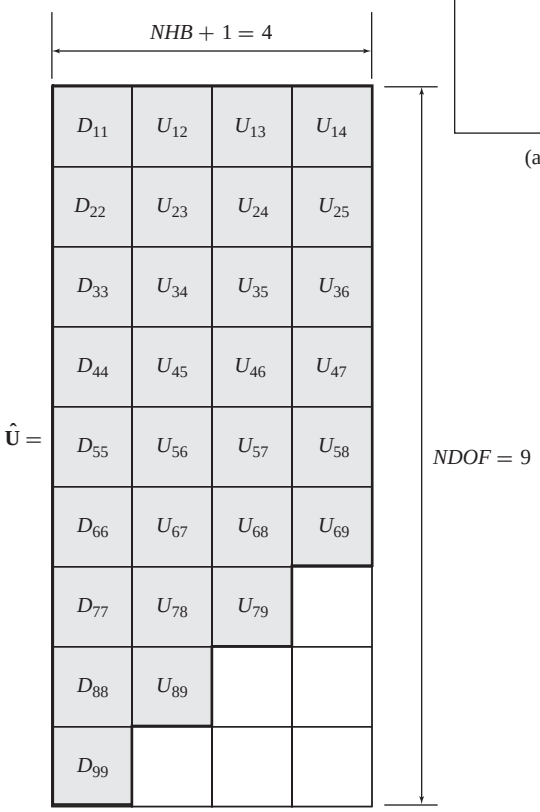

(b) Storage of **D** and **U** in Compact Form

Fig. 9.25

As stated before, the elements on the diagonal and in the upper half-bandwidth of **S** can be compactly stored in computer memory in a rectangular array $\hat{\mathbf{S}}$ of order $NDOF \times (NHB + 1)$ (see Fig. 9.24(b)). In an analogous manner, a rectangular array $\hat{\mathbf{U}}$, of the same order as $\hat{\mathbf{S}}$, can be defined to store the elements on the diagonal of **D** and in the upper half-bandwidth of **U**, as depicted in Fig. 9.25(b). As indicated there, the diagonal elements of **D** are stored in the first column of $\hat{\mathbf{U}}$, and the elements, in each row of **U**, in the half-bandwidth, are stored in the same order in the corresponding row of $\hat{\mathbf{U}}$. The locations of the relevant elements of **D** and **U** in the compact matrix $\hat{\mathbf{U}}$ can be determined by using the following relationships.

$$\begin{aligned} D_{ii} &= \hat{U}_{i1} && \text{for } i = 1, 2, \ldots, NDOF \\ U_{ij} &= \hat{U}_{i,(1+j-i)} && \text{for } i = 1, 2, \ldots, NDOF - 1; \\ & && j = i + 1, i + 2, \ldots, NHB + i \leq NDOF \end{aligned} \tag{9.89}$$

Applying Eqs. (9.74) and (9.89), we obtain the following modified algorithm for solving the banded systems of structure stiffness equations, in terms of the elements of compact matrices $\hat{\mathbf{S}}$ and $\hat{\mathbf{U}}$.

Decomposition

$$\hat{U}_{i1} = \begin{cases} \hat{S}_{i1} & \text{for } i = 1 \\ \hat{S}_{i1} - \sum_{k=m_1}^{i-1} \hat{U}_{k1} \hat{U}^2_{k,(1+i-k)} & \text{for } i = 2, 3, \ldots, NDOF \end{cases}$$

with $m_1 = i - NHB \geq 1$

$$\hat{U}_{ij} = \begin{cases} \dfrac{\hat{S}_{ij}}{\hat{U}_{i1}} & \text{for } i = 1;\ j = 2, 3, \ldots, NHB + 1 \\ \dfrac{1}{\hat{U}_{i1}} (\hat{S}_{ij} - \hat{B}_{ij}) & \text{for } i = 2, 3, \ldots, NDOF - 1;\ j = 2, 3, \ldots, NHB + 1 \leq NDOF - i + 1 \end{cases} \tag{9.90}$$

with

$$\hat{B}_{ij} = \begin{cases} \sum_{k=\hat{m}_2}^{i-1} \hat{U}_{k1} \hat{U}_{k,(1+i-k)} \hat{U}_{k,(i+j-k)} & \text{for } \hat{m}_2 \leq i - 1 \\ 0 & \text{for } \hat{m}_2 > i - 1 \end{cases}$$

in which $\hat{m}_2 = i + j - NHB - 1 \geq 1$

Forward Substitution

$$\hat{d}_i = \begin{cases} \dfrac{\overline{P}_i}{\hat{U}_{i1}} & \text{for } i = 1 \\ \dfrac{1}{\hat{U}_{i1}} \left(\overline{P}_i - \sum_{k=m_1}^{i-1} \hat{U}_{k1} \hat{U}_{k,(1+i-k)} \hat{d}_k \right) & \text{for } i = 2, 3, \ldots, NDOF \end{cases} \tag{9.91}$$

Back Substitution

$$d_i = \begin{cases} \hat{d}_i & \text{for } i = NDOF \\ \hat{d}_i - \sum_{k=i+1}^{m_3} \hat{U}_{i,(1+k-i)} d_k & \text{for } i = NDOF-1, NDOF-2, \ldots, 1 \end{cases}$$

$$\text{with } m_3 = i + NHB \leq NDOF$$

(9.92)

In the computer implementation of the foregoing procedure, computer memory requirements can be reduced by creating only the $\hat{\mathbf{S}}$ matrix, but not the $\hat{\mathbf{U}}$ matrix. Each element $\hat{U}_{ij}$ of the $\hat{\mathbf{U}}$ matrix is now computed and stored in the $\hat{\mathbf{S}}$ matrix in the location originally occupied by the corresponding $\hat{S}_{ij}$ element. Thus, at the end of the decomposition part of the solution process, the $\hat{\mathbf{S}}$ matrix contains all the elements of the $\hat{\mathbf{U}}$ matrix, and can be used in the substitution part of the solution. Also, this $\hat{\mathbf{S}}$ matrix, now containing the elements of $\hat{\mathbf{U}}$ (or $\mathbf{D}$ and $\mathbf{U}$), can be stored for any future reanalysis of the structure for different loading conditions.

In this section, we have considered only one of the many available methods for solving large systems of structural stiffness equations. For a comprehensive coverage of the various solution methods, the reader should refer to references [2, 14, 26].

SUMMARY

In this chapter, we have considered some extensions and modifications of the matrix stiffness method developed in previous chapters. We have also considered techniques for modeling some special features and details of structures, so that more realistic structural responses can be predicted from the analysis.

We studied an alternative formulation of the stiffness method, which involves the structure stiffness matrix for all the coordinates (including the restrained coordinates) of the structure. The advantages of this alternative formulation are that the support displacement effects can be incorporated into the analysis in a direct and straightforward manner, and the reactions can be calculated using the structure stiffness relations. The main disadvantage of this formulation is that it requires significantly more computer memory than the standard formulation.

We presented an approximate method for the analysis of rectangular building frames, neglecting the effects of member axial deformations. This approach significantly reduces the number of structural degrees of freedom to be considered in an analysis. This approximate approach is appropriate only for frames in which the member axial deformations are small enough, as compared to bending deformations, to have a negligible effect on their responses.

The basic concepts of condensation of structural degrees of freedom, and analysis using substructures, were discussed. These approaches can be used in the analysis of large structures to reduce the number of stiffness equations that must be processed, and solved simultaneously.

A commonly used technique for modeling an inclined roller support was described, in which the support is replaced with an imaginary axial force member with large axial stiffness, and oriented in the direction perpendicular to the incline. Modified member stiffness relations, considering the effects of rigid end offsets, were also presented. Procedures for including the effects of semirigid connections, and shear deformations, in the analysis, were discussed, and the analysis of structures composed of nonprismatic members considered.

Finally, we defined the half-bandwidth of structural stiffness matrices; and discussed procedures for efficiently numbering the structure's degrees of freedom, and for storing its stiffness matrix in computer memory by taking advantage of its symmetry and bandedness. Also considered was the commonly used $\mathbf{U}^T\mathbf{D}\mathbf{U}$ decomposition method for solving large banded systems of structure stiffness equations.

PROBLEMS

Section 9.1

9.1 Determine the joint displacements, member axial forces, and support reactions for the plane truss shown in Fig. P9.1, due to the combined effect of the loading shown and a settlement of $\frac{1}{2}$ in. of support 2. Use the alternative formulation of the matrix stiffness method.

9.2 Determine the joint displacements, member axial forces, and support reactions for the plane truss shown in Fig. P9.2, due to the combined effect of the loading shown and a settlement of $\frac{1}{4}$ in. of support 3. Use the alternative formulation of the matrix stiffness method.

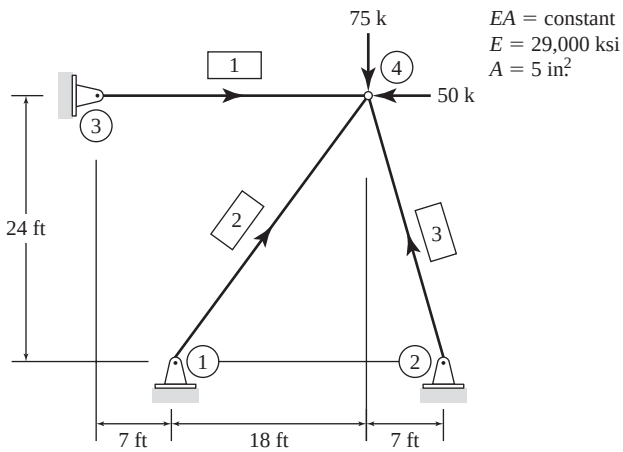

Fig. P9.1

9.3 Determine the joint displacements, member end forces, and support reactions for the three-span continuous beam shown in Fig. P9.3 on the next page, due to settlements of 8 and 30 mm, respectively, of supports 2 and 3. Use the alternative formulation of the matrix stiffness method.

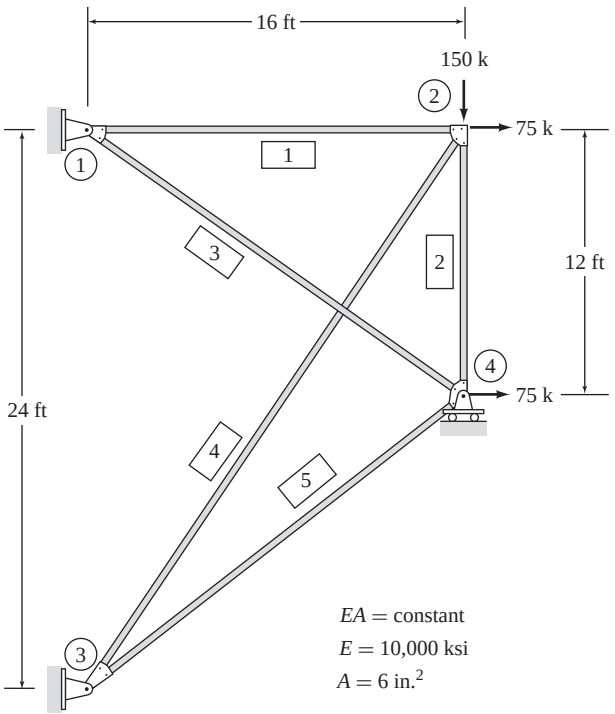

Fig. P9.2

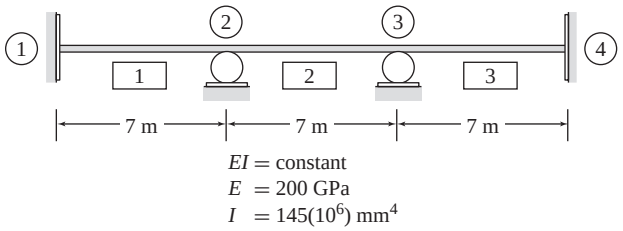

Fig. P9.3

9.4 Determine the joint displacements, member local end forces, and support reactions for the plane frame shown in Fig. P9.4, due to the combined effect of the following: (a) the loading shown in the figure, (b) a clockwise rotation of 0.017 radians of the left support, and (c) a settlement of $\frac{3}{4}$ in. of the right support. Use the alternative formulation of the matrix stiffness method.

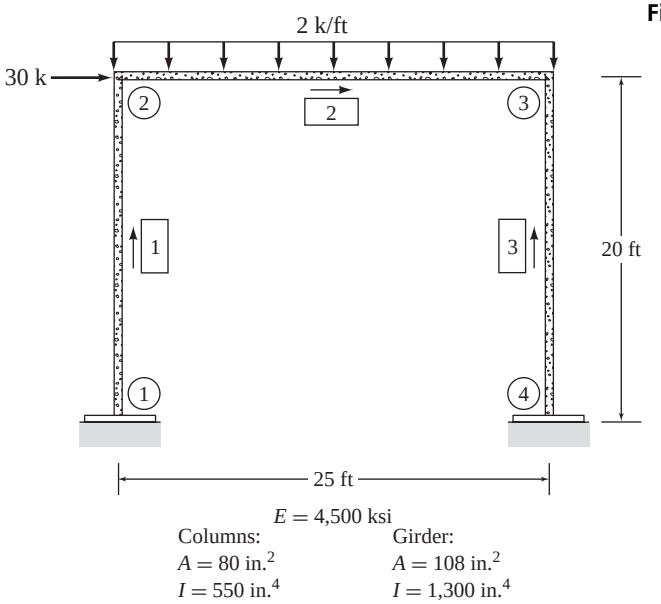

Fig. P9.4, P9.7, P9.10

Section 9.2

9.5 through 9.8 Determine the approximate joint displacements, member local end forces, and support reactions for the frames shown in Figs. P9.5 through P9.8, assuming the members to be inextensible.

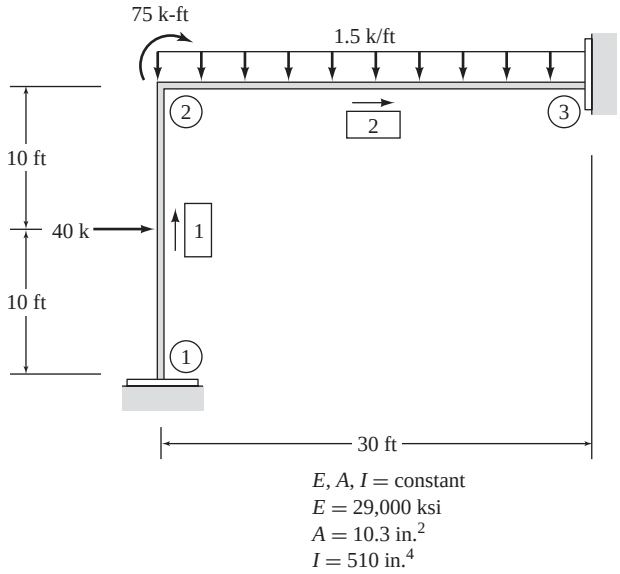

Fig. P9.5, P9.9

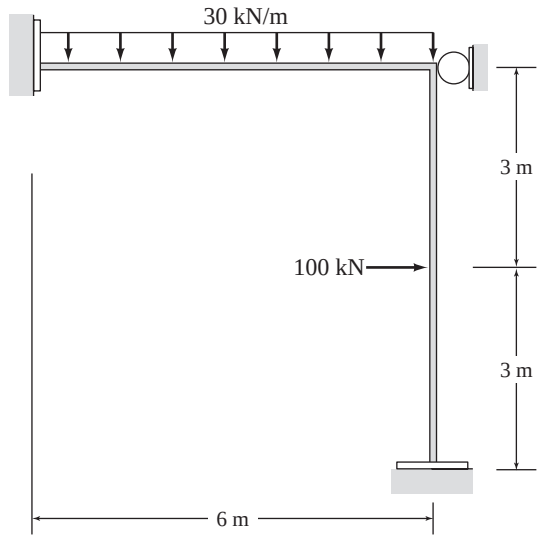

Fig. P9.6

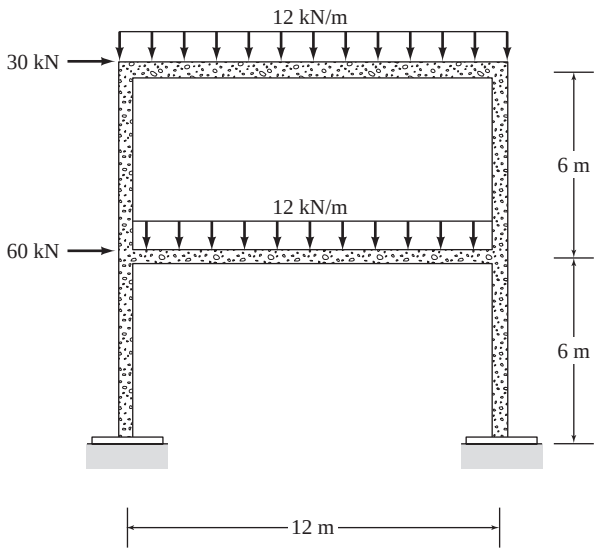

Fig. P9.8

Section 9.3

9.9 and 9.10 Analyze the plane frames shown in Figs. P9.9 and P9.10 using condensation, by treating the rotations of free joints as internal degrees of freedom.

Section 9.8

9.11 and 9.12 Derive the equations of fixed-end forces due to the member loads acting on the nonprismatic beams shown in Figs. P9.11 and P9.12.

Section 9.9

9.13 Solve the following system of simultaneous equations using the $\mathbf{U}^T\mathbf{D}\mathbf{U}$ decomposition method.

$$\begin{bmatrix} 20 & -9 & 15 \\ -9 & 16 & -5 \\ 15 & -5 & 18 \end{bmatrix} \begin{bmatrix} d_1 \\ d_2 \\ d_3 \end{bmatrix} = \begin{bmatrix} 354 \\ -275 \\ 307 \end{bmatrix}$$

9.14 Solve the following system of simultaneous equations using the $\mathbf{U}^T\mathbf{D}\mathbf{U}$ decomposition method.

$$\begin{bmatrix} 5 & -2 & 1 & 0 & 0 \\ -2 & 3 & -2 & 4 & 0 \\ 1 & -2 & 1 & -1 & 3 \\ 0 & 4 & -1 & 6 & -3 \\ 0 & 0 & 3 & -3 & 4 \end{bmatrix} \begin{bmatrix} d_1 \\ d_2 \\ d_3 \\ d_4 \\ d_5 \end{bmatrix} = \begin{bmatrix} 44 \\ -19 \\ 38 \\ -31 \\ 23 \end{bmatrix}$$

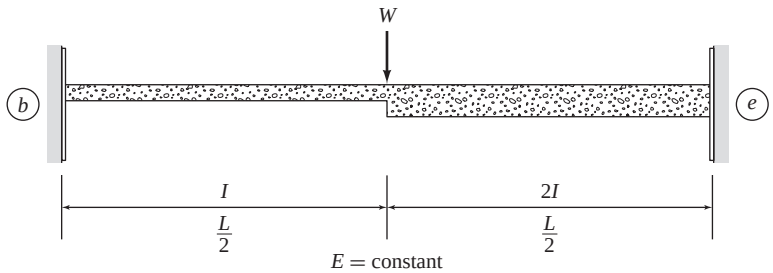

Fig. P9.11

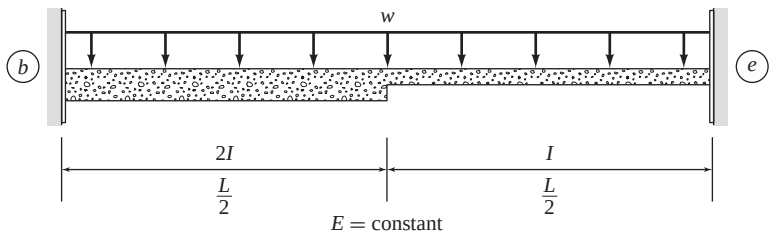

Fig. P9.12